T-1169

# NUMERICAL INVESTIGATION OF REFLECTION AND TRANSMISSION OF SPHERICAL COMPRESSIONAL WAVES

By

Russell L. Gray



ProQuest LLC.
789 East Eisenhower Parkway
P.O. Box 1346
Ann Arbor, MI 48106 – 1346

T-1169

A Thesis submitted to the Faculty and the Board of Trustees of the Colorado School of Mines in partial fulfillment of the requirements for the degree of Doctor of Science in Geophysical Engineering.

Signed: Russell L. Gray
Russell L. Gray

Golden, Colorado

Date: March 25, 1968

Approved: Frank A. Hadsell
Frank A. Hadsell
Thesis Advisor

John C. Hollister
Head of Department

Golden, Colorado

Date: March 27, 1968

# ABSTRACT

A fundamental problem of seismology which has received considerable attention during the past thirty years is to describe the pulse shape of a spherically symmetric compressional wave upon reflection and transmission at an interface. This thesis presents a credible solution to this problem, together with numerical examples to illustrate the relevant mathematical concepts. The main feature of the solution is the insight and understanding of the laws governing spherical wave propagation. The mathematical model used for the investigation consists of two homogeneous and isotropic semi-infinite elastic half spaces in welded contact at a plane interface.

Existing elastic ray theory is extended to a form more tractable to numerical computation. Components of displacement are expressed as convolutions of a pressure, a source excitation, and a propagation term, thus allowing the independent variation of significant parameters. The

propagation term consists of an integral associated with the incident wave and integrals that account for the contribution from the interface. The former is evaluated in closed form, but the latter do not yield to such an evaluation. A plausible interpretation of these integrals is given in terms of generalized functions. Such an interpretation yields a solution which is sanctioned by fulfilling the displacement boundary conditions and by analogy with plane wave theory. The very nature of the solution is such that for many practical purposes, numerical integration is not required to compute reflection and transmission waveforms, thus rendering the solution simpler than has generally been recognized.

# CONTENTS

# ILLUSTRATIONS

Page

Figure

# INDEX OF SYMBOLS

(used in text portion of thesis, p. 1-57)

| Symbol | Definition | Eq. | Page |
|---|---|---|---|
| $A(p,\lambda)$ | | 3 | 6, 7 |
| $A_R(p,\lambda)$, $A_T(p,\lambda)$ | | | 8, 9 |
| $a_n$ | $a_n = [v^2 - S_n^2]^{\frac{1}{2}}$ | | 15 |
| $B_n$, $\overline{B}_n$ | Vertical and horizontal component boundary functions, respectively, for medium n = 1, 2 | | 10 |
| $B_R(p,\lambda)$, $B_T(p,\lambda)$ | | | 8, 9 |
| $BP_t$ | Branch point for time t | | 25 |
| BP | Branch point of $Z_{nP}$ | | 27 |
| $b_n$ | $b_n = [v^2 - s_n^2]^{\frac{1}{2}}$ | | 15 |
| $C_n$, $\overline{C}_n$ | Vertical and horizontal component operational reflection (n = 1) and transmission (n = 2) coefficients for compressional waves | | 11 |
| $c_n$, $\overline{c}_n$ | Same as $C_n$, $\overline{C}_n$ above, but for shear waves | | 11 |
| $d_n$, $\overline{d}_n$ | Vertical and horizontal components of displacement, respectively, in medium n = 1, 2. | | |

| Symbol | Definition | Eq. | Page |
|---|---|---|---|
| $f(t)$ | Source function | | 10 |
| $F(p)$ | Transformed source function | 4 | 7 |
| $g(t,r,z)$ | Propagation function | 5 | 9 |
| $h$ | Vertical distance, source to interface | 3 | 6 |
| $h_{nP}$, $\bar{h}_{nP}$ | Vertical and horizontal primary component of displacement, respectively, for medium n = 1,2 | | 47 |
| $I(t,r)$ | Integral of $K''_{1P}(t,r,0,v)$ | 18 | 36 |
| $Im[\ ]$ | Imaginary part of [ ] | | |
| $J_o$, $J_1$ | Bessel functions | 3 | 6 |
| $K_{nP}$, $\bar{K}_{nP}$ | Vertical and horizontal component kernels, respectively, for compressional waves in medium n = 1, 2. | 8, 9, 10 | 17, 18, 19 |
| $m$ | Integer 1, 2, 3 | | 30 |
| $n$ | Medium designated 1 or 2 | | |
| $p$ | Laplace transform variable | 3 | 6 |
| $\vec{P}(p)$ | Transformed pressure | 4 | 7 |
| $P(t)$ | Pressure | 5 | 9 |
| $q_{nP}$, $\bar{q}_{nP}$ | Vertical and horizontal secondary component of displacement, respectively, for compressional waves in medium n = 1, 2 | | 47 |
| $Q''_n(v)$ | | | 34 |
| $r$ | Horizontal distance, source to receiver | 1 | 4 |
| $r_1$ | Horizontal distance | | 5 |

| Symbol | Definition | Eq. | Page |
|---|---|---|---|
| $r_o$ | Radius of spherical source | | 7 |
| $r_c$ | Critical distance | | 22 |
| $R_o$ | $R_o = [r^2 + (h-z)^2]^{\frac{1}{2}}$. Radius vector from source to receiver | 4 | 7 |
| R | $R = [r^2 + (h+z)^2]^{\frac{1}{2}}$. Length of raypath for reflections | | 20 |
| $R_1$, $R_2$ | Raypath distances for transmissions | | 5 |
| Re[ ] | Real part of [ ] | | |
| $R_p(v)$, $\bar{R}_p(v)$ | Vertical and horizontal component spherical reflection coefficients, respectively, for compressional waves. | | 16 |
| $S_n$, $s_n$ | Compressional and shear wave slownesses, respectively, of medium n = 1, 2 | 1 | 4 |
| t | time | 1 | 4 |
| $t_{nP}$, $t_{nS}$ | Arrival times | | 25 |
| $T_p(v)$, $\bar{T}_p(v)$ | Vertical and horizontal component spherical transmission coefficients, respectively, for compressional waves | | 16 |
| $u_n(t,r,z)$ | Shear wave potential for medium n = 1, 2 | 1 | 4 |
| $U_R$, $U_T$ | Transformed shear wave potential for reflections and transmissions, respectively. | | 8 |
| v | variable | | 15 |
| $v_o$ | Position of singularity on postive real v-axis | | 29 |
| $v_1$, $v_2$, $v_n$ | Pole position on positive real v-axis | | 33 |

| Symbol | Definition | Eq. | Page |
|---|---|---|---|
| $x_{nP}$, $\bar{x}_{nP}$, $x_{nS}$, $\bar{x}_{nS}$ | Vertical and horizontal mathematical components of boundary functions, respectively, for compressional waves (P-subscript) and shear waves (S-subscript). | 6 | 11 |
| $y_{nP}(t,r,z)$ | Auxiliary function | 16 | 31 |
| $y_{nP}(t_{nP})$, $\bar{y}_{nP}(t_{nP})$ | Vertical and horizontal component weights of doublet, respectively, for medium n = 1, 2. | 13 | 31 |
| $y'_{nP}(t_{nP})$ $\bar{y}'_{nP}(t_{nP})$ | Vertical and horizontal component weights of singlet, respectively, for medium n = 1, 2. | 14 | 31 |
| $z$ | Vertical distance, receiver to interface | 1 | 4 |
| $Z_{nP}$ | $Z_{nP} = r^2v^2 + \tau_{nP}^2$ | 10 | 19 |
| $\alpha_n$, $\beta_n$ | | | 8 |
| $\gamma$ | $\omega_o[1 - \zeta^2]^{\frac{1}{2}}$ | | 10 |
| $\gamma_k$ | Sequence of differentiable functions | | 37 |
| $\delta^{-1}(t)$, $\delta(t)$, $\delta'(t)$ | Unit step, singlet, and doublet generalized functions, respectively | 12 | 31 |
| $\zeta$ | $S_1/s_1$ | | 7 |
| $\lambda$ | real variable | 3 | 6 |
| $\xi_n$ | $\alpha_1 h + \alpha_n \lvert z \rvert - pt$ | 6 | 11 |
| $\rho_1$, $\rho_2$ | Density of medium 1, 2 | | 7 |
| $\sigma_1$ | Poisson's ratio of medium 1 | | 49 |
| $\tau_{nP}$ | $\tau_{nP} = a_1 h + a_n \lvert z \rvert - it$ | | 15 |
| $\tau_{nS}$ | $\tau_{nS} = a_1 h + b_n \lvert z \rvert - it$ | | 15 |

| Symbol | Definition | Eq. | Page |
|---|---|---|---|
| $\varphi_n(t,r,z)$ | Compressional wave potential for medium n = 1, 2 | 1 | 4 |
| $\Phi(p,r,z)$ | Transformed compressional wave potential for incident wave | 3 | 6 |
| $\Phi_R$, $\Phi_T$ | Transformed compressional wave potential for reflections and transmissions, respectively. | | 8 |
| $\Psi_n$ | $\alpha_1 h + \beta_n \lvert z \rvert - pt$ | 6 | 11 |
| $\omega_o$ | $2/r_o s_1$ | | |
| $\omega$ | Real integration variable | | 15 |

# ACKNOWLEDGMENTS

This research had its inception during a series of lectures on Cagniard's theory delivered by Professor Frank Hadsell during the 1964-65 academic year at the Colorado School of Mines. Our mutual feeling that "there must be a better way" was the inducement for doing my doctoral research in spherical wave propagation. Professor Hadsell acted as thesis advisor and benefactor, giving freely of both his time and talents. His devotion, patience, and encouragement are deeply acknowledged.

Counsel on matters pertaining to programming the computer was received from J.M. Tucker and D.L. Obitts of the ESSA Boulder Computing Laboratory. Dr. E. Eisner, Texaco Inc., and Dr. J.E. White, Marathon Oil Co., noted ways to improve the text.

Appreciation is expressed to Texaco Inc., for granting an educational leave of absence, for providing fellowships for four years, and for direct financial support over a period of ten months.

The Boulder Earth Science Laboratories of ESSA invited me to be a guest worker at the Computing Laboratory. The office space and computer facilities which were made available over a fifteen month period are gratefully acknowledged.

I am very appreciative of the generous grant from the American Petroleum Institute which contributed toward the purchase of a Calcomp off-line plotter. Adequate plotting facilities made presentation of the large quantities of data computed for this study feasible.

# INTRODUCTION

This thesis deals with the application of exact ray theory to the study of reflection and transmission of spherically symmetric compressional waves at a single plane boundary. Certain of the mathematical details of the problem have been described by Cagniard (1962), Dix (1954), Bortfeld (1962a, 1962b), and many others[1/]. The theory is here extended to obtain expressions for particle displacement that are amenable to numerical evaluation. A formal solution to the problem is obtained following a procedure suggested by Spencer (1960). Double integral expressions appearing in the solution are reduced to single integrals by analytic continuation of the Lipschitz integral, as suggested by Bortfeld (1962a, 1962b).

---

1/ An extensive bibliography may be found in Appendix III of Cagniard (1962) and in Appendix G of this thesis.

General expressions for the vertical and horizontal components of displacement include the time convolution of an arbitrary pressure function, a source function, and a boundary function. The source function describes the excitation of the source, and when convolved with the appropriate functions, describes the incident wave. This function depends only on the source radius and the elastic parameters of the medium in which the source is located. The boundary function accounts for reflection and transmission at the plane interface. For a general solid-solid interface, the boundary function consists of both a compressional component and a shear component. Each of these components consists of the sum of a weighted singlet[2/], a weighted doublet, and an integral transform of the spherical reflection or transmission coefficient of the particular interface under study.

Bortfeld (1962a) has pointed out that the shear waves which are involved in the general case of a solid-solid interface increase the difficulties of the mathematical treatment, but do not contribute correspondingly to the

---

2/ The terms singlet and doublet are used to describe the delta function and its first derivative, respectively.

understanding of the fundamentals of the reflection and transmission process. In view of certain numerical difficulties associated with the general case, an interface which does not generate shear waves is used to illustrate reflection and transmission waveforms. One such interface is the special solid-solid for which the shear wave speeds of the two media are equal and the densities of the two media are equal. In order to visualize the general problem, the essential mathematical development will include shear wave terms.

## FORMAL SOLUTION

The three-dimensional mathematical model consists of two homogeneous and isotropic semi-infinite elastic half spaces in welded contact at a plane interface (Fig. 1). A cylindrical coordinate system $(r,z,\theta)$ with the positive z-axis passing through the source at $z = h$, is used. The interface is the plane $z = 0$. An arbitrary pressure $P(t)$ over a spherical surface of radius $r_o$ generates spherically symmetric compressional waves. The problem is to determine the displacement at an arbitrary point in either medium as a function of time.

Formally, the problem is to find scalar potentials $\varphi_n$ and $u_n$ which satisfy the wave equations

$$\left[\nabla^2 - S_n^2 \frac{\partial^2}{\partial t^2}\right] \varphi_n(t,r,z) = 0 \ ;$$

$$\left[\nabla^2 - \frac{1}{r^2} - s_n^2 \frac{\partial^2}{\partial t^2}\right] u_n(t,r,z) = 0 \qquad (1)$$

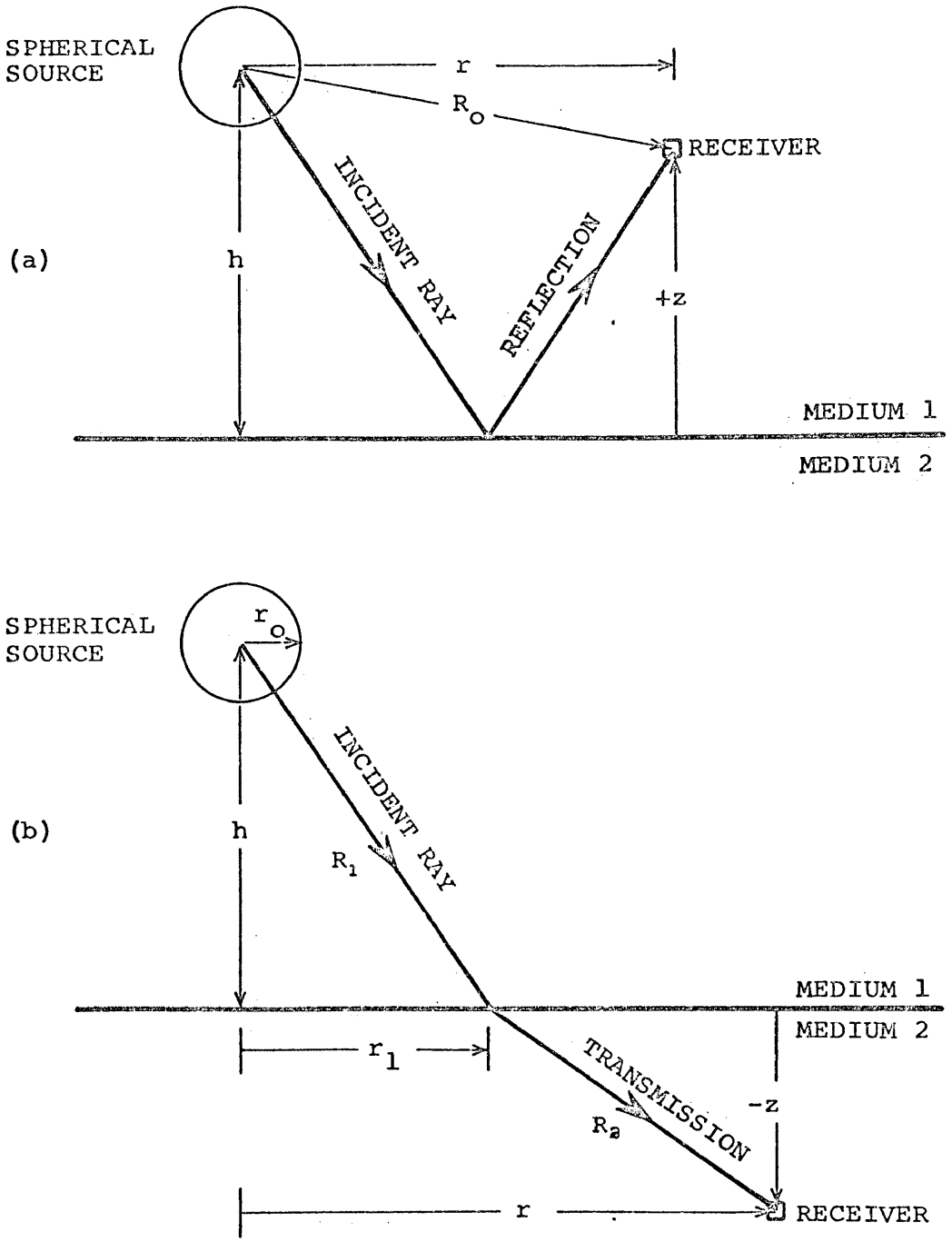


FIGURE 1. Geometrical configuration of source and receiver. (a) Receiver is in medium 1. Raypath distance $R = [r^2 + (h+z)^2]^{\frac{1}{2}}$. (b) Receiver is in medium 2. Raypath distance is $R_1 + R_2$.

Here, $S_n$ and $s_n$ represent wave slownesses defined as the reciprocal of the compressional and shear wave speeds, respectively, and $\nabla^2$ is the Laplace operator

$$\nabla^2 = [\partial^2/\partial r^2 + (1/r)\partial/\partial r + \partial^2/\partial z^2].$$

The subscript n = 1 refers to medium 1 and n = 2 to medium 2. Since axial symmetry persists during the propagation, the displacement vector can have no component in the $\theta$-direction. The vertical displacement $d_n(t,r,z)$ and the horizontal displacement $\bar{d}_n(t,r,z)$ may be obtained from

$$d_n = \frac{\partial \omega_n}{\partial z} + \frac{1}{r}\frac{\partial}{\partial r}(ru_n) \qquad (2)$$

$$\bar{d}_n = \frac{\partial \varphi_n}{\partial r} - \frac{\partial u_n}{\partial z}$$

Source Potential -- General solutions for equations (1) may be obtained using integral transform techniques (see Spencer, 1960). From these solutions, the Laplace transformed potential for an axially symmetric source of compressional waves in an unbounded medium is found to be expressible as

$$\Phi(p,r,z) = \int_0^\infty \lambda A(p,\lambda) J_o(r\lambda) e^{-\alpha_1 |z-h|} d\lambda \qquad (3)$$

where p is the transform variable and $J_o$ is the Bessel function of zero-order. The restriction that

$$\text{Re}\,[\alpha_1 = (\lambda^2+p^2S_1^2)]^{\frac{1}{2}} \geq 0$$

is imposed to assure a bounded potential. The function $A(p,\lambda)$ is determined from the boundary conditions at the source.

The transformed source potential due to a pressure P(t) over a spherical surface of radius $r_o$ is given by (Cagniard, 1962, p. 11)

$$\Phi\ (p,r,z) = \frac{1}{R_o}\, e^{-pRS_1}\, \tilde{P}(p)F(p) \qquad (4)$$

where

$$R_o = [r^2 + (h-z)^2]^{\frac{1}{2}}$$

$$F(p) = - r_o\rho_1[p^2 + 2\zeta\omega_o p + \omega_o^2]^{-1}$$

$$\zeta = S_1/s_1; \quad \omega_o = 2/r_o s_1$$

$\tilde{P}(p)$ in equation (4) is the transform of the pressure and F(p) is the transform of what will be called the source function, f(t).

Equating equations (3) and (4) gives an integral equation in $A(p,\lambda)$ whose solution may be readily derived from the Sommerfeld result (Cagniard, 1962, p. 39; Dix, 1954, p. 726):

$$A(p,\lambda) = \frac{1}{\alpha_1}\, \tilde{P}(p)F(p)$$

Reflection and Transmission Potentials -- A compressional wavefront incident upon a general solid-solid interface gives rise to both compressive and shear stresses due to the discontinuity in the elastic properties. The reflected stress field may be described with two potentials, denoted $\Phi_R$ for compressional waves and $U_R$ for shear waves. Similarly, the transmitted stress field may be described with potentials $\Phi_T$ and $U_T$. These potentials, which may be obtained from the general transformed solutions of equation (1), are given below

$$\Phi_R(p,r,z) = \int_0^\infty \lambda A_R(p,\lambda) J_o(r\lambda) e^{-\alpha_1 z} d\lambda$$

$$U_R(p,r,z) = \int_0^\infty \lambda B_R(p,\lambda) J_1(r\lambda) e^{-\beta_1 z} d\lambda$$

$$\Phi_T(p,r,z) = \int_0^\infty \lambda A_T(p,\lambda) J_o(r\lambda) e^{\alpha_2 z} d\lambda$$

$$U_T(p,r,z) = \int_0^\infty \lambda B_T(p,\lambda) J_1(r\lambda) e^{\beta_2 z} d\lambda$$

with

$$\alpha_n = [\lambda^2 + p^2 S_n^2]^{\frac{1}{2}}; \quad \beta_n = [\lambda^2 + p^2 s_n^2]^{\frac{1}{2}}$$

The functions $A_R$, $B_R$, $A_T$, and $B_T$ are determined from the boundary conditions at the interface, namely continuity of stresses and displacements. The transformed boundary conditions form a system of linear algebraic equations from

which these functions may be derived (Cagniard, 1962, p. 40). For a special solid-solid interface, it can be shown that

$$A_R(p,\lambda) = \frac{\alpha_1 - \alpha_2}{\alpha_1 + \alpha_2} A(p,\lambda) e^{-\alpha_1 h}$$

$$A_T(p,\lambda) = \frac{2\alpha_1}{\alpha_1 + \alpha_2} A(p,\lambda) e^{-\alpha_1 h}$$

$$B_R(p,\lambda) = B_T(p,\lambda) = 0$$

In the case of the general solid-solid interface for which $s_1 = s_2$ and $\rho_1 = \rho_2$, $B_R$ and $B_T$ are non-zero. The linear equations for the general and special solid-solid interface, together with their solution, are given in Appendix A.

Components of Displacement -- A formal solution to the problem is obtained by performing the required differentiations (equation (2)) of the inverse Laplace transforms for $\Phi_1 = \Phi + \Phi_R$, $\Phi_2 = \Phi_T$, $U_1 = U_R$, and $U_2 = U_T$. With the symbol * used to denote convolution with respect to t, the formal solution is given by the equations:

$$d_1(t,r,z) = P(t) * f(t) * \left[\frac{z-h}{R_o} g(t-R_o S_1) + B_1(t,r,z)\right]$$

$$d_2(t,r,z) = -P(t) * f(t) * B_2(t,r,z)$$

$$\bar{d}_1(t,r,z) = P(t) * f(t) * \left[\frac{r}{R_o} g(t-R_oS_1) + \bar{B}_1(t,r,z)\right]$$

$$\bar{d}_2(t,r,z) = P(t) * f(t) * \bar{B}_2(t,r,z) \qquad (5)$$

The overbar represents a horizontal component. The term $g(t-R_oS_1)$ is associated with the incident wave and the $B_n$, $\bar{B}_n$ terms represent the boundary functions. The source function, the incident term, and the boundary functions are given below.

$$f(t) = -\delta^{-1}(t) \frac{r_o}{\gamma\rho_1} e^{-\omega_o\zeta t} \sin \gamma t \; ; \quad \gamma = \omega_o[1 - \zeta^2]^{\frac{1}{2}}$$

$$g(t,r,z) = -\frac{S_1}{R_o} \delta'(t) - \frac{1}{R_o^2} \delta(t)$$

$$B_n(t,r,z) = -\frac{d^2}{dt^2}\left[x_{nP}(t,r,z) + x_{nS}(t,r,z)\right]$$

$$\bar{B}_n(t,r,z) = -\frac{d^2}{dt^2}\left[\bar{x}_{nP}(t,r,z) + \bar{x}_{nS}(t,r,z)\right]$$

where $\delta^{-1}(t)$ represents the unit step and where $\rho_1$ is the density of medium 1. The terms $x_{nP}$ and $x_{nS}$ represent compressional (P-subscript) and shear (S-subscript) components of the boundary functions. The relevant equations for these terms follow:

$$x_{nP}(t,r,z) = \frac{1}{2\pi i} \int_{Br} \int_{o}^{\infty} C_n \frac{\lambda}{p^2} J_o(r\lambda) e^{-\xi_n} \, d\lambda dp$$

$$x_{nS}(t,r,z) = \frac{1}{2\pi i} \int_{Br} \int_{o}^{\infty} c_n \frac{\lambda}{p^2} J_o(r\lambda) e^{-\psi_n} \, d\lambda dp$$

$$\bar{x}_{nP}(t,r,z) = \frac{1}{2\pi i} \int_{Br} \int_{o}^{\infty} \bar{C}_n \frac{\lambda^2}{p^2 \alpha_1} J_1(r\lambda) e^{-\xi_n} \, d\lambda dp$$

$$\bar{x}_{nS}(t,r,z) = \frac{1}{2\pi i} \int_{Br} \int_{o}^{\infty} \bar{c}_n \frac{\lambda^2}{p^2 \alpha_1} J_o(r\lambda) e^{-\psi_n} \, d\lambda dp \qquad (6)$$

$$\xi_n = \alpha_1 h + \alpha_n |z| - pt \; ; \quad \psi_n = \alpha_1 h + \beta_n |z| - pt \; .$$

Here, Br represents the Bromwich path of integration. The factors $C_n$ and $c_n$, which depend on <u>both</u> $\lambda$ and p, represent operational reflection (n = 1) and transmission (n = 2) coefficients for compressional and shear wave propagation, respectively. Coefficients for the special solid-solid interface are given by

$$C_1 = \bar{C}_1 = \frac{\alpha_1 - \alpha_2}{\alpha_1 + \alpha_2}$$

$$C_2 = \frac{2\alpha_2}{\alpha_1 + \alpha_2} \; ; \quad \bar{C}_2 = \frac{2\alpha_1}{\alpha_1 + \alpha_2}$$

$$c_n = \bar{c}_n = 0$$

The shear coefficients $c_n$ and $\bar{c}_n$ are non-zero for the general solid-solid interface.

## REDUCTION OF DOUBLE INTEGRALS

One of the principal mathematical tasks in dealing with problems in spherical wave propagation is to reduce unmanageable double integrals (equations (6)) to single integrals. Cagniard (1962), Pekeris (1956), Longman (1961), Bortfeld (1962a, 1962b), and possibly others, have devised techniques to do this. The techniques of Cagniard, Pekeris, and Longman are similar in many respects. With the Cagniard method, the Bessel functions are replaced by their integral representations. Then, through a sequence of intricate transformations, the integrands are cast in the form of a direct Laplace transform allowing inversion by inspection, thus leaving single integral expressions to be evaluated by numerical means. The Bortfeld approach is based on recognizing that the Lipschitz integral comprises one of the double integrals. The Lipschitz integrals may be evaluated in closed-form, obviating the need to perform a double integration. In many respects, Bortfeld's approach is more straightforward

than Cagniard's and is therefore used here.

Analytic Properties in the p-Plane -- Both $\alpha_n$ and $\beta_n$ may be made single valued by placing a branch cut between their branch points $\pm i\lambda/S_n$ and $\pm i\lambda/s_n$, respectively. The requirement imposed earlier that $\mathrm{Re}[\alpha_n] \geq 0$ and $\mathrm{Re}[\beta_n] \geq 0$, which assured bounded potentials, specifies on which sheet of the Riemann surface the square roots are positive real for positive real p. On this sheet, the right-half p-plane maps in a single-valued manner onto the right-half of the $\alpha_n$- and $\beta_n$-planes such that $\alpha_n$ and $\beta_n$ are analytic everywhere except on their branch cuts.

The coefficients $C_n$, $\bar{C}_n$, $c_n$, and $\bar{c}_n$ are analytic in the p-plane everywhere except at the branch points[3/] because they represent sums, products, and quotients of analytic functions. Also, the exponential terms are analytic in the p-plane everywhere except on the branch cuts and $p^{-2}$ is analytic everywhere except at the origin. Consequently, the integrands are analytic over the entire p-plane except at branch cuts

---

3/ Cagniard demonstrated that the branch points are the only singularities except in the very special case where the interface can support a Stoneley wave. These singularities, called by Cagniard the Rayleigh poles, do not affect the formulation at this stage and do not exist for the special solid-solid interface.

and perhaps poles on the imaginary axis. Moreover, the integrands are real when p is real. This important property and the Schwartz reflection principle (Morse and Feshbach, 1953, p. 393) imply that equations (6) may be expressed as twice the real part of the integrals over half the Bromwich path of integration.

The v-Plane -- The p-dependence of the integrands can be simplified by specifying half the Bromwich path along the positive imaginary axis $p = i\omega$, and making the transformation $\lambda = \omega v$. Since $\omega$ is real, the transformation is merely a change in scale, but the following simplifications result:

$$\alpha_n = \omega a_n \quad ; \quad \beta_n = \omega b_n$$

$$\xi_n = \omega \tau_{nP} \quad ; \quad \psi_n = \omega \tau_{nS}$$

where

$$a_n = [v^2 - S_n^2]^{\frac{1}{2}}; \quad b_n = [v^2 - s_n^2]^{\frac{1}{2}}$$

$$\tau_{nP} = a_1 h + a_n |z| - it$$

$$\tau_{nS} = a_1 h + b_n |z| - it$$

Both $a_n$ and $b_n$ are made analytic functions of v by placing cuts between the branch points $\pm S_n$ and $\pm s_n$, respectively. These branch cuts are placed slightly below the real axis.

The radical $a_n$ is defined on a sheet of the Riemann surface for which points on the real v-axis map onto the positive imaginary $a_n$-axis for $-S_n < v < S_n$, and onto the positive real $a_n$-axis for $v > S_n$. A point in the v-plane maps to a corresponding quadrant in the $a_n$-plane for such a branch. The radical $b_n$ is similarly defined.

Of particular importance is the simplification of $C_n$, $\overline{C}_n$, $c_n$, and $\overline{c}_n$ to functions of the single integration variable v. For the reflection coefficient $C_1 = C_1(p,\lambda)$, the transformation of variables gives $C_1(i\omega, \omega v) = R_P(v)$. Similarly, $C_2(i\omega, \omega v) = T_P(v)$ for a vertical component transmission coefficient. An overbar is used to represent the horizontal component. A P subscript associates a coefficient with compressional wave propagation. For the special solid-solid interface, the relevant equations for the reflection and transmission coefficients are given by

$$R_P(v) = \overline{R}_P(v) = \frac{a_1 - a_2}{a_1 + a_2}$$

$$T_P(v) = \frac{2a_2}{a_1 + a_2}$$

$$\overline{T}_P(v) = \frac{2a_1}{a_1 + a_2}$$

Coefficients for the general solid-solid interface include the shear terms $R_S(v)$, $\bar{R}_S(v)$, $T_S(v)$, and $\bar{T}_S(v)$. Each of the eight equations for the general reflection and transmission coefficients is functions of $S_n$, $s_n$, $\rho_n$, and v, and is considerably more complicated than those above.

With $p = i\omega$ and $\lambda = \omega v$, the double integrals defining $x_{nP}$ and $\bar{x}_{nP}$ in equations (6) are expressible in the following form:

$$x_{1P}(t,r,z) = -\frac{1}{\pi} \mathrm{Re} \int_0^\infty R_P(v)\ K_{1P}(t,r,z,v)\ dv$$

$$x_{2P}(t,r,z) = -\frac{1}{\pi} \mathrm{Re} \int_0^\infty T_P(v)\ K_{2P}(t,r,z,v)\ dv$$

$$\bar{x}_{1P}(t,r,z) = -\frac{1}{\pi} \mathrm{Re} \int_0^\infty \bar{R}_P(v)\ \bar{K}_{1P}(t,r,z,v)\ dv$$

$$\bar{x}_{2P}(t,r,z) = -\frac{1}{\pi} \mathrm{Re} \int_0^\infty \bar{T}_P(v)\ \bar{K}_{2P}(t,r,z,v)\ dv \qquad (7)$$

where

$$K_{nP}(t,r,z,v) = v \int_0^\infty e^{-\omega\ \tau_{nP}}\ J_o(rv\omega)\ d\omega$$

$$\bar{K}_{nP}(t,r,z,v) = \frac{v^2}{a_1} \int_0^\infty e^{-\omega\ \tau_{nP}}\ J_1(rv\omega)\ d\omega \qquad (8)$$

Similar expressions for $x_{nS}$ and $\bar{x}_{nS}$ are obtained from equations (7) and (8) by replacing the P subscript with an S.

The integrals appearing in equations (8) can be evaluated in closed form. The evaluation is discussed in the next section. The functions $K_{nP}$ and $\bar{K}_{nP}$ define kernels of integral transforms of spherical reflection and transmission coefficients. The kernels depend on the characteristic wave slownesses, time t, coordinates of the source and receiver, and the integration variable v. The reflection and transmission coefficients, on the other hand, depend entirely on v and the elastic parameters of the interface under study, and are independent of the geometry of the problem. Specifying a particular interface such as a solid-solid or liquid-solid simply designates the particular equations for $R_P(v)$, ..., $\bar{T}_S(v)$. This feature has been discussed by Spencer (1960) for an arbitrary axially symmetric source.

The Kernels -- The integrals appearing in equations (8) are known to converge for $\mathrm{Re}[\tau_{nP}] \geq 0$. The first is known as the Lipschitz integral for $\mathrm{Re}[\tau_{nP}] > 0$ (Watson, 1966, p. 384). For $\mathrm{Re}[\tau_{nP}] = 0$, the integral is a special case of the discontinuous Weber-Schafheitlin integrals (Abramowitz and Stegun, 1964, p. 487) and converges when $\mathrm{Im}[\tau_{nP}] \neq rv$. The value of the latter may be obtained from the former by analytic continuation (Appendix B). The second integral

appearing in equations (8) is readily evaluated from the first using integration by parts. The kernels are found to be:

$$K_{nP}(t,r,z,v) = \begin{cases} v[Z_{nP}]^{-\frac{1}{2}}; \ Re(\tau_{nP}) > 0 \\ -iv \ sgn \ \hat{\tau}_{nP}[-\hat{Z}_{nP}]^{-\frac{1}{2}}; \ Re(\tau_{nP}) = 0, \ \hat{Z}_{nP} < 0 \\ v[\hat{Z}_{nP}]^{-\frac{1}{2}}; \ Re(\tau_{nP}) = 0, \ \hat{Z}_{nP} > 0 \end{cases} \tag{9}$$

$$\bar{K}_{nP}(t,r,z,v) = \begin{cases} (v/ra_1)\left[1 - \tau_{nP}(Z_{nP})^{-\frac{1}{2}}\right]; \ Re(\tau_{nP}) > 0 \\ (v/ra_1)\left[1 - |\hat{\tau}_{nP}|(-\hat{Z}_{nP})^{-\frac{1}{2}}\right]; \ Re(\tau_{nP}) = 0, \ \hat{Z}_{nP} < 0 \\ (v/ra_1)\left[1 - i\hat{\tau}_{nP}(\hat{Z}_{nP})^{-\frac{1}{2}}\right]; \ Re(\tau_{nP}) = 0, \ \hat{Z}_{nP} > 0 \end{cases} \tag{10}$$

where

$$\hat{\tau}_{nP} = Im(\tau_{nP})$$

$$Z_{nP} = r^2v^2 + \tau_{nP}^2 \ ; \ \hat{Z}_{nP} = r^2v^2 - \hat{\tau}_{nP}^2$$

Branch cuts are placed adjacent to the negative real axis of the $Z_{nP}$-plane in order to arrive at the above expressions. The mapping of these cuts onto the v-plane is discussed in a following section. With the kernels $K_{nP}$ and $\bar{K}_{nP}$ defined according to equations (9) and (10) above, the double integral

expressions of equation (6) are reduced to the single integrals given by equation (7). The convergence of the single integrals is discussed in the next section.

Establishing the singularities of the kernels is requisite for the interpretation of the single integrals. Time independent singularities of the horizontal component kernels occur at $\pm S_n$, the branch points of $a_n$. Roots of $Z_{nP} = 0$ define the time-dependent singularities. For n = 1, the roots may be obtained from the expression

$$v = R^{-2}[\pm rt + (z+h)(t_{1P}^2 - t^2)^{\frac{1}{2}}]$$

where $R = [r^2 + (h+z)^2]^{\frac{1}{2}}$ is the length of the reflection raypath and $t_{1P} = RS_1$ is the reflection arrival time. There are four real roots for $t < t_{1P}$. For $t > t_{1P}$, there are two complex roots, one in the first quadrant of the v-plane and one in the second quadrant. The conjugate of the two complex roots satisfies $Z_{1P} = 0$ on the second sheet of the Riemann surface. At the arrival time $t_{1P}$, two roots merge on the real axis, forming a simple pole there.

Figure 2 is a plot of a root locus of $Z_{1P} = 0$ for r = h = z = 100 ft, and $S_1 = .0001$ sec/ft, $S_2 = .0000625$ sec/ft. Additional roots for corresponding times may be visualized by rotating the locus curve about the imaginary axis. The arrows in Figure 2 indicate the direction the

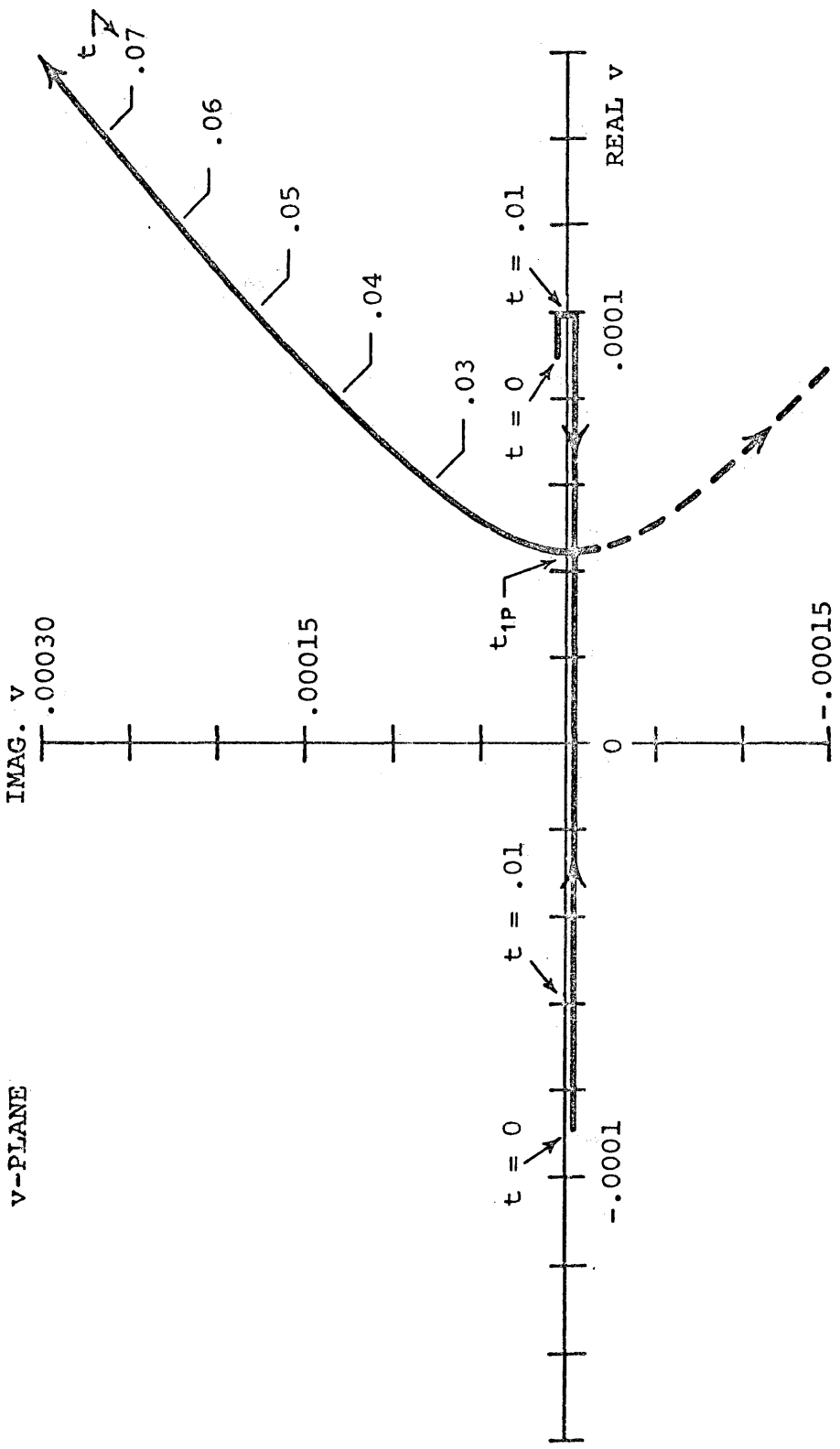


FIGURE 2. Root locus of $Z_{1p} = 0$. r = h = z = 100 ft, $S_1$ = .0001 sec/ft, $S_2$ = .0000625 sec/ft. $t_{1p}$ = .02236 sec. Real roots appear apart from axis for sake of clarity.

roots move as t increases. The dashed curve indicates those complex roots on the second sheet of the Riemann surface.

Figure 3 illustrates the root loci of $Z_{1P} = 0$ for various radial distances r between 0 and 400 ft. Here, $S_1 > S_2$, and curves meet the positive real axis in the interval $v < S_2$ for $r < r_c$ and in the interval $S_2 < v < S_1$ for $r > r_c$[4/]. This important feature yields the critical refraction arrival (head waves). It should be remembered in examining Figures 2 and 3 that for given coordinates r, h, and z, and for a given value of t, $Z_{1P}$ possesses either two complex or four real roots. While for sake of clarity these figures may indicate a smaller or greater number of roots, the implication is unintentional.

The zeros of $Z_{2P}$ and $Z_{nS}$ are more difficult to obtain than those for $Z_{1P}$ because two radicals are involved instead of one. In these three cases, the zeros may be obtained by solving two quartic equations in v whose real coefficients depend on r, h, z, t, $S_1$, and on either $S_2$, $s_1$, or $s_2$. Two complex or four real roots are then established from the eight possibilities. Roots on the positive real axis lie to the left of the minimum wave slowness appearing in the appropriate $\tau_{2P}$ or $\tau_{nS}$. The locus of the complex roots is very similar to the locus for $Z_{1P}$, which is

---

4/ The critical distance $r_c$ is given by

$$r_c = S_2(h+z)\left[S_1^2 - S_2^2\right]^{-\frac{1}{2}};\ S_1 > S_2$$

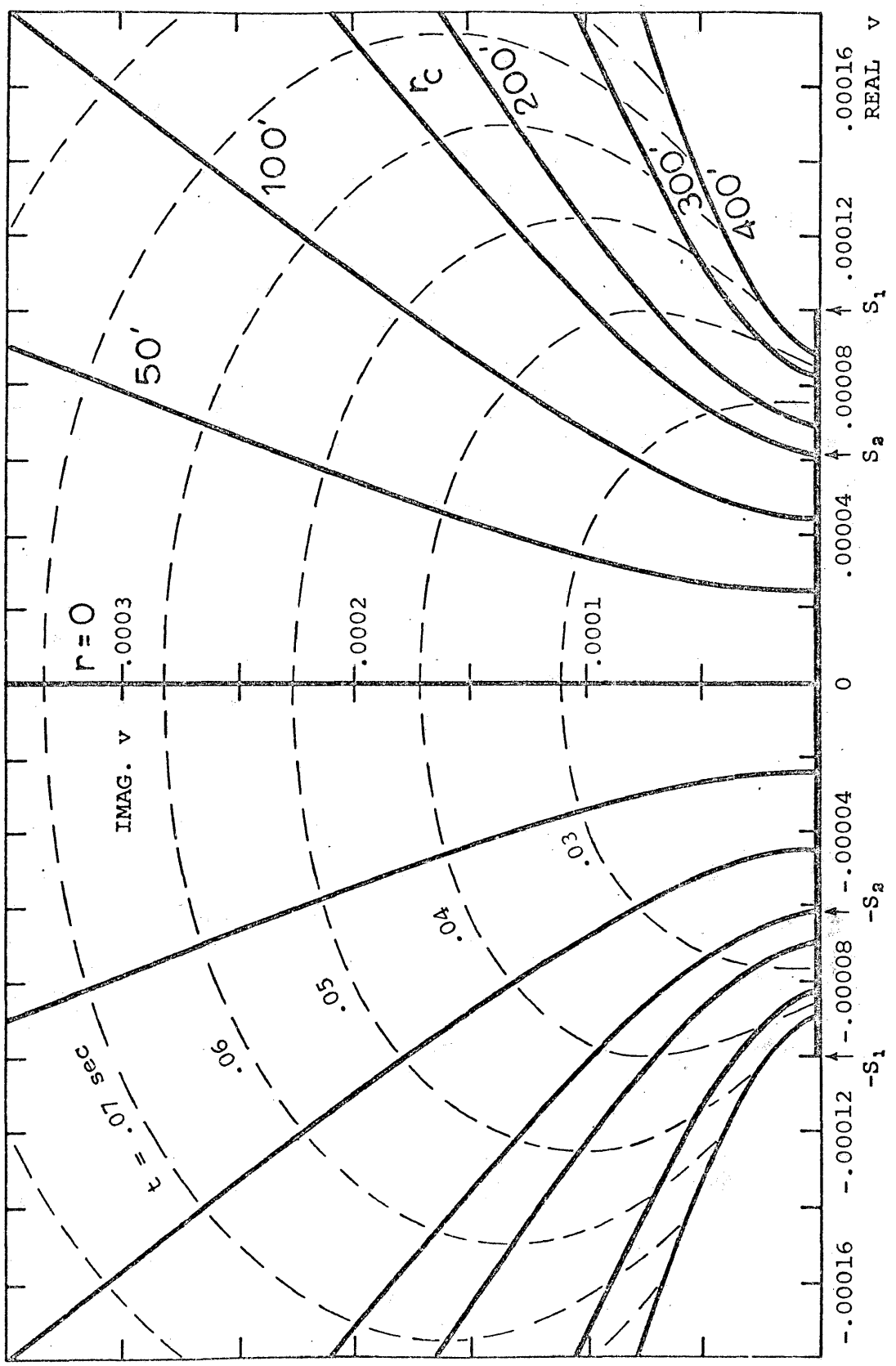


FIGURE 3. Root locus of $Z_{1P} = 0$ for several values of r. $r_c$ = 160 ft, h = z = 100 ft, $S_1$ = .0001 sec/ft, $S_2$ = .0000625 sec/ft.

certainly to be expected. The details of finding the zeros of $Z_{2P}$ and $Z_{nS}$, together with examples of root loci, are given in Appendix C.

## THE BOUNDARY FUNCTIONS

The relative position of branch points and cuts in the v-plane is fundamental to the interpretation of $x_{nP}$, ..., $\bar{x}_{nS}$ and their derivatives. Branch cuts associated with the kernels were specified in the $Z_{nP}$ and $Z_{nS}$ planes; consequently these cuts must be mapped onto the v-plane. One such mapping is shown in Figure 4 for a cut on the negative real axis of the $Z_{1P}$-plane and for several values of t. Here it will be noted that the v-plane image of the cut lies on the axes for $t < t_{1P}$ ($t_{1P}$ = .02236 sec), with segments moving into the first and second quadrants for $t > t_{1P}$.[5/] The positions of the branch points for each value of t are denoted by $BP_t$. The multiple branch point feature is a direct consequence of placing the cut on the negative real axis of the $Z_{1P}$-plane.

---

5/ The notation $t_{nP}$ and $t_{nS}$ is used for the reflection (n = 1) or transmission (n = 2) arrival time of a compressional and shear wave, respectively.

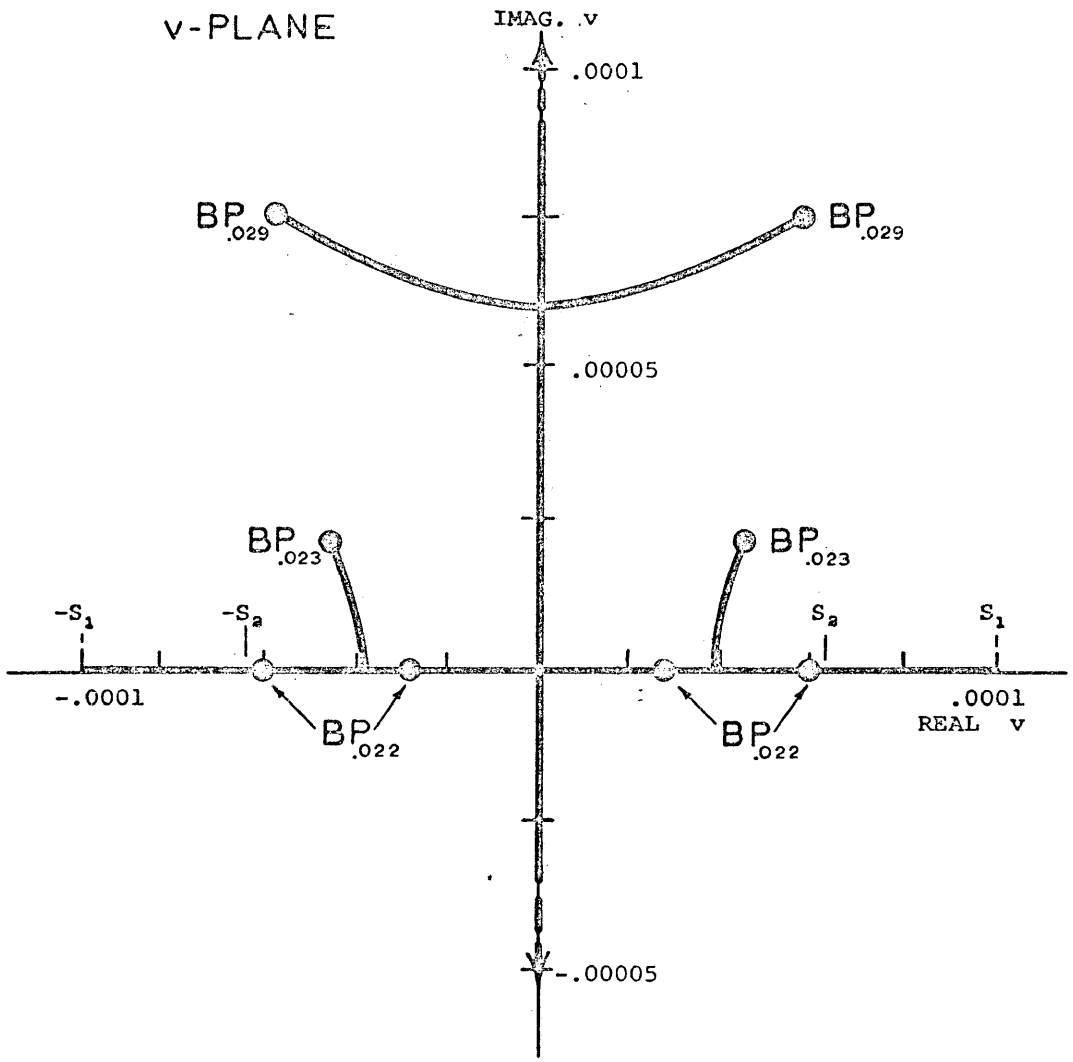


FIGURE 4. The v-plane mapping of the negative real axis of the $Z_{1P}$-plane for t = .022, .023, .029 sec. $t_{1P}$ = .02236 sec. r = h = z = 100 ft, $S_1$ = .0001 sec/ft, $S_2$ = .0000625 sec/ft. The mapping includes the entire imaginary v-axis and the real segment $-S_1<v<S_1$. $BP_t$ denote multiple branch points for the respective t.

If the cut is placed in the manner shown in Figure 5b ($t < t_{1P}$), the v-plane image occurs to the left of the positive imaginary axis and slightly above the real axis, finally terminating at a single branch point BP on the real axis (Fig. 5a). The moving branch point is the smallest positive real root of $Z_{1P} = 0$. The other three zeros of $Z_{1P}$ lie apart from BP for $t < t_{1P}$; two lie on the negative real axis and one on the positive real axis between the minimum and maximum wave slowness.

Several features may assist in understanding the moving branch point BP. When t is less than the travel time via the minimum time path, BP lies to the left of the minimum wave slowness. When t is greater than the reflection or transmission arrival time, BP and its image in the second quadrant lie apart from the real axis. When the receiver is on the critical cone ($r = r_c$), BP = $S_2$ when $S_2 < S_1$ and $t = t_{nP}$ (see Fig. 3). When the receiver is outside the critical cone ($r > r_c$) and when t is greater than the critical refraction arrival time, but less than the reflection arrival time, the branch point lies on the positive real axis between the minimum and maximum wave slowness.

The analytic regions for the integrands are established with the specification of the moving branch cut. Clearly, when t is less than the travel time via the minimum time

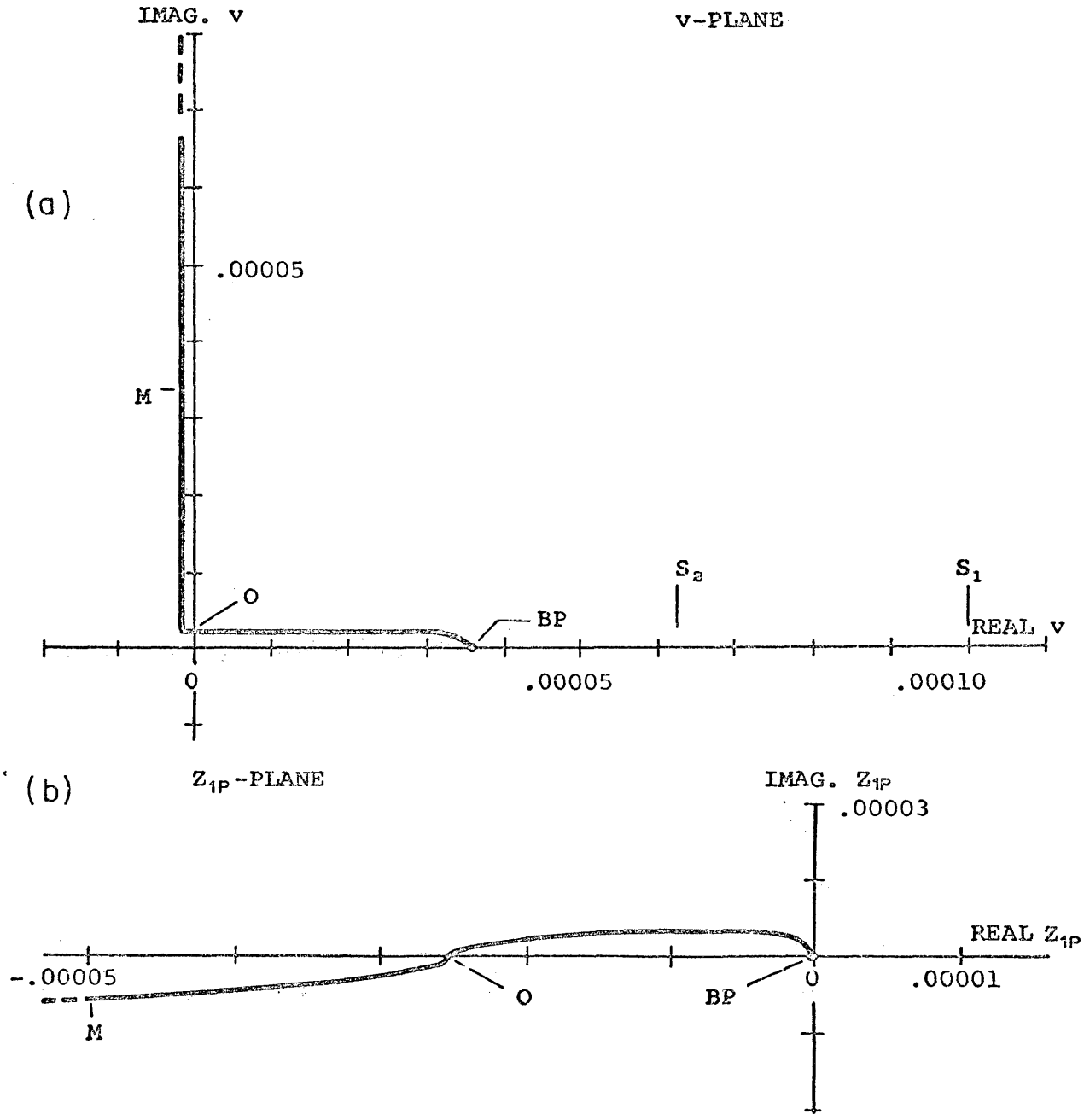


FIGURE 5. (a) v-plane mapping of the $Z_{1p}$-plane branch cut shown in (b) for t = .015, r = h = z = 100 ft, $S_1$ = .0001 sec/ft. $S_2$ = .0000625 sec/ft. The $Z_{1p}$-plane cut is placed arbitrarily close to the negative real axis in the manner shown.

path, the integrands are analytic everywhere within the first quadrant, excluding a segment $0 \leqslant v \leqslant BP$ adjacent to the real axis and excluding the zeros of $Z_{nP}$ and $a_1$. The real part of the integrands is zero over the interval extending from the origin to the minimum wave slowness. The real-axis segment of the moving branch cut is therefore of little consequence until $r > r_c$, because there is no contribution to the integrals over this portion of the path. Only the case $r \leqslant r_c$ will be considered in the sequel.

The singularities that lie on the real axis when $t < t_{nP}$ are integrable because the integrands behave as $(v-v_o)^{-\frac{1}{2}}$ in arbitrarily small neighborhoods of these points. When $t = t_{nP}-0$, the singularities merge with BP at $v = v_n$, forming a simple pole there. Equivalently, when $t = t_{nP}+0$, the complex branch points from both sheets of the Riemann surface merge at $v_n$, forming a simple pole there.

The analyticity of the integrands in the first quadrant for $t < t_{nP}$ suggests using the Cauchy-Goursat theorem to deform the real-axis integration path to one which offers greater convenience. A contour up the positive imaginary axis, thence along a quarter-circle back to the positive real axis is one possibility. Since the integrands are real on the imaginary axis, integration over this portion of the equivalent contour yields only imaginary values and therefore contributes nothing to $x_{nP}$, ..., $\bar{x}_{nS}$. The quarter circle

yields no contribution to $x_{1P}$ and $\bar{x}_{1P}$ for a special solid-solid because $R_p(v) = \bar{R}_p(v) \to 0$ as $|v| \to \infty$. Consequently, $x_{1P} = \bar{x}_{1P} = 0$ for $t < t_{1P}$. For all other cases, however, the integrands behave as $v^m$ as $|v| \to \infty$, where $m \geq 0$. This means that the integrals defining $x_{nP}$, ..., $\bar{x}_{nS}$ do not converge and are hence meaningless in the classical sense.

One must remember that $x_{nP}$, ..., $\bar{x}_{nS}$ are not displacements; they are mathematical components which may be unbounded and yet yield meaningful results. Particle displacement is obtained by convolving the second derivative of the mathematical components with f(t) and P(t). The feature of unboundedness requires that a tentative solution be "constructed", so to speak, such that the wave equations (eq. (1)) and the boundary conditions are satisfied. Such a solution, if one can be found, is the only solution by virtue of the uniqueness theorem of Kirchoff and Neumann (see Love, 1944, p. 176; Sokolnikoff, 1956, p. 86).

Although the physical components of the elastic field, such as particle displacement or stress, must be expressible as functions, the mathematical components are not so limited. These mathematical components may, and frequently do, fall within the larger set of generalized functions. Generalized functions are sometimes necessary to describe and explain mathematically a continuous but very rapid variation of the mathematical components.

A Tentative Solution -- A tenative solution may be deduced by adopting a plausible interpretation of equations (6) or (7), or the derivatives of these integrals. One possible interpretation of the integrals

$$x''_{1P}(t,r,z) = \frac{d^2}{dt^2} x_{1P}(t,r,z)$$

$$= \frac{1}{2\pi i} \int_{Br} \int_{o}^{\infty} C_1 \lambda J_o(r\lambda) e^{-\xi_1} \, d\lambda dp$$

$$= -\frac{1}{\pi} \mathrm{Re} \int_{o}^{\infty} R_p(v) K''_{nP}(t,r,z,v) \, dv \qquad (11)$$

is given by the following equation with n = 1:

$$x''_{nP}(t,r,z) = y_{nP}(t_{nP})\delta'(t-t_{nP}) + y'_{nP}(t_{nP})\delta(t-t_{nP}) \qquad (12)$$

$$+ y''_{nP}(t,r,z)\delta^{-1}(t-t_{nP})$$

where

$$y_{nP}(t_{nP}) = \lim_{t \to t^+_{nP}} x_{nP}(t,r,z) = \pi i \, \mathrm{Res}[v_n] \qquad (13)$$

$$y'_{nP}(t_{nP}) = \lim_{t \to t^+_{nP}} x'_{nP}(t,r,z) = \pi i \, \mathrm{Res}[v_n]' \qquad (14)$$

$$y''_{nP}(t,r,z) = x''_{nP}(t,r,z) \text{ for } t > t_{nP} \qquad (15)$$

In the definitions above, $\mathrm{Res}[v_n]$ means the residue of $R_P(v)K_{1P}(t_{1P},r,z,v)$, $(n = 1)$, or $T_P(v)K_{2P},r,z,v)$, $(n = 2)$, at $v_n$. $\mathrm{Res}[v_n]'$ is similarly defined using $K'_{nP}$ in place of $K_{nP}$. The weight of the doublet, $y_{nP}(t_{nP})$, and the weight of the singlet, $y'_{nP}(t_{nP})$, are both functions of the coordinates r, h, and z. Integrals corresponding to equation (11) which define $x''_{2P}$, $\bar{x}''_{nP}$, $x''_{nS}$, and $\bar{x}''_{nS}$ may be interpreted in a like manner.

Equation (12) was chosen as a tentative solution to the problem for two reasons. First, when n = 1 this equation can be derived directly from $x_{1P}$ for a special solid-solid interface. Second, equation (12), and analogs for $\bar{x}''_{nP}$, $x''_{nS}$, and $\bar{x}''_{nS}$, satisfy the displacement boundary conditions. Each of these reasons will be briefly discussed.

For a special solid-solid interface, the mathematical components $x_{1P}$ and $\bar{x}_{1P}$ are zero for $t < t_{nP}$. This discontinuous feature is expressible mathematically in the following form:

$$x_{1P}(t,r,z) = \delta^{-1}(t-t_{1P})y_{1P}(t,r,z) \qquad (16)$$

and similarly for $\bar{x}_{1P}$. $y_{1P}(t,r,z)$ is a bounded and continuous auxiliary function which is introduced to facilitate the differentiation of $x_{1P}$. The generalized derivative of equation (16) yields equation (12) for n = 1.

For the arrival time $t_{1P}$, the integrals $x_{1P}$ and $x'_{1P}$ have a Cauchy principal value (Morse and Feshbach, 1953, p. 368) equal to $\pi i$ times the residue at $v_n$. This feature yields the weights $y_{1P}(t_{1P})$ and $y'_{1P}(t_{1P})$.

It must be understood that equation (16), and its horizontal component analog, can be established only for the special solid-solid interface. While this form may be valid for other cases as well, and the physics of the problem indicates that it should, a consistent mathematical proof has yet to be formulated. The methods of Cagniard (1962), Pekeris (1956), and Longman (1961) can be used to show that the reflection and transmission potentials are zero for $t < t_{nP}$, but this does not necessarily mean that $x_{nP}$, ..., $\bar{x}_{nS}$ are zero. One should be aware of the fact that it is not necessary for $x_{nP}$ to be zero for $t < t_{nP}$ in order to arrive at equation (12). Other possibilities are discussed in Appendix D.

Weights of the Doublet and Singlet -- Derivation of the weights of the doublet and singlet is predicated on finding the residue of the various integrands at the poles $v_n$ which occur when $t = t_{nP}$. The position of these poles is found from the relations

$$v_1 = rS_1/R; \; v_2 = r_1S_1/R_1 = (r-r_1)S_2/R_2,$$

where $R = [r^2 + (h+z)^2]^{\frac{1}{2}}$ and where $r_1$, $R_1$, and $R_2$ are defined according to Figure 1b.

A Laurent series expansion of $rv - i\tau_{nP}$ about $v_n$ yields the following approximation (Appendix E):

$$Z_{nP} \approx -(v-v_n)^2[\tfrac{1}{2}(rv + i\tau_{nP})|Q_n''(v_n)|]$$

wherein

$$Q_n''(v) = -i[hS_1^2/a_1^3 + |z|S_n^2/a_n^3].$$

The residue for the $x_{1P}$ integrand is given by

$$(v-v_1)R_P(v)K_{1P}(t,r,z,v)\Big|_{v-v_1} = iR_P(v_1)v_1[rv_1|Q_1''(v_1)|]^{-\frac{1}{2}}$$

$$= i[(h+z)/R][S_1/R]R_P(v_1)$$

Residues of the other integrands are similarly obtained.

The required weights of the doublet follow from equation (13), which gives

$$y_{1P}(t_{1P}) = [(h+z)/R][S_1/R]\mathrm{Re}[R_P(v_1)];\ r,z \geq 0$$

$$y_{2P}(t_{2P}) = \begin{cases} \dfrac{(h/R_1)(S_1/R_1)(r_1/r)^{\frac{1}{2}}\mathrm{Re}[T_P(v_2)]}{[1 + (R_2/R_1)^3(h/z)^2(S_1/S_2)]^{\frac{1}{2}}}; & r > 0,\ z < 0 \\ (S_1/h)(1 + S_1|z|/S_2h)^{-1}\mathrm{Re}[T_P(0)]; & r = 0,\ z \leq 0 \end{cases}$$

(17)

Expressions for $\bar{y}_{nP}(t_{nP})$ may be obtained from equations (17) by replacing [(h+z)/R] with (r/R) (n = 1) and $(h/R_1)$ with $(r_1/R_1)$ (n = 2), and by using the appropriate reflection and transmission coefficients. The shear analogs may be similarly obtained.

The integrals for $x'_{nP}$ and $\bar{x}'_{nP}$, from which the weights $y'_{nP}(t_{nP})$ and $\bar{y}'_{nP}(t_{nP})$ are obtained, display a third order pole at $v_n$ when $t = t_{nP}$. These integrals can be transformed into integrals involving only simple poles on the real v-axis. To do this, the t-variable differentiations of the kernels are interchanged with space-variable differentiations. Using equations (8), it is easy to derive the following useful transformations

$$K'_{nP}(t,r,z,h,v) = -i \frac{\partial}{\partial h}\left[\frac{1}{a_1} K_{nP}(t,r,z,h,v)\right]$$

$$\bar{K}'_{nP}(t,r,z,h,v) = -i \frac{\partial}{\partial r}\left[\frac{1}{a_1} K_{nP}(t,r,z,h,v)\right]$$

With the foregoing transformations, it can be shown that the weights of the singlets can be derived from the weights of the doublets. Some of the details of this derivation are given in Appendix E. Using equation (14), the required weights of the singlet appearing in equation (12) are found to be

$$y'_{1P}(t_{1P}) = (RS_1)^{-1} y_{1P}(t_{1P})$$

$$y'_{2P}(t_{2P}) = (R_1 S_1)^{-1} y_{2P}(t_{2P})$$

The analogous weights are obtained in the same way.

It is instructive to note the similarity between $g(t,r,z)$ of equation (5) and $x''_{nP}(t,r,z)$ of equation (12). Each contains a doublet and singlet term. The weight of the doublet terms of g, $x''_{1P}$, and $x''_{2P}$ contain the factors $R_o^{-1}$, $R^{-1}$, and $R_1^{-1}$, respectively. The weight of the corresponding singlet terms contain the factors $R_o^{-2}$, $R^{-2}$, and $R_1^{-2}$, respectively. The doublet is therefore a far field term and the singlet a near field term. When both the singlet and $y''_{nP}$ contribution are negligible, the reflection and transmission waveforms are the same as the incident waveform; only the relative amplitudes differ. In other words, there is no change in pulse shape on reflection and transmission at the interface.

Continuity of Displacement at z = 0 -- Continuity of the vertical component of displacement is realized when

$$d_1(t,r,0) - d_2(t,r,0) = 0$$

and similarily for the horizontal component. Using the relations $t_o = t_{1P} = t_{2P} = R_o S_1$ and $K_{1P} = K_{2P}$ for $z = 0$, it can be shown that (see Appendix F):

$$d_1(t,r,0) - d_2(t,r,0) = P(t)*f(t)*\delta^{-1}(t-t_o)\,I(t,r,), \qquad (18)$$

where

$$I(t,r) = \frac{1}{\pi}\,\mathrm{Re}\int_o^\infty K''_{1P}(t,r,0,v)\,dv$$

for a special solid-solid interface. The integral

definition of the kernel (eq. (8)), and the Sommerfeld result, are used to show that

$$I(t,r) = (h/R_o)g(t-t_o,r,0)$$

But $g(t,r,0) = 0$ for $t \neq 0$ because it represents the sum of a doublet and a singlet. Consequently, the right hand side of equation (18) vanishes when the step is interpreted according to

$$\delta^{-1}(t) = \begin{matrix} 1 \text{ for } t > 0 \\ 0 \text{ for } t \leqslant 0 \end{matrix}$$

A proof of the last statement may be constructed by replacing $\delta^{-1}(t)$ in equation (18) with a sequence of ordinary differentiable functions $\gamma_k(t)$. One such sequence is given by

$$\gamma_k(t) = (k/\pi)^{\frac{1}{2}} \int_{-\infty}^{t} e^{-k\nu^2} \, d\nu$$

The following limits, taken in the order indicated, establishes the proof:

$$[\delta^{-1}(t-t_o)g(t-t_o,r,0)] = \lim_{\substack{k\to\infty \\ \epsilon\to 0}} [\gamma_k(t-t_o-\epsilon)g(t-t_o,r,0)]$$

$$= 0$$

Continuity of the horizontal component of displacement is demonstrated in the same manner. In the development for the general solid, the algebra becomes much more involved, but is otherwise the same as that given above for the special solid.

Continuity of displacement for z = 0 has been verified numerically. Computations were carried out for both vertical and horizontal components and for several values of r and h, thus serving as a partial check on the computer programs which produced the numerical examples of the next section.

Clearly, a solution has been found which satisfies the displacement boundary conditions. This is a necessary condition for the solution to be valid, but not a sufficient condition. In addition to satisfying the displacement boundary conditions, equation (12) must satisfy the stress conditions and the equations of motion. No mathematical proof has yet been devised to verify that the latter conditions are fulfilled. Rather, an attempt is made to sanction the solution by analogy with plane wave theory. The analogy is predicated on the assumption that in the far field, the laws governing reflection and transmission of spherical waves are similar to those laws for plane waves. For spherical wave theory to be consistent with plane wave theory, reflection and transmission waveforms in the far field must approximate the incident waveform. An appraisal of the solution using the plane wave analogy is facilitated with examples of the next section.

## NUMERICAL EXAMPLES

Certain of the preceding mathematical expressions will be illustrated in order to provide a better understanding of the theory. Examples of reflection and transmission coefficients, the second time derivative of the kernels, and the real part of the integrands will provide a better understanding of the integral transforms. Examples of reflection and transmission waveforms will illustrate the relative importance of the pressure function, the source function, and the doublet, singlet, and $y''_{nP}$, ..., $\bar{y}_{nS}$ terms of the boundary functions. Simple synthetic seismograms will illustrate the relative shape and magnitude of the incident and reflection waveforms. A solid-solid interface with $s_1 = s_2$, $\rho_1 = \rho_2$, $S_1 > S_2$, and $r < r_c$ will be used.

The first example shows the real and imaginary parts of the reflection coefficients (Fig. 6). The transmission

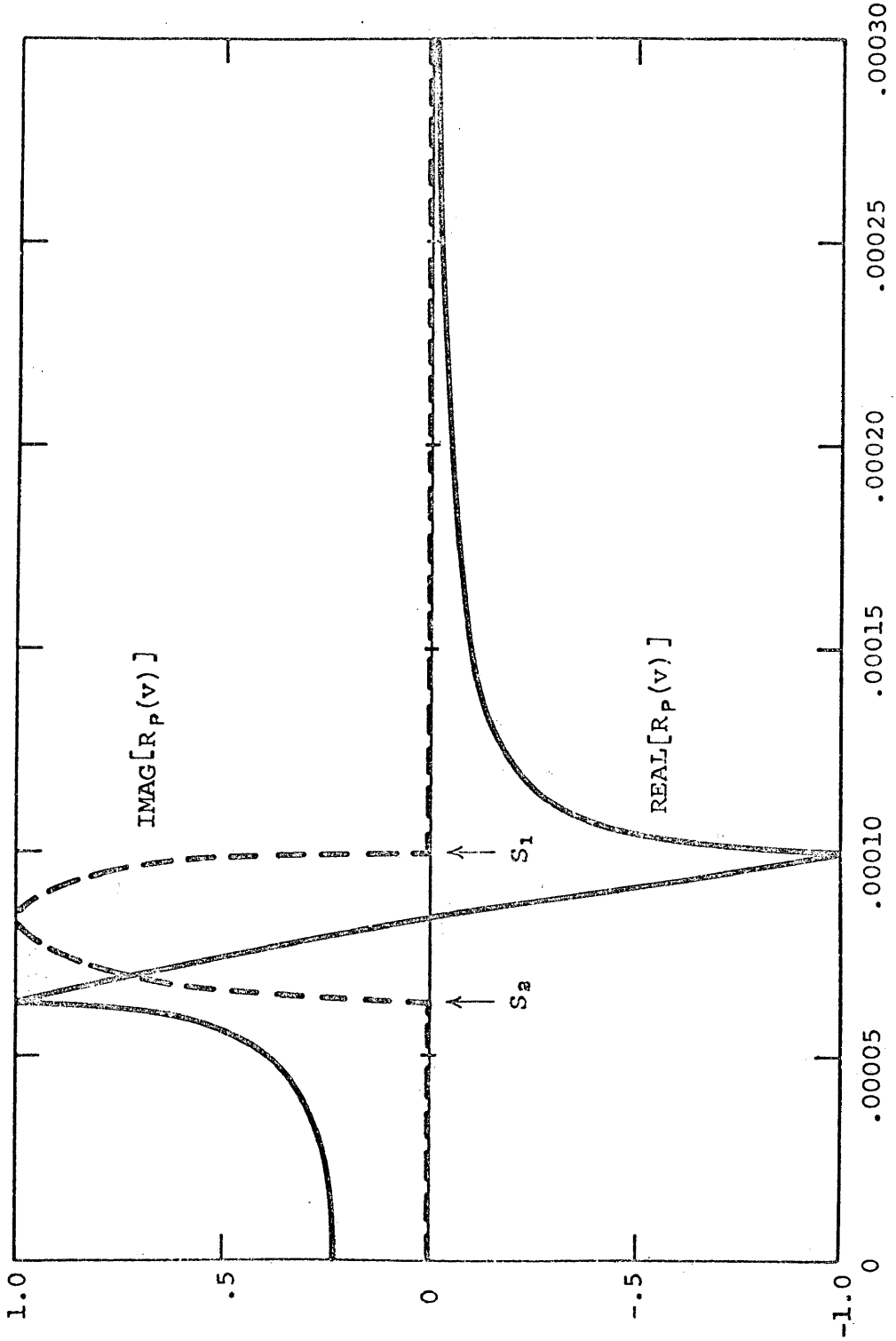


FIGURE 6. Real and imaginary parts of reflection coefficients $R_p(v) = \bar{R}_p(v)$ for a special solid-solid interface with $s_1 = s_2$, $\rho_1 = \rho_2$, $S_1 = .0001$ sec/ft, and $S_2 = .0000625$ sec/ft.

coefficients may be visualized using the simple relationships $T_P(v) = 1 - R_P(v)$ and $\bar{T}_P(v) = 1 + \bar{R}_P(v)$. It is helpful to note that outside of the interval $S_2 < v < S_1$, $Im(R_P) = -Im(T_P) = Im(\bar{T}_P) = 0$.

The real and imaginary parts of $K''_{1P}(t,r,z,v)$ and $\bar{K}''_{2P}(t,r,v,z)$ are shown in Figure 7 for several values of $t > t_{nP}$. The effect of the $a_1^{-1}$ factor in $\bar{K}_{2P}$ is clearly seen at $v = S_1 = .0001$. It will be noted that the real parts of both $K''_{1P}$ and $K''_{2P}$ are zero in the interval $0 < v < S_2$, whereas the imaginary parts attain a maximum there. It should be understood that the kernels depend on the two wave slownesses appearing in the appropriate $\tau_{nP}$ or $\tau_{nS}$, but are otherwise independent of the interface under study. Clearly, the differentiated kernels shown in Figure 7 characterize any interface whose compressional wave slownesses are given by $S_1 = .0001$ sec/ft and $S_2 = .0000625$ sec/ft.

The real parts of all four integrands are shown in Figure 8 for several values of $t > t_{nP}$. Several features are noteworthy. First, all curves are zero for $v \leq S_2$. Second, the dominant portion of the curves lies in the interval $S_2 < v < S_1$. Third, the (integrable) singularity at $v = S_1$ is clearly displayed for the horizontal component integrand associated with medium 1, but not for medium 2.

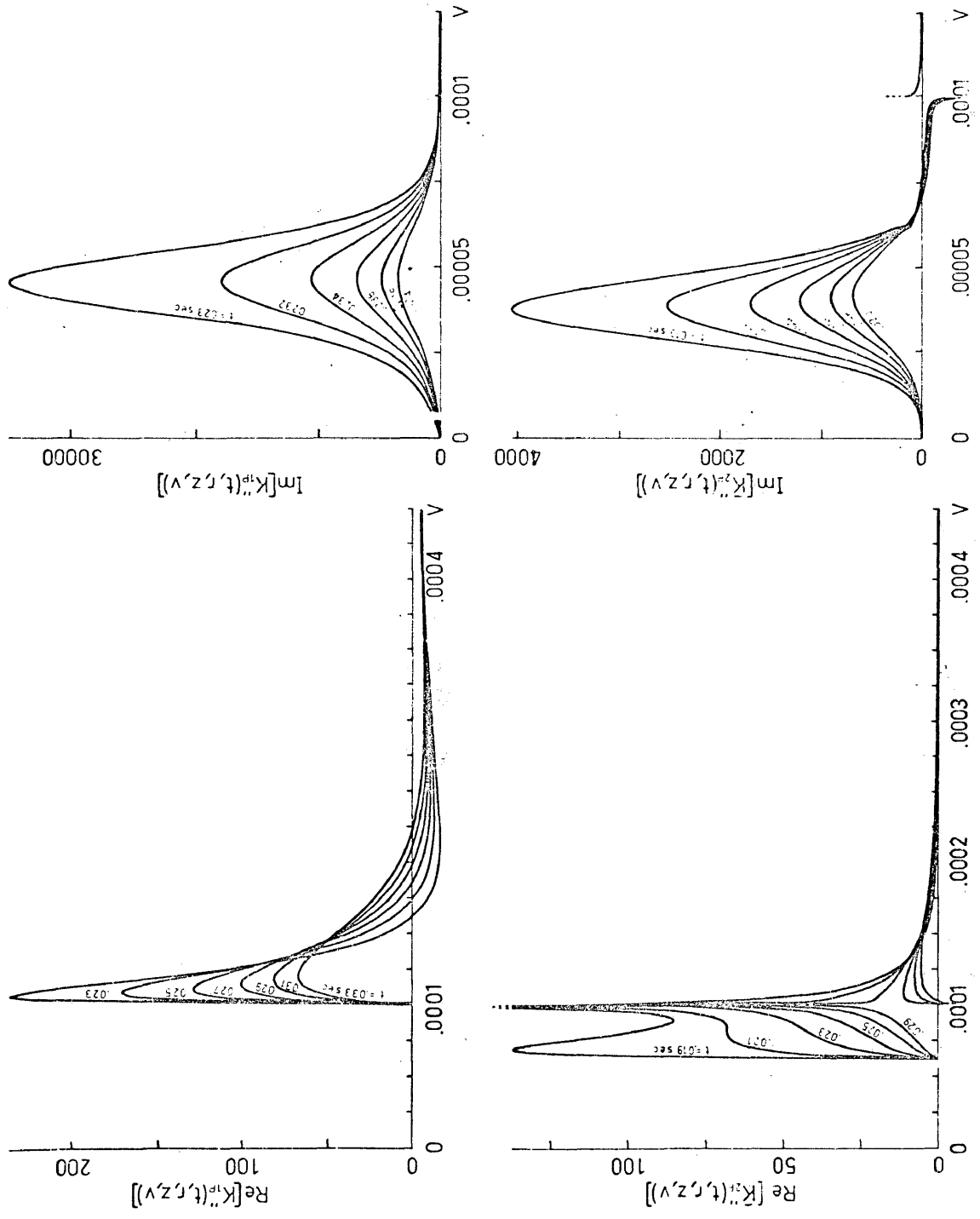


FIGURE 7. Real and imaginary parts of differentiated kernels $K''_{1p}(t,r,z,v)$ and $\bar{K}''_{2p}(t,r,z,v)$ for $r = h = \pm z = 100$ ft, $S_1 = .0001$ sec/ft, $S_2 = .0000625$ sec/ft. $t_{1p} = .02236$ sec, $t_{2p} = .01805$ sec.

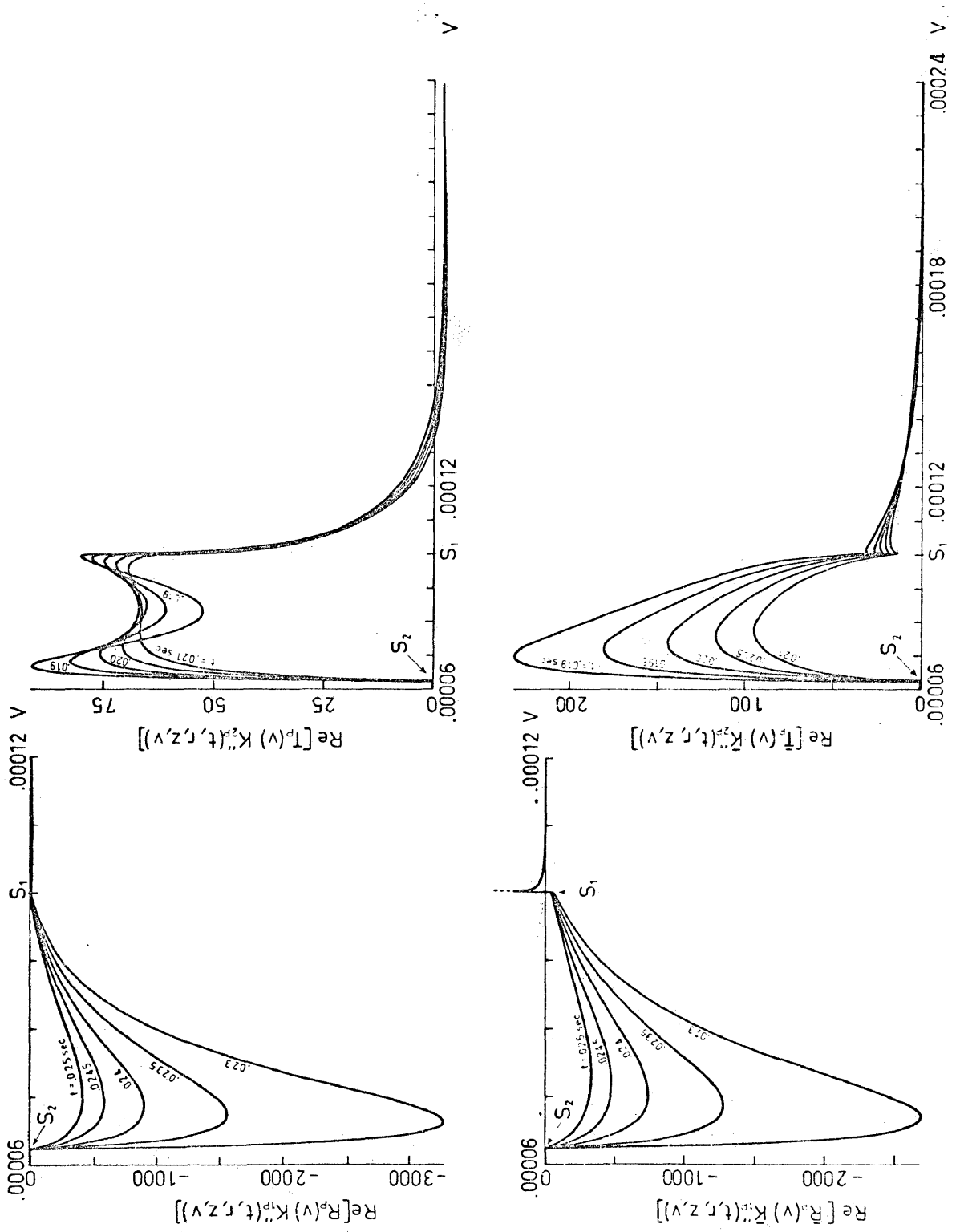


FIGURE 8. Real parts of all four $y''_{np}(t,r,z)$ and $\bar{y}''_{np}(t,r,z)$ integrands for a special solid-solid interface with $s_1 = s_2$, $\rho_1 = \rho_2$, $S_1 = .0001$ sec/ft, $S_2 = .0000625$ sec/ft. $r = h = \pm z = 100$ ft. Arrival times $t_{1p} = .02236$ sec, $t_{2p} = .01805$ sec.

The real part of the integrand associated with medium 2 is an indeterminant form at $v = S_1$, but nevertheless yields a finite value there. Note that the magnitude of the integrands decreases quite rapidly with increasing t.

Examples of $y''_{2P}$ and $\bar{y}''_{2P}$ are shown in Figure 9. These values were obtained using Romberg quadrature, an iterative nonadaptive scheme for evaluating integrals to prescribed accuracy (Davis and Rabinowitz, 1967). The important feature here is the bounded, smooth, and continuous nature of the functions, and the fact that they die out in a fraction of a millisecond. As the vertical distance from the interface increases, the amplitudes decrease and the functions become more step-like. Increasing r has the converse effect, as the next example will demonstrate.

Figure 10 shows the singlet and $y''_{1P}$ terms of $B_1$ (eq. 5) for several values of r. The spike at $t = t_{1P}$ represents the weighted singlet. The amplitude of the spike equals $y'_{1P}(t_{1P})/\Delta t$, where $\Delta t$ is the time increment between successive values of $y''_{1P}$. This makes a comparison of the two terms possible and illustrates the relative contribution of the weighted singlet and $y''_{1P}$ when convolved with f(t). A careful examination of Figure 10 will reveal that the amplitude of the spike increases as r increases. The $R^{-2}$ decrease in spike amplitude is compensated by $\mathrm{Re}[R_p(v_1)]$ as r increases. As h and z increase, however,

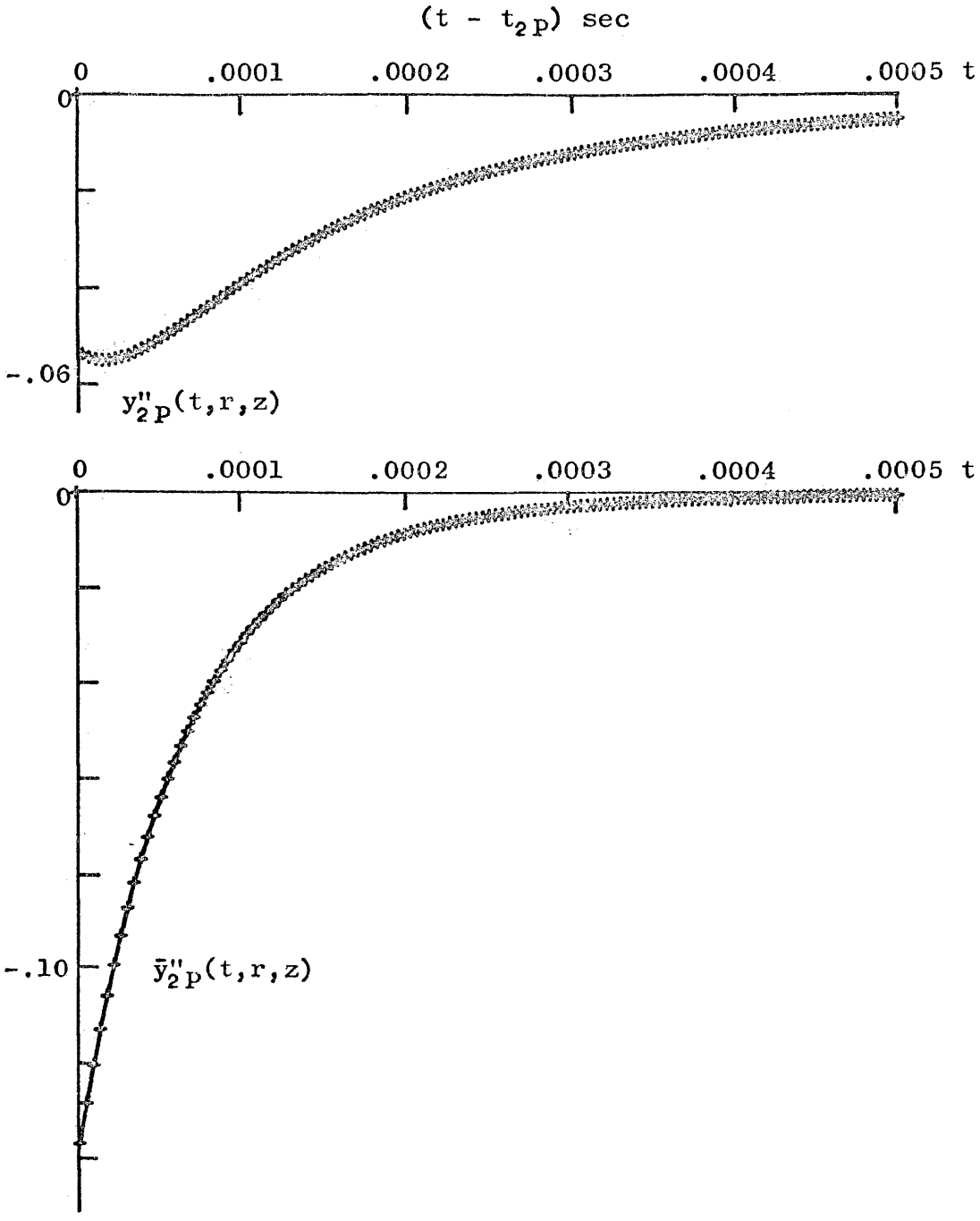


FIGURE 9. Examples of $y''_{2p}(t,r,z)$ and $\bar{y}''_{2p}(t,r,z)$ for a special solid-solid interface with $s_1 = s_2$, $\rho_1 = \rho_2$, $S_1 = .0001$ sec/ft, $S_2 = .0000625$ sec/ft. $r = 20$ ft, $h = -z = 25$ ft, $t_{2p} = .0043569$ sec.

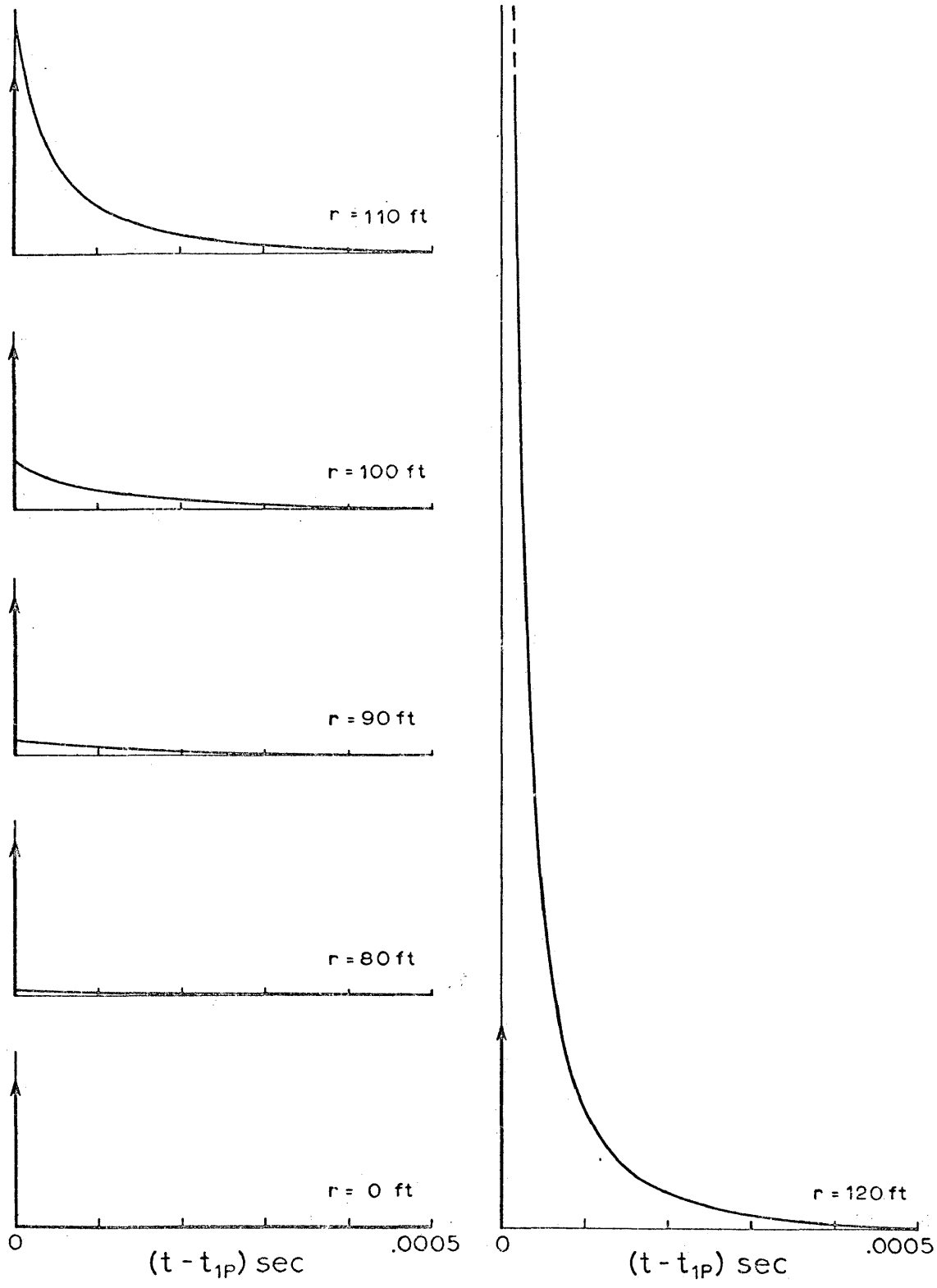


FIGURE 10. Variation of $y'_{1P}(t_{1P})\delta(t-t_{1P}) + y''_{1P}(t,r,z)\delta^{-1}(t-t_{1P})$ with r for a special solid-solid interface. $s_1 = s_2$, $\rho_1 = \rho_2$, $S_1 = .0001$ sec/ft, $S_2 = .0000625$ sec/ft. $h = z = 80$ ft, $r_c = 128$ ft.

both $R^{-2}$ and $Re[R_P(v_1)]$ decrease. Although the spike dominates well inside the critical cone, it becomes of lesser importance as r approaches $r_c$. This is an important feature of the boundary functions as will be seen in the examples of reflection and transmission waveforms which follow.

It is both convenient and logical to introduce the following notation:

$$h_{nP}(t,r,z) = -f(t) * y_{nP}(t_{nP})\delta'(t-t_{nP}) = -y_{nP}(t_{nP})f'(t-t_{nP})$$

$$q_{nP}(t,r,z) = -f(t) * \left[y'_{nP}(t_{nP})\delta(t-t_{nP}) + y''_{nP}(t,r,z)\delta^{-1}(t-t_{nP})\right]$$

An overbar is used for horizontal components. The units of $h_{nP}$ and $q_{nP}$ in the CGS system are $cm/(sec \cdot dynes/cm^2)$. When convolved with pressure ($dynes/cm^2$), the resulting expressions have units of displacement. Indeed, $h_{nP} + q_{nP}$ represent the reflection (n = 1) and transmission (n = 2) waveforms for a unit pressure impulse. It is altogether fitting, therefore, that $h_{nP}$ and $q_{nP}$ be called components of the appropriate waveforms. In the ensuing discussion, $h_{nP}$ will be called the "primary component" and $q_{nP}$ the "secondary component".

Examples of displacement waveforms and their components are shown in Figure 11. Note that both the magnitude and shape of the primary and secondary components differ quite substantially. Here, with relatively small h and z and with

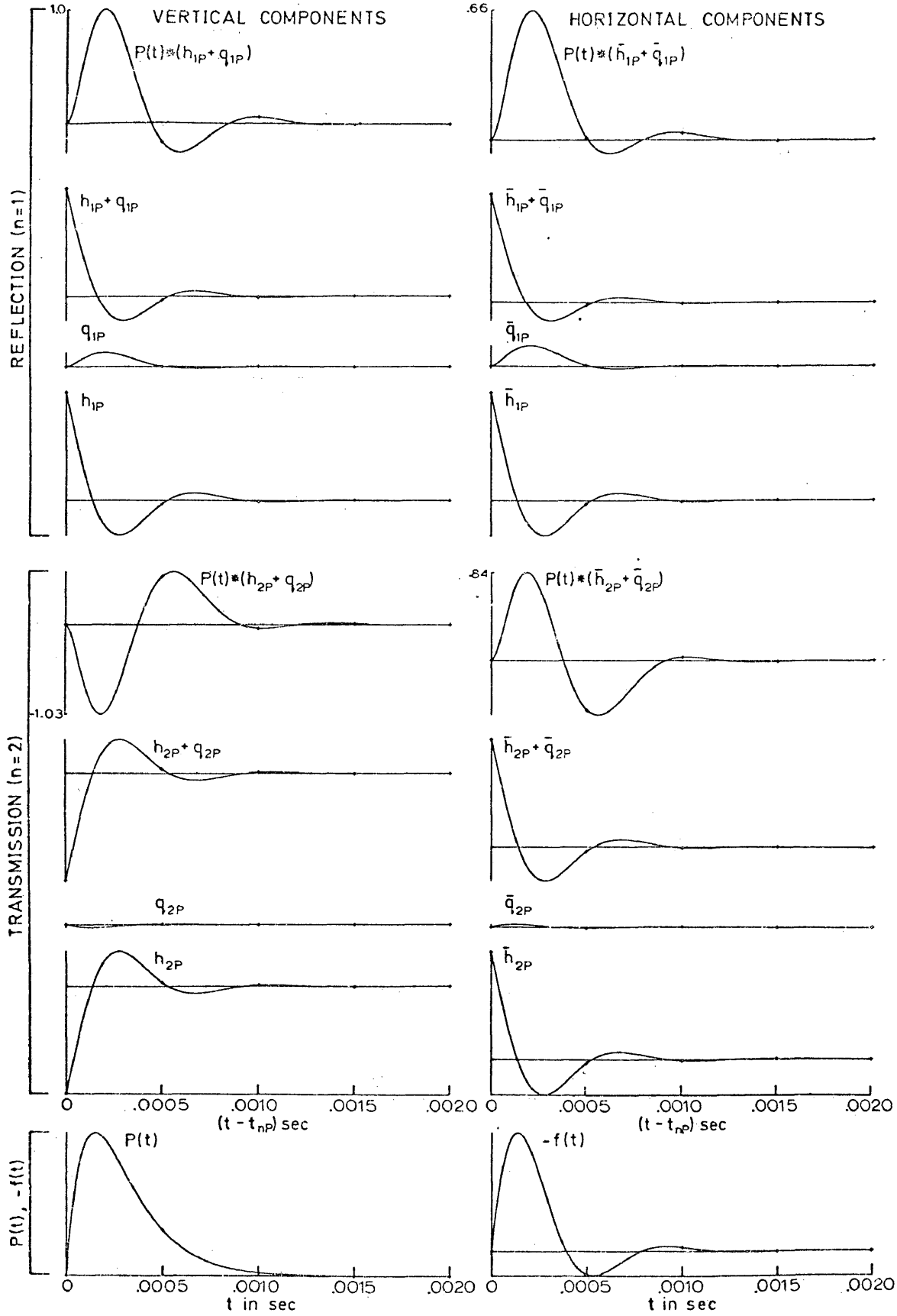


FIGURE 11. Displacement waveforms and their components for a special solid-solid interface with $s_1 = s_2 = .0002222$ sec/ft, $\rho_1 = \rho_2 = 2.4$ gm/cm$^3$, $S_1 = .0001$ sec/ft, $S_2 = .0000625$ sec/ft (Poisson's ratio for medium 1 is .373) $r_o = 1$ ft, $r = .25$ ft, $h = \pm z = 20$ ft, $t_{1P} = .004717$ sec, $t_{2P} = .003794$ sec.

$r = .78\ r_c$, the primary components dominate, especially for the transmitted pulses. Consequently, the complete reflection and transmission waveforms for a pressure impulse retain the essential features of the primary components. For $r \approx r_c$, this would have not been the case. The pulses labeled $P(t)*[h_{nP} + q_{nP}]$ and $P(t)*[\bar{h}_{nP} + \bar{q}_{nP}]$ illustrate the components of displacement for a pressure input P(t) over a spherical surface 2 ft in diameter. The P(t) used for this example was selected to simulate an explosive charge (Toksöz, Ben-Menahem, and Harkrider, 1964). The pressure has the form $P(t) = P_o t^{\mu} e^{-\eta t}$, where $\mu$ and $\eta$ are yield-dependent positive parameters which control the rise time and decay time.

It should be mentioned in passing that the short time duration (1.5-ms) of the various pulses shown in Figure 11 is a consequence of using a Poisson ratio of $\sigma_1 = .373$ and a source radius of $r_o = 1$ ft. Both $\sigma_1$ and $r_o$ have a pronounced effect on the source function. Increasing $\sigma_1$ makes f(t) more oscillatory and increases the time duration of significant amplitudes. Increasing $r_o$ also increases the time duration of significant amplitudes.

Changes in waveform due to increasing r are illustrated in Figure 12. Both f(t) and P(t) are as shown in Figure 11. The important feature of Figure 12 is the buildup of the secondary component as r increases to the critical

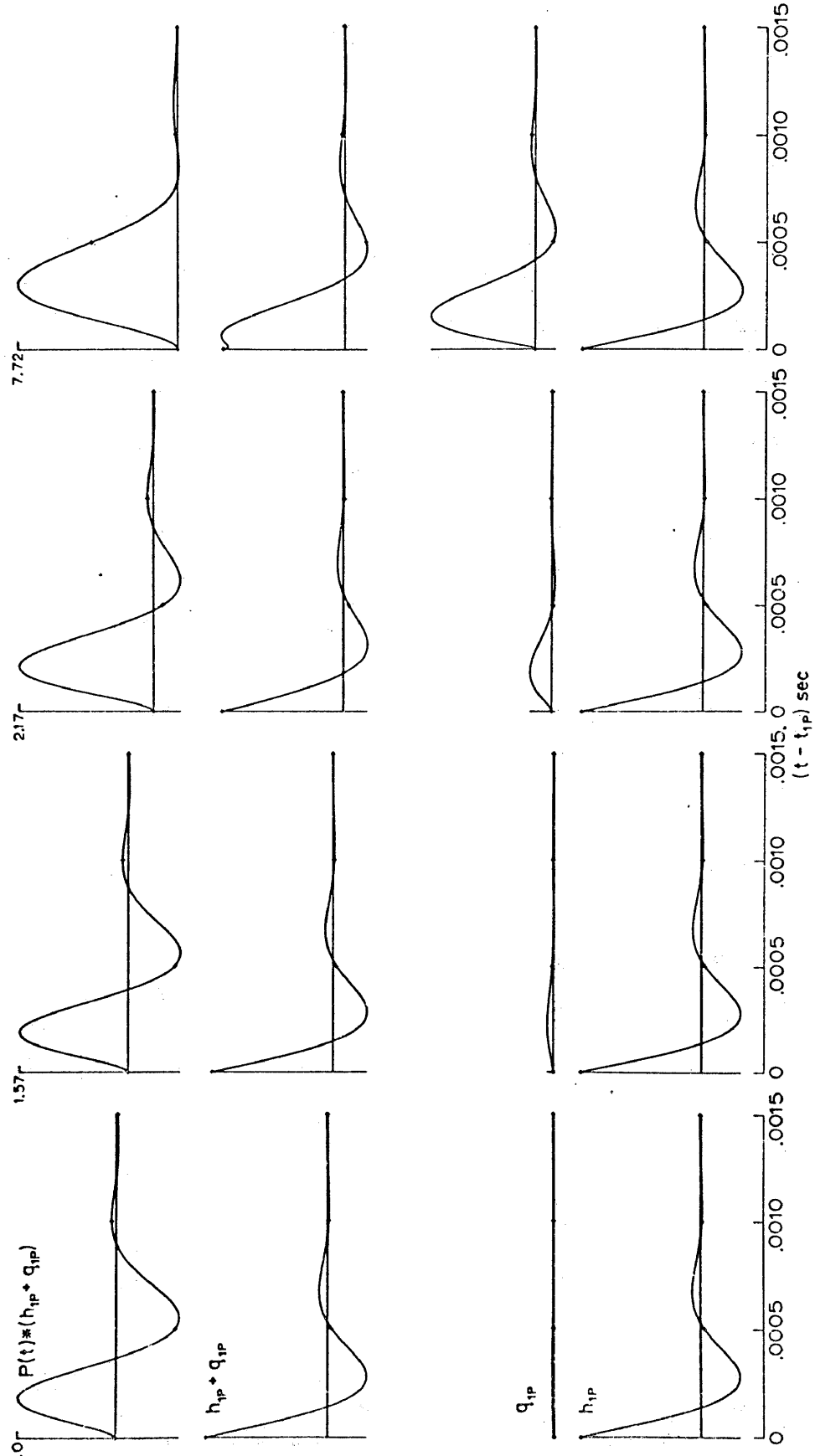


FIGURE 12. Variation of vertical component reflection waveforms (displacement) and their components with r for the special solid-solid interface, pressure P(t), and source function f(t) described in Figure 11. h = z = 80 ft.

distance, where its amplitude is seen to be quite pronounced. This increase in amplitude is attributed to the $y''_{1P}$ term, and not to the singlet term. Clearly, when the magnitude of h and z is less than about 80 $r_o$ and $r \approx r_c$, the secondary component can dominate the primary component. Usually, however, the secondary component is, as the name implies, subordinate to the primary component.

The final example includes the incident waveform (Fig. 13). The source is 1000 ft from the interface and the horizontal source-to-receiver distance r is 500 ft, which corresponds to .61 $r_c$, .59 $r_c$, and .57 $r_c$ for z = 25, 50, and 100 ft, respectively. The pressure has the same form as the previous examples with a peak at .001 sec and half-amplitude at .003 sec. Poisson's ratio and the source radius are .405 and 5 ft, respectively. The traces are aligned to the arrival time of the incident wave. On the bottom traces (z = 25 ft), the incident and reflection events overlap. These events are well separated on the top traces (z = 100 ft), however, and a waveform comparison can be made. A careful examination will reveal little, if any, difference in the shape of the incident and reflection waveforms other than amplitude. This implies that the secondary (near field) components are insignificant, leaving only the primary (far field) components.

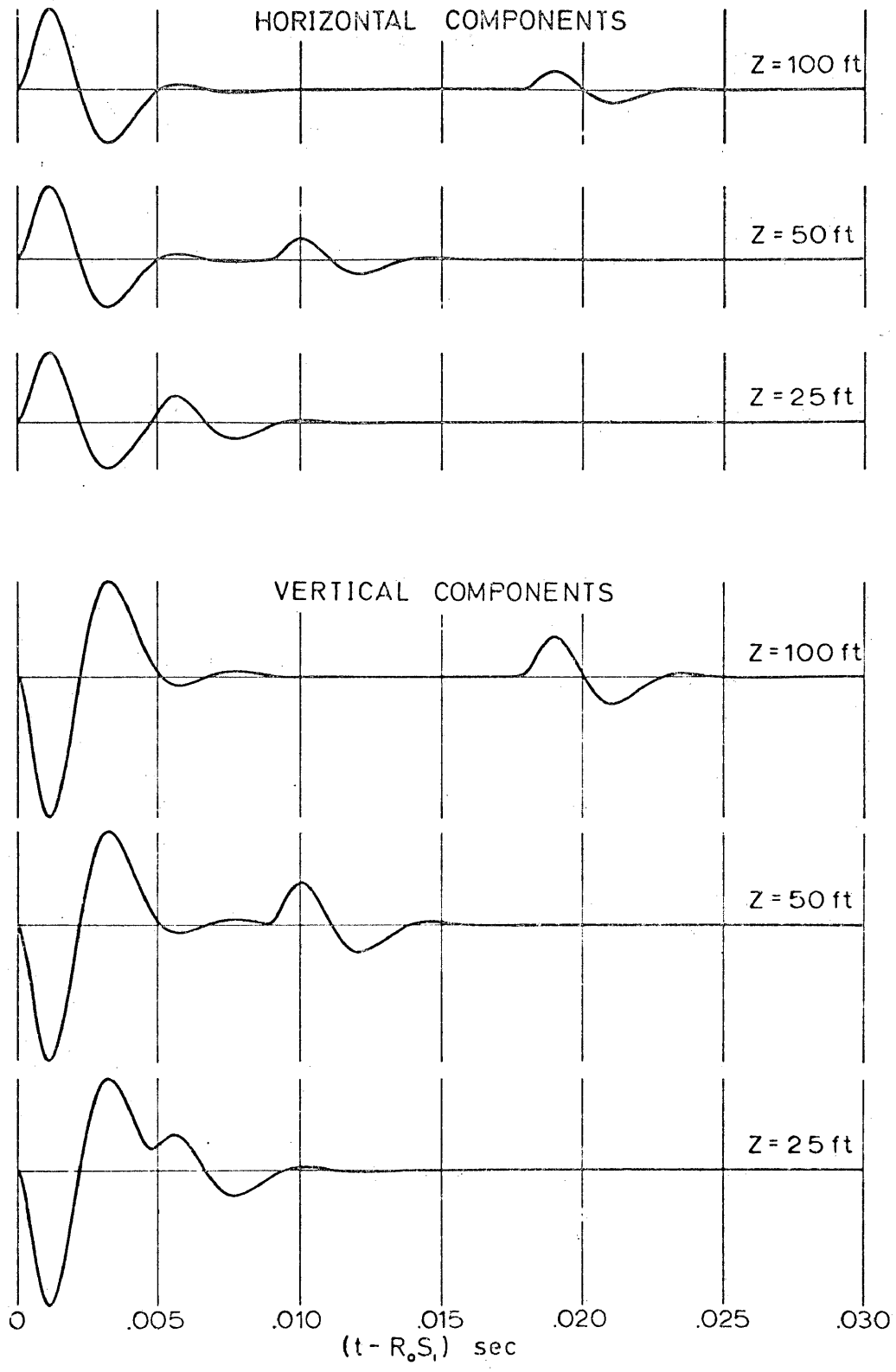


FIGURE 13. Simple synthetic seismograms $d_1(t,r,z)$ and $\overline{d}_1(t,r,z)$ for a special solid-solid interface with $s_1 = s_2 = .00025$ sec/ft, $\rho_1 = \rho_2 = .0000625$ sec/ft (Poisson's ratio for medium 1 is .405). $r_o = 5$ ft, $r = 500$ ft, $h = 1000$ ft, $z = 25$, 50, and 100 ft. P(t) peaks at .001 sec and is down -6 db at .003 sec. Traces are time aligned.

# CONCLUSIONS

Interpreting the integrals which account for the contribution from the interface in the domain of generalized functions gives reasonable results. The interpretation yields equations which fulfill the displacement boundary conditions and which are consistent with plane wave theory in the far field. Several noteworthy features of the solution are given below.

When the least time path associated with a particular ray is either a reflection or transmission path, and not a critical refraction path, the exact contribution from the interface consists of the sum of three terms. For a pressure impulse, these terms are the convolution of a source function with: (1) a weighted doublet; (2) a weighted singlet; and (3) an integral transform of an appropriate spherical reflection or transmission coefficient of the interface. The functional values of the first two terms are obtained from explicit expressions, whereas values of the third term

are obtained by numerical integration. The weight of the second term divided by the weight of the first term decreases in magnitude as $R^{-1}$ for reflections and $R_1^{-1}$ for transmissions. Hence the amplitude of the second term decreases faster than the first and is negligible in the far field.

Numerical examples for a solid-solid interface which does not generate shear waves indicate that the third term is negligible when the source and receiver are more than about 80 source radii from the interface. When this is the case, the reflection and transmission waveforms are the same as the incident waveform; only the relative amplitudes differ, as in plane wave theory. However, when the source and receiver are near the boundary and the receiver is near the edge of the critical cone, pronounced distortion of the waveform can result. A similar "rule of the thumb" has yet to be established for the general solid-solid interface.

The doublet weights of the primary component play the same role as the reflection and transmission coefficients for plane wave theory. For the case of spherical waves, the various weights depend on the angle of incidence, the relevant elastic parameters of the two media, and the raypath distances R for reflections and $R_1$ together with the ratios $(R_2/R_1)^3$, $(h/z)^2$, and $(r_1/r)^{\frac{1}{2}}$, for transmissions.

Of practical importance is the conclusion that for many purposes, the laws governing reflection and transmission of spherical compressional waves within the critical cone are as simple as those laws for plane waves. More elaborate mathematical models for wave propagation studies and synthetic seismogram synthesis using spherical sources are feasible because of this. These studies will provide a better understanding of principles which are fundamental to seismology.

# REFERENCES

Abramowitz, M., and Stegun, I.A., (ed.), 1964, Handbook of mathematical functions: Washington, U.S. Govt. Printing Office, Appl. Math. Ser. 55.

Bortfeld, R., 1962a, Exact solution of the reflection and refraction of arbitrary spherical compressional waves at liquid-liquid interfaces and at solid-solid interfaces with equal shear velocities and equal densities: Geophys. Prosp., v. 10, p. 35-67.

_____1962b, Reflection and refraction of spherical compressional waves at arbitrary plane interfaces: Geophys. Prosp., v. 10, p. 517-538.

Cagniard, L., 1962, Reflection and refraction of progressive seismic waves, translated by E.A. Flinn and C.H. Dix: New York, McGraw-Hill Book Co., Inc.

Davis, P.J., and Rabinowitz, P., 1967, Numerical integration: Waltham, Blaisdell Div., Ginn and Co.

Dix, C.H., 1954, The method of Cagniard in seismic pulse problems: Geophysics, v. 19, p. 722-738.

Longman, I.M., 1961, Solution of an integral equation occurring in the study of certain wave propagation problems in layered media: Jour. Acoustical Soc. America, v. 33, p. 954-958.

Love, A.E.H., 1944, The mathematical theory of elasticity, 4th ed.: New York, Dover Pub. Inc.

Morse, P.M., and Feshbach, H., 1953, Methods of theoretical physics, pt. I: New York, McGraw-Hill Book Co., Inc.

Pekeris, C.L., 1956, Solution of an integral equation occurring in impulsive wave propagation problems: U.S. Natl. Acad. Sci. Proc., v. 42, p. 439-443.

Sokolnikoff, I.S., 1956, Mathematical theory of elasticity: New York, McGraw-Hill Book Co., Inc.

Spencer, T.W., 1960, The method of generalized reflection and transmission coefficients: Geophysics, v. 25, p. 625-641.

Toksöz, M.N., Ben-Menahem, A., and Harkrider, D.G., 1964, Determination of source parameters of explosions and earthquakes by amplitude equalization of seismic surface waves. 1. underground nuclear explosions: Jour. Geophys. Research, v. 69, p. 4355-4365.

Watson, G.N., 1966, A treatise on the theory of Bessel functions: Cambridge, Cambridge Univ. Press.

# APPENDIX A

## LINEAR EQUATIONS AND THEIR SOLUTION FOR $A_R$, $B_R$, $A_T$, AND $B_T$

The functions $A_R(p,\lambda)$, $B_R(p,\lambda)$, $A_T(p,\lambda)$ and $B_T(p,\lambda)$ depend on the physical conditions imposed at the plane boundary $z = 0$. For a solid-solid with no slippage along the boundary, four conditions must be fulfilled:

1: Continuity of vertical displacement

2: Continuity of horizontal displacement

3: Continuity of normal stresses

4: Continuity of tangential stresses

These four conditions are expressed in terms of the transformed potentials by the following equations (Cagniard, 1962, p. 3):

1: $(\Phi_1)_z + (U_1/r)_r = (\Phi_2)_z + (U_2/r)_r$

2: $(\Phi_1)_r - (U_1)_z = (\Phi_2)_r - (U_2)_z$

3: $\rho_1 \left[e_1 p^2 \Phi_1 + \hat{e}_1[(\Phi_1)_{zz} + (U_1)_{rz} + r^{-1}(U_1)_z]\right]$

$= \rho_2 \left[e_2 p^2 \Phi_2 + \hat{e}_2[(\Phi_2)_{zz} + (U_2)_{rz} + r^{-1}(U_2)_z]\right]$

$$4: \quad \rho_1 \left[p^2 U_1 + \hat{e}_1[(\Phi_1)_{rz} - (U_1)_{zz}]\right]$$

$$= \rho_2 \left[p^2 U_2 + \hat{e}_2[(\Phi_2)_{rz} - (U_2)_{zz}]\right] \qquad \text{(A-1)}$$

where

$$(\Phi_n)_z = \frac{\partial \Phi n}{\partial z} \quad ; \quad (U_n)_{rz} = \frac{\partial^2 U_n}{\partial r \partial z} \quad ; \quad \text{etc.}$$

$$e_n = 1 - 2S_n^2/s_n^2 \; ; \quad \hat{e}_n = 2/s_n^2 \; ; \; n = 1, 2$$

Substitution of the appropriate integral expressions for the potentials into equations (A-1) yields the following system of linear algebraic equations:

$$1: \; \alpha_1 A_R - \lambda B_R + \alpha_2 A_T + \lambda B_T = \alpha_1 A e^{-\alpha_1 h}$$

$$2: \; \lambda A_R - \beta_1 B_R - \lambda A_T - \beta_2 B_T = -\lambda A e^{-\alpha_1 h}$$

$$3: \; L_1 A_R - N_1 B_R - L_2 A_T - N_2 B_T = -L_1 A e^{-\alpha_1 h}$$

$$4: \; M_1 A_R - L_1 B_R + M_2 A_T + L_2 B_T = M_1 A e^{-\alpha_1 h} \qquad \text{(A-2)}$$

where

$$L_n = \rho_n(\lambda^2/s_n^2 + p^2/2)$$

$$M_n = \rho_n \lambda \alpha_n / s_n^2$$

$$N_n = \rho_n \lambda \beta_n / s_n^2$$

$$A = A(p,\lambda) = \alpha_1^{-1} \tilde{P}(p) F(p)$$

Solving equations (A-2) gives the required functions:

$$A_R(p,\lambda) = \frac{Q_1(p,\lambda)}{D(p,\lambda)} A(\rho,\lambda)e^{-\alpha_1 h}$$

$$B_R(p,\lambda) = \frac{Q_2(p,\lambda)}{D(p,\lambda)} \lambda\alpha_1 A(p,\lambda)e^{-\alpha_1 h}$$

$$A_T(p,\lambda) = \frac{Q_3(p,\lambda)}{D(p,\lambda)} \alpha_1 A(p,\lambda)e^{-\alpha_1 h}$$

$$B_T(p,\lambda) = \frac{Q_4(p,\lambda)}{D(p,\lambda)} \lambda\alpha_1 A(p,\lambda)e^{-\alpha_1 h} \qquad \text{(A-3)}$$

where

$$\begin{aligned} D(p,\lambda) = {} & \lambda^2(\lambda^2 + p^2E_1s_1^2 + p^2E_2s_2^2)^2 \\ & + \lambda^2\alpha_1\alpha_2\beta_1\beta_2 - \alpha_1\beta_1(\lambda^2 + p^2E_2s_2^2)^2 \\ & - \alpha_2\beta_2(\lambda^2 + p^2E_1s_1^2)^2 \\ & + p^4E_1E_2s_1^2s_2^2(\alpha_1\beta_2 + \alpha_2\beta_1) \end{aligned}$$

$$\begin{aligned} Q_1(p,\lambda) = {} & -\lambda^2(\lambda^2 + p^2E_1s_1^2 + p^2E_2s_2^2)^2 \\ & + \lambda^2\alpha_1\alpha_2\beta_1\beta_2 - \alpha_1\beta_1(\lambda^2 + p^2E_2s_2^2)^2 \\ & + \alpha_2\beta_2(\lambda^2 + p^2E_1s_1^2)^2 \\ & + p^4E_1E_2s_1^2s_2^2(\alpha_1\beta_2 - \alpha_2\beta_1) \end{aligned}$$

$$Q_2(p,\lambda) = 2[\alpha_2\beta_2(\lambda^2 + p^2E_1s_1^2) - (\lambda^2 + p^2E_1s_1^2 + p^2E_2s_2^2)(\lambda^2 + p^2E_2s_2^2)]$$

$$Q_3(p,\lambda) = 2p^2E_1s_1^2[\beta_1(\lambda^2 + p^2E_2s_2^2) - \beta_2(\lambda^2 + p^2E_1s_1^2)]$$

$$Q_4(p,\lambda) = 2p^2E_1s_1^2[\lambda^2 + p^2E_1s_1^2 + p^2E_2s_2^2) - \alpha_2\beta_2]$$

$$E_1 = [2(1 - \rho_2s_1^2/\rho_1s_2^2)]^{-1};\ E_2 = [2(1 - \rho_1s_2^2/\rho_2s_1^2)]^{-1}$$

$$\alpha_n = [\lambda^2 + p^2S_n^2]^{\frac{1}{2}};\quad \beta_n = [\lambda^2 + p^2s_n^2]^{\frac{1}{2}}$$

$$n = 1,\ 2$$

Special Solid-Solid Interface

A special solid-solid is defined for $s_1 = s_2$ and $\rho_1 = \rho_2$. With $\beta_1 = \beta_2$, $L_1 = L_2$, and $N_1 = N_2$, equations (A-2) simplify to

$$1:\ \alpha_1A_R - \lambda B_R + \alpha_2A_T + \lambda B_T = \alpha_1Ae^{-\alpha_1h}$$

$$2:\ \lambda A_R - \beta_1B_R - \lambda A_T - \beta_1B_T = -\lambda Ae^{-\alpha_1h}$$

$$3:\ \epsilon A_R - \lambda\beta_1B_R - \epsilon A_T - \lambda\beta_1B_T = -\epsilon Ae^{-\alpha_1h}$$

$$4:\ \lambda\alpha_1A_R - \epsilon B_R + \lambda\alpha_2A_T + \epsilon B_T = \lambda\alpha_1Ae^{-\alpha_1h} \qquad \text{(A-4)}$$

where

$$\epsilon = \lambda^2 + p^2s_1^2/2$$

Multiplying expression (1:) by $-\lambda$ and adding to expression (4:) gives $B_R = -B_T$. Multiplying expression (2:) by $\epsilon$ and

adding to $-\lambda$ times expression (3:) gives the same result. Equations (A-4) are therefore equivalent to

$$\alpha_1 A_R + \alpha_2 A_T + 2\lambda B_T = \alpha_1 A e^{-\alpha_1 h}$$

$$\lambda\alpha_1 A_R + \lambda\alpha_2 A_T + 2\varepsilon B_T = \lambda\alpha_1 A e^{-\alpha_1 h}$$

Multiplying the first by $-\lambda$ and adding to the second gives

$$(p^2 s_1^2) B_T = 0$$

which must be valid for all p. Thus, $B_R = B_T = 0$ and the 4 x 4 system of linear equations reduces to the following 2 x 2 system

$$\alpha_1 A_R + \alpha_2 A_T = \alpha_1 A e^{-\alpha_1 h}$$

$$A_R - A_T = - A e^{-\alpha_1 h} \qquad \text{(A-5)}$$

Solving equations (A-5) gives the required functions:

$$A_R(p,\lambda) = \frac{\alpha_1 - \alpha_2}{\alpha_1 + \alpha_2} A(p,\lambda) e^{-\alpha_1 h}$$

$$A_T(p,\lambda) = \frac{2\alpha_1}{\alpha_1 + \alpha_2} A(p,\lambda) e^{-\alpha_1 h}$$

# APPENDIX B

## DERIVATION OF THE KERNELS $K_{nP}(t,r,z,v)$, $\overline{K}_{nP}(t,r,z,v)$, AND THEIR DERIVATIVES

The kernels are based on the analytic continuation of the integral

$$\int_0^\infty e^{-bx} J_o(ax)dx = + [a^2 + b^2]^{-\frac{1}{2}}; \; b \geq 0 \qquad \text{(B-1)}$$

established by Lipschitz in 1859 (Watson, 1966, p. 384). Here, a, b, and c are real variables[1]. The integral

$$I(\beta) = \int_0^\infty e^{-\beta x} J_o(ax)\, dx$$

is an analytic function of the complex variable $\beta = b + ic$ in the domain of its existence, namely, $Re(\beta) = b \geq 0$.

The radical

$$W = \sqrt{Z}$$

where

$$Z = a^2 + \beta^2$$

---

1/ The notation applies only to this appendix.

can be made an analytic function of $\beta$ by placing a cut slightly to the left of the imaginary $\beta$-axis between the branch points $\pm ia$. W is defined on a sheet of the Riemann surface for which points on the positive real $\beta$-axis map onto the positive real W-axis. On this surface, points on the positive imaginary $\beta$-axis map onto the positive real W-axis for $0 < c < a$, and onto the positive imaginary W-axis for $c > a$. Moreover, points on the negative imaginary $\beta$-axis map onto the positive real W-axis for $-a < c < 0$, and onto the negative imaginary W-axis for $c < -a$.

Since a function that is analytic in a domain D is uniquely determined throughout D by its values along a curve or a domain interior to D, it follows from the analytic continuation of equation (B-1) that

$$I(\beta) = \begin{cases} (a^2 + \beta^2)^{-\frac{1}{2}} \; ; \; b > 0 \\ (a^2 - c^2)^{-\frac{1}{2}} \; ; \; a^2 > c^2, \; b=0 \\ -i \operatorname{sgn} c \; (c^2 - a^2)^{-\frac{1}{2}} \; ; \; a^2 < c^2, \; b=0 \end{cases} \quad \text{(B-2)}$$

Equations (B-2) may be interpreted in terms of a branch cut in the Z-plane. The domain $b > 0$ of the $\beta$-plane maps onto the entire Z-plane except the negative real axis. Consequently, if one is to use $I[\beta(Z)] = Z^{-\frac{1}{2}}$, the branch cut of $Z^{-\frac{1}{2}}$ must be on the negative real Z-axis. To include $b = 0$ in the definition of the Z-plane branch cut, one must

visualize the cut slightly below or slightly above the negative real Z-axis for positive and negative values of c, respectively.

Corresponding integrals involving $J_1(ax)$ may be evaluated from equation (B-2). The following substitutions are made

$$u = J_o(ax); \quad du = -aJ_1(ax)\, dx$$

$$dv = e^{-\beta x}\, dx; \quad v = -\beta^{-1}e^{-\beta x}$$

Integration by parts gives

$$\int_o^\infty e^{-\beta x}J_o(ax)\,dx = -\beta^{-1}e^{-\beta x}J_o(ax)\Big|_{x=o}^{\infty} - a\beta^{-1}\int_o^\infty e^{-\beta x}J_1(ax)\,dx$$

$$= \beta^{-1}\left[1 - a\int_o^\infty e^{-\beta x}J_1(ax)\,dx\right].$$

Rearranging terms gives the result

$$\int_o^\infty e^{-\beta x}J_1(ax)\,dx = a^{-1}\left[1 - \beta\int_o^\infty e^{-\beta x}J_o(ax)\,dx\right]$$

$$= a^{-1}\left[1 - \beta(a^2 + \beta^2)^{-\frac{1}{2}}\right]; \quad b > 0 \qquad \text{(B-3)}$$

When b = 0, the integral becomes

$$\int_o^\infty e^{icx}\, J_1(ax)\,dx = \begin{cases} a^{-1}\left[1 - ic(a^2 - c^2)^{-\frac{1}{2}}\right]; & a^2 > c^2 \\ a^{-1}\left[1 - |c|(c^2 - a^2)^{-\frac{1}{2}}\right]; & a^2 < c^2 \end{cases} \qquad \text{(B-4)}$$

The integrals defining the kernels, namely

$$K_{nP}(t,r,z,v) = v\int_0^\infty e^{-\omega\tau_{nP}} J_o(rv\omega)\,d\omega$$

$$\overline{K}_{nP}(t,r,z,v) = \frac{v^2}{a_1}\int_0^\infty e^{-\omega\tau_{nP}} J_1(rv\omega)\,d\omega \qquad \text{(B-5)}$$

are readily evaluated using equations (B-2), (B-3), and (B-4). With the notation

$$\hat{\tau}_{nP} = Im(\tau_{nP})$$

$$Z_{nP} = r^2v^2 + \tau_{nP}^2$$

$$\hat{Z}_{nP} = r^2v^2 - \hat{\tau}_{nP}^2$$

the following results are obtained from equations (B-5):

$$K_{nP}(t,r,z,v) = \begin{cases} vZ_{nP}^{-\frac{1}{2}} ; & Re(\tau_{nP}) > 0 \\ -iv\,sgn\hat{\tau}_{nP}(-\hat{Z}_{nP})^{-\frac{1}{2}} ; & Re(\tau_{nP}) = 0,\ \hat{Z}_{nP} < 0 \\ v\hat{Z}_{nP}^{-\frac{1}{2}} ; & Re(\tau_{nP}) = 0,\ \hat{Z}_{nP} > 0 \end{cases} \qquad \text{(B-6)}$$

$$\overline{K}_{nP}(t,r,z,v) = \begin{cases} \frac{v}{ra_1}\left[1 - \tau_{nP}Z_{nP}^{-\frac{1}{2}}\right] ; & Re(\tau_{nP}) > 0 \\ \frac{v}{ra_1}\left[1 - |\hat{\tau}_{nP}|(-\hat{Z}_{nP})^{-\frac{1}{2}}\right] ; & Re(\tau_{nP}) = 0,\ \hat{Z}_{nP} < 0 \\ \frac{v}{ra_1}\left[1 - i\hat{\tau}_{nP}\hat{Z}_{nP}^{-\frac{1}{2}}\right] ; & Re(\tau_{nP}) = 0,\ \hat{Z}_{nP} > 0 \end{cases} \qquad \text{(B-7)}$$

Corresponding shear component kernels are obtained in a similar manner.

The first two derivatives of the kernels with respect to t are given below.

$$K'_{nP}(t,r,z,v) = \begin{cases} iv\tau_{nP}Z_{nP}^{-3/2}; & \mathrm{Re}(\tau_{nP}) > 0 \\ -iv|\hat{\tau}_{nP}|(-\hat{Z}_{nP})^{-3/2}; & \mathrm{Re}(\tau_{nP}) = 0,\ \hat{Z}_{nP} < 0 \\ -v\hat{\tau}_{nP}\hat{Z}_{nP}^{-3/2}; & \mathrm{Re}(\tau_{nP}) = 0,\ \hat{Z}_{nP} > 0 \end{cases} \tag{B-8}$$

$$\bar{K}'_{nP}(t,r,z,v) = \begin{cases} irv^3/[a_1 Z_{nP}^{3/2}]; & \mathrm{Re}(\tau_{nP}) > 0 \\ -rv^3 \mathrm{sgn}\hat{\tau}_{nP}/[a_1(-\hat{Z}_{nP})^{3/2}]; & \mathrm{Re}(\tau_{nP}) = 0,\ \hat{Z}_{nP} < 0 \\ -rv^3/[a_1\hat{Z}_{nP}^{3/2}]; & \mathrm{Re}(\tau_{nP}) = 0,\ \hat{Z}_{nP} > 0 \end{cases} \tag{B-9}$$

$$K''_{nP}(t,r,z,v) = \begin{cases} v(r^2v^2 - 2\tau_{nP}^2)Z_{nP}^{-5/2}; & \mathrm{Re}(\tau_{nP}) > 0 \\ -iv\mathrm{sgn}\hat{\tau}_{nP}(r^2v^2 + 2\hat{\tau}_{nP}^2)(-\hat{Z}_{nP})^{-5/2}; & \mathrm{Re}(\tau_{nP}) = 0,\ \hat{Z}_{nP} < 0 \\ v(r^2v^2 + 2\hat{\tau}_{nP}^2)Z_{nP}^{-5/2}; & \mathrm{Re}(\tau_{nP}) = 0,\ \hat{Z}_{nP} > 0 \end{cases} \tag{B-10}$$

$$\overline{K}''_{nP}(t,r,z,v) = \begin{cases} -3rv^3\tau_{nP}/[a_1 Z_{nP}^{5/2}]; & \mathrm{Re}(\tau_{nP}) > 0 \\ -3rv^3\,|\hat{\tau}_{nP}|/[a_1(-\hat{Z}_{nP})^{5/2}]; & \mathrm{Re}(\tau_{nP}) = 0,\ \hat{Z}_{nP} < 0 \\ -i3rv^3\hat{\tau}_{nP}/[a_1\hat{Z}_{nP}^{5/2}]; & \mathrm{Re}(\tau_{nP}) = 0,\ \hat{Z}_{nP} > 0 \end{cases} \tag{B-11}$$

# APPENDIX C

## ZEROS OF $Z_{1P}$, $Z_{2P}$, $Z_{1S}$, AND $Z_{2S}$

Zeros of the function $Z_{nP}$ and $Z_{nS}$ (n=1,2) are obtained by solving the equation

$$rv \pm i\tau = 0 \qquad \text{(C-1)}$$

for v. Here, $\tau$ represents a particular $\tau_{nP}$ or $\tau_{nS}$ associated with $Z_{nP}$ or $Z_{nS}$, respectively. When $\tau = \tau_{1P}$, the solution of equation (C-1) is straightforward because only one radical is involved. The other three cases are considerably more difficult because two radicals are involved instead of one. The two classes of solution are discussed below.

### CLASS 1: $\tau = \tau_{1P}$

The equation to be solved is given by

$$rv \pm i\,[v^2 - S_1^2]^{\frac{1}{2}}\,(z+h) \pm t = 0 \qquad \text{(C-2)}$$

Transposing $rv \pm t$ and squaring both sides of equation (C-2) gives

$$(rv \pm t)^2 = -(v^2 - S_1^2)(z+h)^2$$

or

$$[r^2 + (z+h)^2]\,v^2 \pm (2rt)v - [S_1^2(z+h)^2 - t^2] = 0$$

The four roots of the above quadratics are given by

$$v = R^{-2}[\pm rt \mp (z+h)[t_{1P}^2 - t^2]^{\frac{1}{2}}]$$

where

$$R = [r^2 + (z+h)^2]^{\frac{1}{2}}; \quad t_{1P} = RS_1$$

CLASS 2: $\tau = \tau_{2P}$, $\tau_{1S}$, or $\tau_{2S}$

Let $\eta$ represent a particular $S_2$, $s_1$, or $s_2$ associated with $\tau_{2P}$, $\tau_{1S}$, or $\tau_{2S}$, respectively. The equation to be solved is given by

$$rv \pm i[h(v^2-S_1^2)^{\frac{1}{2}} + |z|(v^2-\eta^2)^{\frac{1}{2}}] \pm t = 0 \qquad \text{(C-3)}$$

One approach to find the roots of equation (C-3) is to express the equation as two quartics, and represent each quartic as the product of two quadratics. Four extraneous roots are introduced by such a procedure. Consequently, the eight possible roots must be substituted back into equation (C-3) to establish which are valid. To proceed with the objective of representing equation (C-3) in terms of quartics, the equation is rewritten in the form

$$(rv\pm t)^2 = -[h^2(v^2-S_1^2) + z^2(v^2-\eta^2) - 2h|z|(v^2-S_1^2)^{\frac{1}{2}}(v^2-\eta^2)^{\frac{1}{2}}]$$

or

$$A_1v^2 \pm A_2v + A_3 = 2h|z|(v^2-S_1^2)^{\frac{1}{2}}(v^2-\eta^2)^{\frac{1}{2}} \qquad \text{(C-4)}$$

where

$$A_1 = r^2 + h^2 + z^2$$

$$A_2 = 2rt$$

$$A_3 = h^2 S_1^2 + z^2 \eta^2 - t^2$$

Squaring both sides of equation (C-4) and rearranging terms gives

$$(A_1^2 - 4h^2z^2)v^4 \pm (2A_1A_2)v^3$$

$$+ [A_2^2 - 2A_1A_3 + 4h^2z^2(S_1^2 + \eta^2)]v^2$$

$$\mp (2A_2A_3)v + [A_3^2 - 4h^2z^2S_1^2\eta^2] = 0$$

The resulting quartics are given by[1]

$$v^4 \pm av^3 + bv^2 \pm cv + d = 0 \qquad \text{(C-5)}$$

where

$$a = D^{-1}[4rt(r^2 + h^2 + z^2)]$$

$$b = 2D^{-1}[r^2(3t^2 - h^2S_1^2 - z^2\eta^2) + h^2z^2(S_1^2+\eta^2) + h^2(t^2-h^2S_1^2) + z^2(t^2-z^2\eta^2)]$$

$$c = -D^{-1}[4rt(h^2S_1^2 + z^2\eta^2 - t^2)]$$

---

1/ Some of the notation applies only to this appendix.

$$d = D^{-1}[h^4 S_1^4 + z^4 \eta^4 + t^4 - 2h^2 z^2 S_1^2 \eta^2$$

$$-2h^2 S_1^2 t^2 - 2z^2 \eta^2 t^2]$$

$$D = (r^2 + h^2 + z^2)^2 - 4h^2 z^2$$

When $t = 0$ and/or $r = 0$ and $|z| \neq h$, the quartics reduce to the form

$$v^4 + bv^2 + d = 0 \qquad \text{(C-6)}$$

When $t \neq 0$, $r = 0$ and $|z| = h \neq 0$, the quartics reduce to the simple quadratic form

$$v^2 - e = 0 \qquad \text{(C-7)}$$

where

$$e = (2ht)^{-2}[2h^2 \left[h^2 S_1^2 \eta^2 + t^2 (S_1^2 + \eta^2)\right] - h^4 (S_1^4 + \eta^4) - t^4]$$

Various algorithms exist for extracting the roots of quartic equations. One such algorithm may be found on page 17 of the Handbook of Mathematical Functions (Abramowitz and Stegun, 1964), but sufficient detail is lacking to warrant further discussion.

A procedure commonly used to find the roots of a quartic is outlined below. The quartic is written in the form

$$X = Y$$

A quantity N is added to each side such that

$$X + N = P^2.$$

With

$$P^2 = Y + N,$$

a quantity M is added to each side making $P^2 + M$ a perfect square and rendering $Y + N + M$ a perfect square when its discriminant is zero. Thus with the appropriate M

$$P^2 + M = O^2$$

$$Y + N + M = Q^2$$

and the quartic is represented as

$$X - Y = O^2 - Q^2 = (O-Q)(O+Q) = 0$$

The details of the foregoing procedure are given below.

Equation (C-5) is written in the equivalent form

$$v^4 \pm av^3 = - bv^2 \mp cv - d$$

and the quantity $a^2v^2/4$ is added. This gives the equation

$$(v \pm av/2)^2 = (\pm a^2/4 - b)v^2 \mp cv - d \qquad (C-8)$$

Adding a term in an arbitrary variable u to both sides gives

$$(v^2 \pm av/2)^2 + u(v^2 \pm av/2) + u^2/4 =$$

$$(u + a^2/4 - b)v^2 + (\pm ua/2 \mp c)v + (u^2/4 - d)$$

Since the left member of the last equation is a perfect square, the quartic becomes

$$(v^2 \pm av/2 + u/2)^2 = (u + a^2/4 - b)v^2$$

$$+ (\pm ua/2 \mp c)v + (u^2/4 - d) \qquad (C-9)$$

The right member of equation (C-9) is a perfect square provided u is so determined that its discriminant is zero; that is, provided

$$(\pm\, ua/2 \mp c)^2 - 4(u + a^2/4 - b)(u^2/4 - d) = 0$$

or

$$u^3 - bu^2 + (ac - 4d)u - (c^2 + a^2d - 4bd) = 0 \qquad \text{(C-10)}$$

Let $u_1$ denote a real root of equation (C-10). When all roots of the cubic are real, a value of $u_1$ must be used which renders

$$u_1 + a^2/4 > b$$
$$u_1/4 > d \qquad \text{(C-11)}$$

If the root $u_1$ is substituted into equation (C-9), the right member will be a perfect square of the form

$$g^2v^2 \pm 2ghv + h^2 = (\pm\, gv \not\lessgtr h)^2$$

where the $\not\lessgtr$ sign represents either $\pm$ or $\mp$, whichever is appropriate. Hence, equation (C-8) can be written as

$$[v^2 \pm \tfrac{1}{2}av + \tfrac{1}{2}u_1]^2 = [\pm(u_1 + a^2/4 - b)^{\frac{1}{2}}\, v \not\lessgtr (u_1^2/4 - d)^{\frac{1}{2}}]^2$$

Extracting the square root gives

$$(v^2 \pm \tfrac{1}{2}av + \tfrac{1}{2}u_1) = \pm\, [u_1 + a^2/4 - b]^{\frac{1}{2}}\, v \not\lessgtr (u^2/4 - d)^{\frac{1}{2}}$$

or

$$v^2 + [\pm\tfrac{1}{2}a \mp (u_1 + a^2/4 - b)^{\frac{1}{2}}]v + \tfrac{1}{2}u_1 \not\lessgtr (u_1^2/4 - d) = 0 \qquad \text{(C-12)}$$

Finally,

$$v^4 + av^3 + bv^2 + cv + d$$

$$= (v^2 + B_1 v + C_1)(v^2 + B_2 v + C_2) = 0$$

and similarly for the other quartic.

The relationship between $B_1$, $B_2$, $C_1$, and $C_2$ and the original coefficients of the quartic a, b, c, and d is very important. It can be shown that for the coefficients of the quadratics to be correct:

$$\begin{aligned} B_1 + B_2 &= a \\ B_1 B_2 + C_1 + C_2 &= b \\ B_1 C_2 + B_2 C_1 &= c \\ C_1 C_2 &= d \end{aligned} \qquad \text{(C-13)}$$

Expressions (C-11) and (C-13) define two constraints which must be imposed on the foregoing algorithm for extracting the roots of a quartic. Equations (C-11) is a necessary, but not sufficient condition to assure correct roots. Equation (C-13), on the other hand, is a necessary and sufficient condition to assure correct roots. Seldom, if ever, will equation (C-13) be satisfied exactly because of numerical errors. Thus, it is helpful (and assuring) to establish an error criterion for the roots which are obtained.

When $t = 0$ and/or $r = 0$ and $|z| \neq h$, an explicit expression for the four roots of one of the quartics is obtained from equation (C-6), namely

$$v = \pm\left[-\tfrac{1}{2}b \pm \tfrac{1}{2}(b^2 - 4d)^{\frac{1}{2}}\right]^{\frac{1}{2}}$$

Finally, when $t \neq 0$, $r = 0$, and $|z| = h \neq 0$, there are only two roots, namely

$$v = \pm \sqrt{e}$$

or

$$v = \pm i\sqrt{|e|}$$

Roots of the quartics obtained from equation (C-3) may be obtained from the foregoing algorithm. In general, there are eight complex roots. Since the coefficients a, b, c, and d are real, complex roots occur in conjugate pairs. As an example, the partial root locus of one of the quartics is shown in Figures C-1 and C-2. Additional roots for corresponding times may be visualized by rotating the locus curves about the imaginary axis.

Not all roots shown in Figures C-1 and C-2 satisfy equation (C-3). The two squarings which were necessary to express equation (C-3) as quartic equations introduced extraneous roots. Moreover, some of the complex roots lie on the

second sheet of the Riemann surface. Consequently, for a given value of t, the eight roots must be substituted back into equation (C-3) to determine which are valid. This has been done for the roots computed for the foregoing example and the results are shown in Figure C-3.

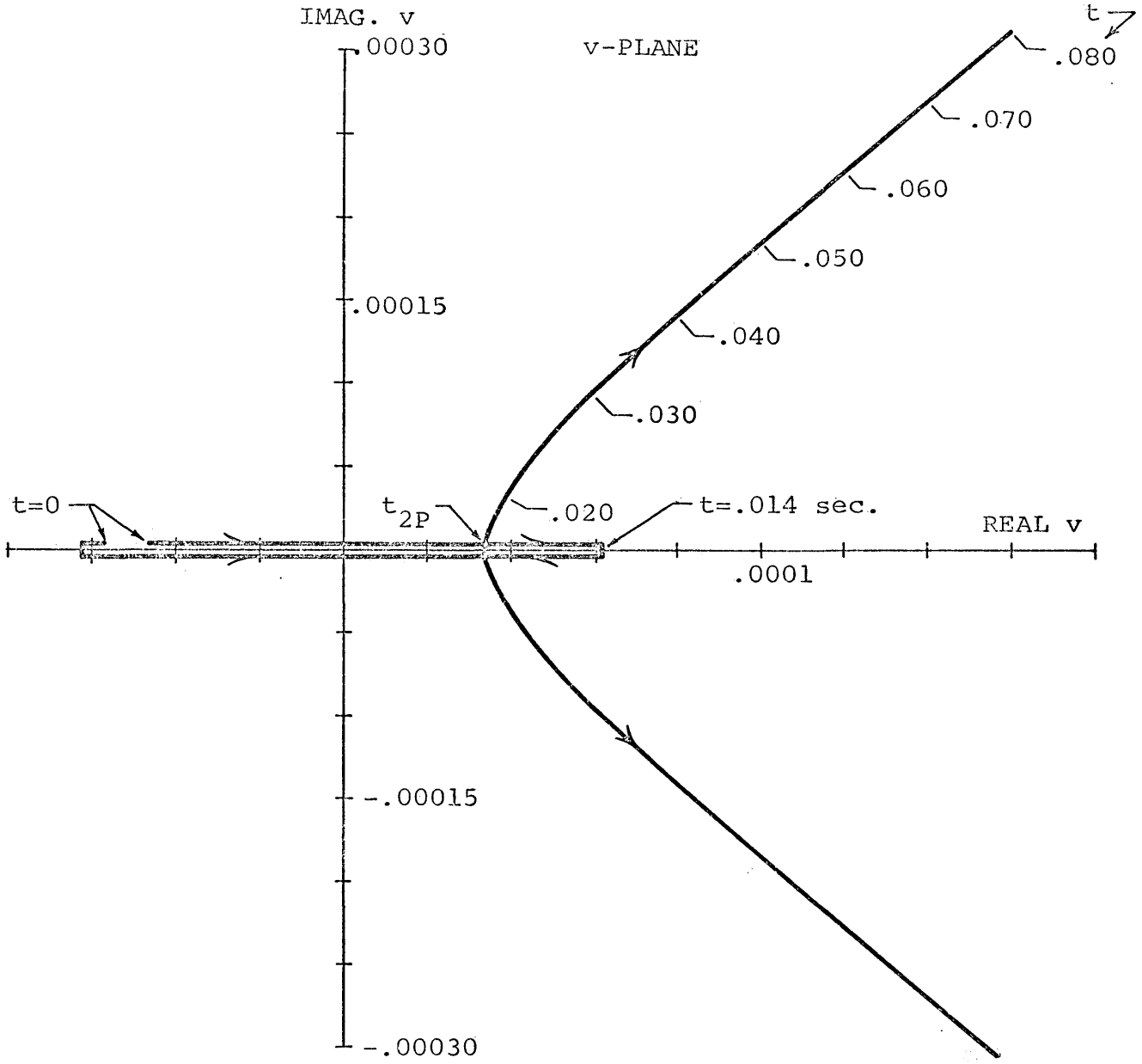


FIGURE C-1. Locus of two roots of the quartic

$$v^4 + av^3 + bv^2 + cv + d = 0$$

for the parameters r = h = -z = 100 ft., $S_1$ = .0001 sec/ft, $S_2$ = .0000625 sec/ft. Arrival time $t_{2P}$ = .018049 sec. Roots lie apart from real axis for sake of clarity.

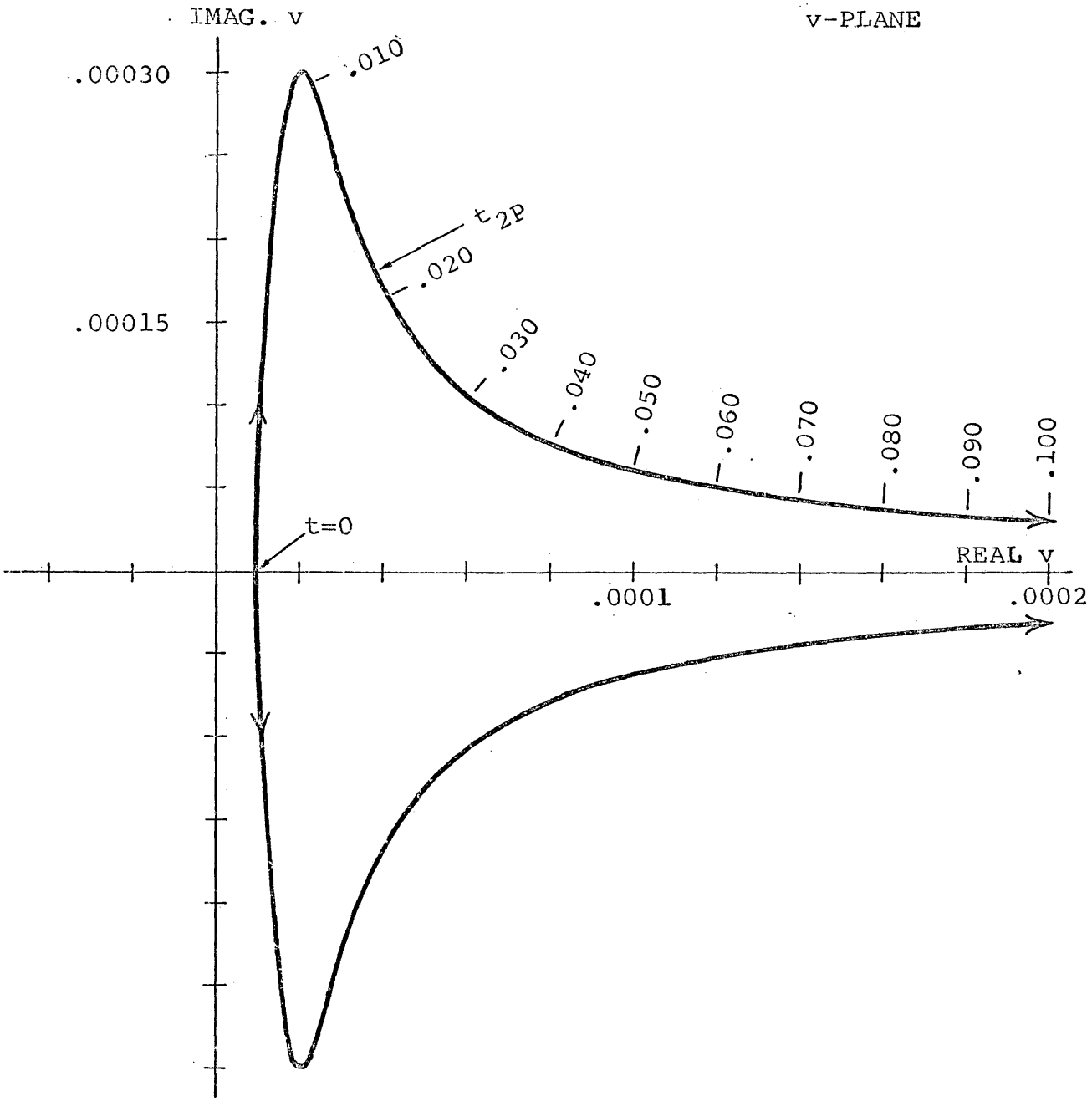


FIGURE C-2. Locus of two roots of the quartic

$$v^4 + av^3 + bv^2 + cv + d = 0$$

which comprise extraneous roots of $Z_{2P} = 0$. Relevant parameters are: $r = h = -z = 100$ ft. $S_1 = .0001$ sec/ft, $S_2 = .0000625$ sec/ft. Arrival time $t_{2P} = .018049$ sec.

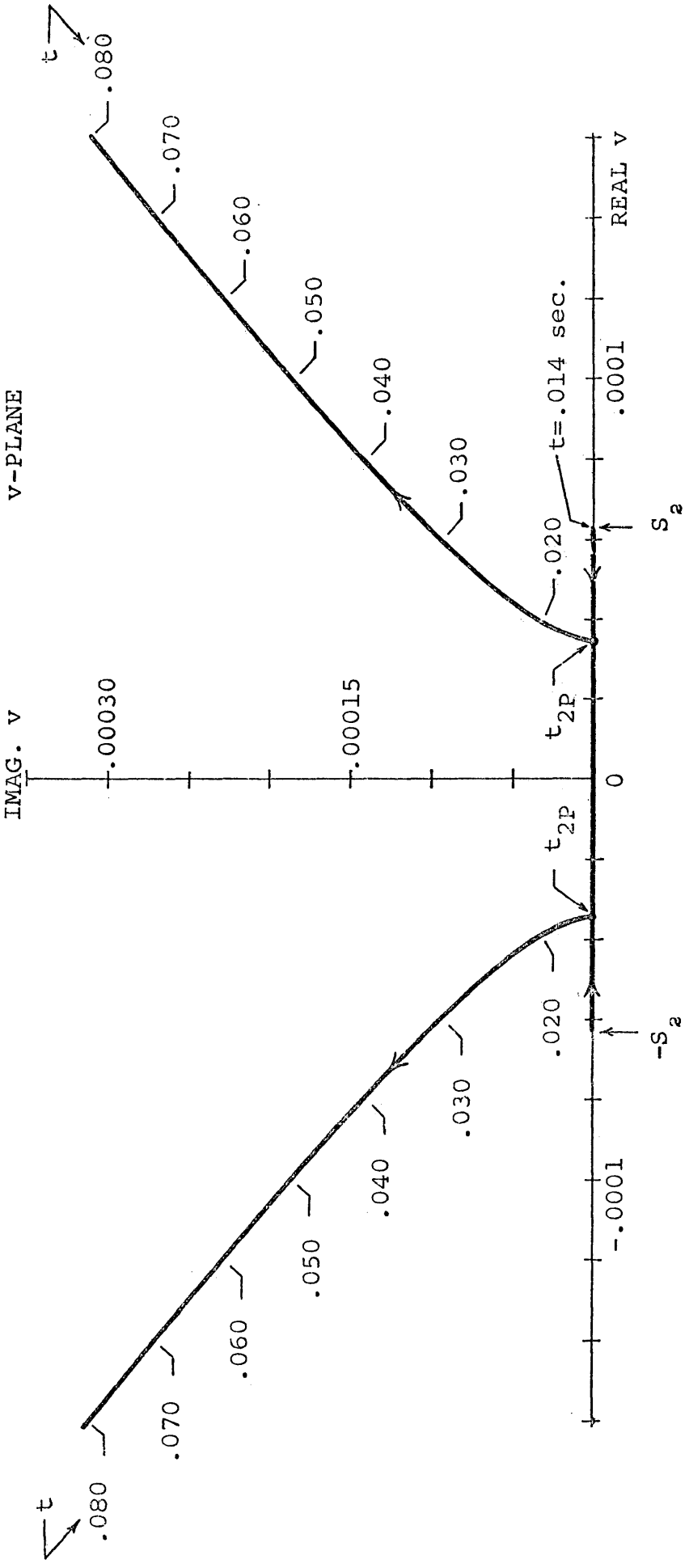


FIGURE C-3. Root locus of $Z_{2P}$ = 0 for r = h = -z = 100 ft., $S_1$ = .0001 sec/ft., $S_2$ = .0000625 sec/ft., Arrival time $t_{2P}$ = .018049 sec.

# APPENDIX D

## REPRESENTATION OF $x_{nP}$ INSIDE THE CRITICAL CONE ($r < r_c$)

The hypothesis $x_{nP}(t,r,z) = 0$ for $t < t_{nP}$ (eq. (16)) is a sufficient condition to yield equation (12), which is a plausible solution to the problem. The purpose of this section is to show that this is not a necessary condition.

Consider the following function

$$\chi_{nP}(t) = \lim_{\substack{k\to\infty \\ \epsilon\to 0}} M[t-t_{nP}][1 - \gamma_k(t-t_{nP}+\epsilon) + \gamma_k(t-t_{nP}-\epsilon)] \qquad \text{(D-1)}$$

The order of the limit shown above is from top to bottom; that is, (1) $k \to \infty$ and then (2) $\epsilon \to 0$. The term $\gamma_k(t)$ represents a sequence of ordinary differentiable functions. One such sequence is given by

$$\gamma_k(t) = (k/\pi)^{\frac{1}{2}} \int_{-\infty}^{t} e^{-k\nu^2}\, d\nu$$

This sequence is discussed in greater detail in Appendix F, where it is shown that

$$\lim_{\substack{k\to\infty \\ \epsilon\to 0}} \gamma_k(t-\epsilon) = \delta^{-1}(t) = \begin{cases} 1 \text{ for } t > 0 \\ 0 \text{ for } t \leq 0 \end{cases}$$

Equation (D-1) is plotted in Figure D-1 for $k \to \infty$. It will be noted that $\chi_{nP}(t) = 0$ in the interval $(t_{nP}-\epsilon) < t < (t_{nP} + \epsilon)$. The ordinate intercept is a function of the constant M and the arrival time $t_{nP}$.

The first and second derivatives of equation (D-1) are given by the following equations:

$$\chi'_{nP}(t) = \lim_{\substack{k\to\infty \\ \epsilon\to 0}} M \Big[ 1 - \gamma_k(t-t_{nP} + \epsilon) + \gamma_k(t-t_{nP}-\epsilon) + [t-t_{nP}][\gamma'_k(t-t_{nP}-\epsilon) - \gamma'_k(t-t_{nP}+\epsilon)] \Big] \quad \text{(D-2)}$$

$$\chi''_{nP}(t) = \lim_{\substack{k\to\infty \\ \epsilon\to 0}} M \Big[ 2\,[\gamma'_k(t-t_{nP}-\epsilon) - \gamma'_k(t-t_{nP}+\epsilon)] + [t-t_{nP}][\gamma''_k(t-t_{nP}-\epsilon) - \gamma''_k(t-t_{nP}+\epsilon)] \Big] \quad \text{(D-3)}$$

Equations (D-2) and (D-3) are plotted in Figure (D-1b) and (D-1c), respectively, for $k \to \infty$. The singlet $\delta(t)$ and the doublet $\delta'(t)$ represent the limit of $\gamma'_k(t)$ and $\gamma''_k(t)$, respectively, as $k \to \infty$.

With the aid of Figure D-1, the following properties may be established:

1: $\chi_{nP}(t_{nP}) = 0$

2: $\chi'_{nP}(t_{nP}) = 0$; $\chi'_{nP}(t_{nP}) = M$ for $t \neq t_{nP}$

3: $\chi''_{nP}(t) = 0$ for all t.

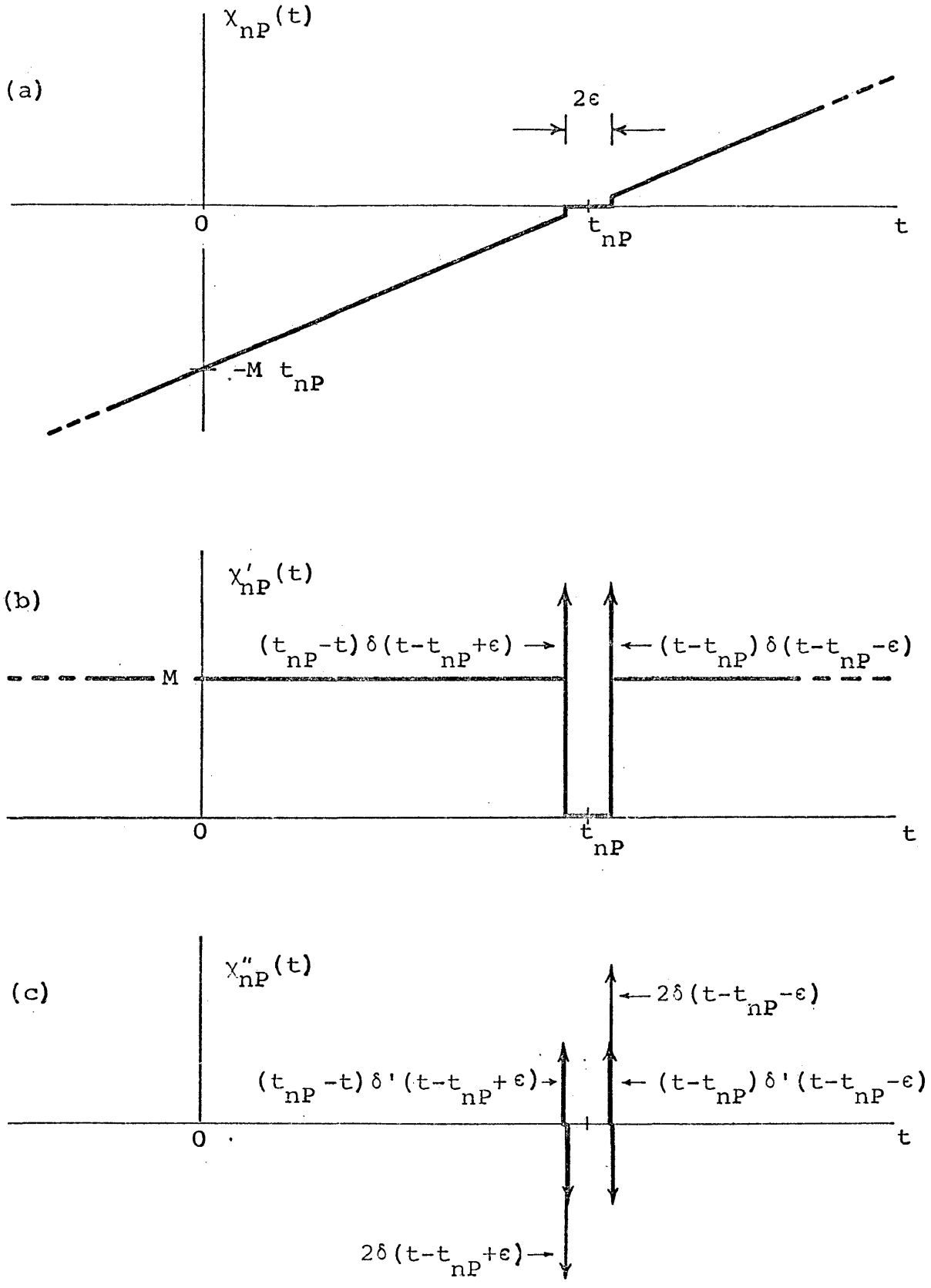


FIGURE D-1. Plots of the discontinuous $\chi_{nP}(t)$ and its first two derivatives.

Let $y_{nP}(t,r,z)$ represent a bounded and continuous function for $t \geq t_{nP}$. If

$$X_{nP}(t,r,z) = \lim_{\substack{k\to\infty \\ \epsilon\to 0}} \gamma_k(t-t_{nP}+\epsilon) y_{nP}(t,r,z) + \chi_{nP}(t), \tag{D-4}$$

then

$$X''_{nP}(t,r,z) = y_{nP}(t_{nP})\delta'(t-t_{nP}) + y'_{nP}(t_{nP})\delta(t-t_{nP}) + y''_{nP}(t,r,z)\delta^{-1}(t-t_{nP}) + 0 \tag{D-5}$$

for all t.[1/] The following limits yield the weights $y_{nP}(t_{nP})$ and $y'_{nP}(t_{nP})$ of equation (D-5):

$$\begin{aligned} \lim_{t\to t_{nP}^+} X_{nP}(t,r,z) &= y_{nP}(t_{nP}) \lim_{\substack{k\to\infty \\ \epsilon\to 0}} \gamma_k(\epsilon) + \chi_{nP}(t_{nP}) \\ &= y_{nP}(t_{nP}) \lim_{\epsilon\to 0} \delta^{-1}(\epsilon) + 0 \\ &= y_{nP}(t_{nP}) \end{aligned} \tag{D-6}$$

$$\lim_{t\to t_{nP}^+} X'_{nP}(t,r,z) = y'_{nP}(t_{nP}) \lim_{\substack{k\to\infty \\ \epsilon\to 0}} \gamma_k(\epsilon) + y_{nP}(t_{nP}) \lim_{\substack{k\to\infty \\ \epsilon\to 0}} \gamma'_k(\epsilon) + \chi'_{nP}(t_{nP})$$

---

1/ The weights $y_{nP}(t_{nP})$ and $y'_{nP}(t_{nP})$ should not be interpreted according to equations (13) and (14) at this stage in the development.

$$= y'_{nP}(t_{nP}) + y_{nP}(t_{nP}) \lim_{\epsilon \to 0} [0] + 0$$

$$= y'_{nP}(t_{nP}) \qquad \text{(D-7)}$$

Equations (D-6) and (D-7) are independent of $\chi_{nP}(t)$ by virtue of properties 1 and 2 above. This feature, together with property 3, implies that $X''_{nP}$ given by equation (D-5) is independent of $\chi_{nP}(t)$.

Comparing equation (D-5) with equation (12) will reveal that these two equations have the same form. In fact, $X''_{nP}(t,r,z) = x''_{nP}(t,r,z)$ whenever

$$\lim_{t \to t^+_{nP}} X_{nP}(t,r,z) = \lim_{t \to t^+_{nP}} x_{nP}(t,r,z) \qquad \text{(D-8)}$$

$$\lim_{t \to t^+_{nP}} X'_{nP}(t,r,z) = \lim_{t \to t^+_{nP}} x'_{nP}(t,r,z) \qquad \text{(D-9)}$$

$$y''_{nP}(t,r,z) = x''_{nP}(t,r,z) \text{ for } t > t_{nP} \qquad \text{(D-10)}$$

Equations (D-8) and (D-9) may be realized by virtue of equations (D-6) and (D-7), respectively. Equation (D-10) may be realized by matter of definition because $y_{nP}(t,r,z)$ appears as an arbitrary bounded and continuous function in equation (D-5). Consequently, the expression

$$x_{nP}(t,r,z) = \delta^{-1}(t-t_{nP}) y_{nP}(t,r,z) + \chi_{nP}(t) \qquad \text{(D-11)}$$

yields equation (12) which is a plausible solution to the problem.

It is instructive to note that equation (16) is a special case of equation (D-11) and results when M = 0. It is also instructive to note that equation (D-11) is unbounded in the limit as $M \to \infty$. Both of these conditions are encountered in dealing with the integral definition of $x_{nP}$ and will be briefly discussed below. The following notation will facilitate the discussion:

$$I_1(t,v) = R_P(v) K_{1P}(t,r,z,v)$$

$$I_2(t,v) = T_P(v) K_{2P}(t,r,z,v)$$

The singularities of $I_n(t,v)$ lie on the real v-axis when $t < t_{nP}$ and are integrable. Therefore, these integrands are analytic everywhere within the first quadrant, excluding only a segment $0 < v < BP$ arbitrarily close to the real axis (Fig. D-2). This real axis segment of the moving branch cut is of little consequence until $r > r_c$ because $\mathrm{Re}[I_n] = 0$ over this portion of the integration path. Thus for $r < r_c$ and $t < t_{nP}$, the Cauchy-Goursat theorem may be used to write

$$\mathrm{Re} \int_{C_1} I_n(t,v)\,dv = - \mathrm{Re} \int_{C_2} I_n(t,v)\,dv - \mathrm{Re} \int_{C_3} I_n(t,v)\,dv \qquad \text{(D-12)}$$

The integrands $I_n(t,v)$ are real on $C_3$; hence the third integral of equation (D-12) vanishes.[2/]

---

2/ Along $C_3$, $dv = i\,d\nu$ and the integral becomes $\int_{C_3} i\, I_n(t,i\nu)\,d\nu$

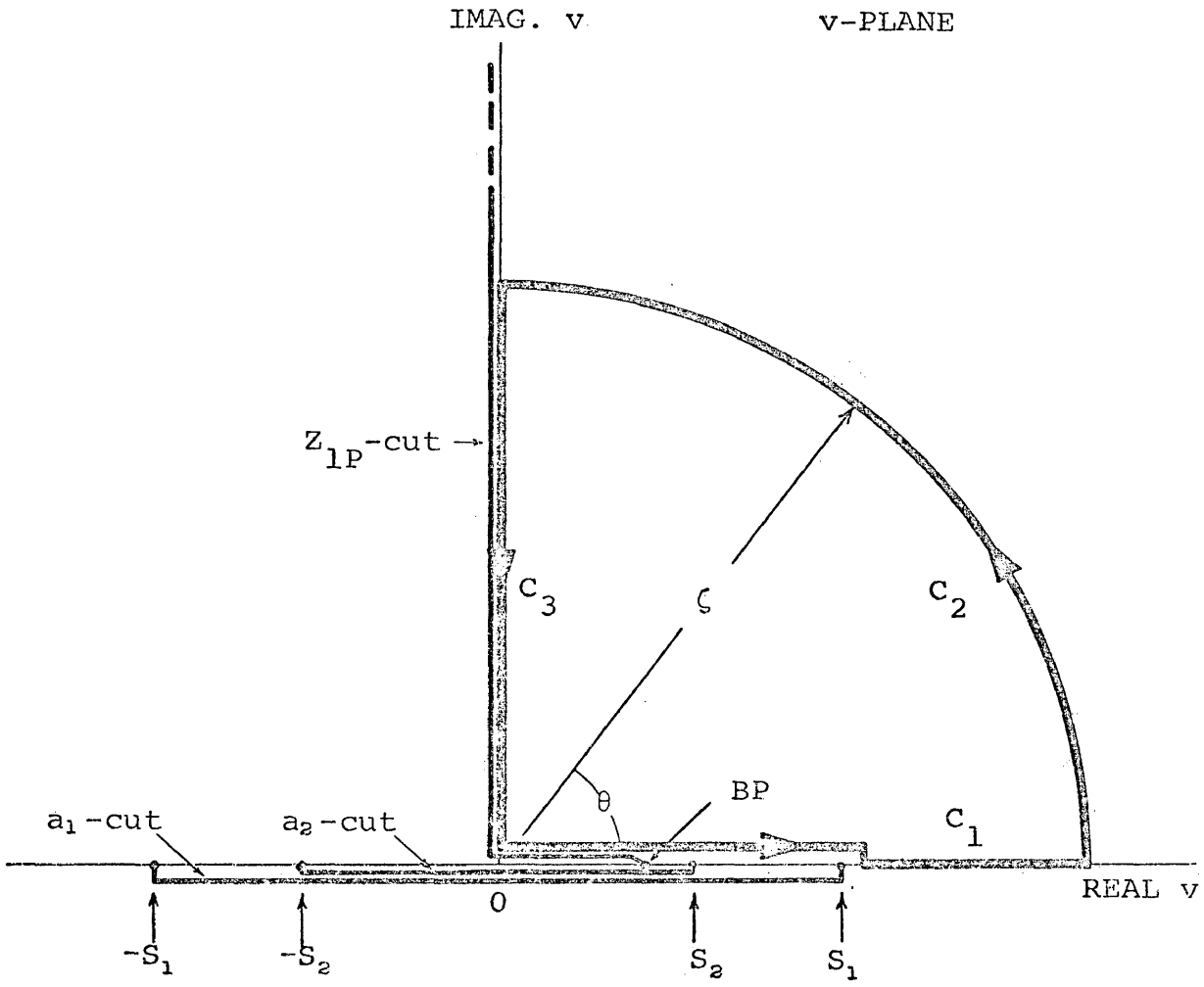


FIGURE D-2. Closed v-plane contour for $t < t_{nP}$.

The radius of the $C_2$ contour, $\zeta$, can be taken large enough that the following approximations are valid:

$$a_1 \approx a_2 \approx v = \zeta e^{i\theta}$$

Since t is bounded for the case under study ($t < t_{nP}$), it follows that[3/]

$$\tau_{nP} \approx \zeta e^{i\theta} \ (h + z)$$

for large $\zeta$. The kernels therefore approach a constant value as $\zeta \to \infty$:

$$K_{nP}(t,r,z,\zeta e^{i\theta}) = [r^2 + (h + z)^2]^{-\frac{1}{2}} = R^{-1}$$

The reflection and transmission coefficients for a special solid-solid interface ($s_1 = s_2$, $\rho_1 = \rho_2$) also approach constant values as $\zeta \to \infty$. These values are given by

$$R_P(\zeta e^{i\theta}) = \overline{R}_P(\zeta e^{i\theta}) \to 0$$

$$T_P(\zeta e^{i\theta}) \to 1$$

$$\overline{T}_P(\zeta e^{i\theta}) \to 1$$

For a general solid-solid interface ($s_1 \neq s_2$, $\rho_1 \neq \rho_2$),

---

3/ In the remainder of this appendix, z will denote the magnitude of the distance from the interface to the receiver. Normally, z is negative when the receiver is in medium 2.

the reflection coefficients increase as $m_1 v^2$ as $|v| \to \infty$, and the transmission coefficients approach constant values, $m_2$. The constants $m_1$ and $m_2$ depend on the elastic parameters of the two media and on the component and mode of wave propagation.

The foregoing results imply that on $C_2$ there are three cases to consider:

1 - $I_1(t,v) \to 0$ (special solid-solid)

2 - $I_1(t,v) \to m_1 R^{-1} \zeta^2 e^{i2\theta}$ (general solid-solid)

3 - $I_2(t,v) \to \eta$ (special solid-solid, $\eta = R^{-1}$; general solid-solid, $\eta = m_2 R^{-1}$)

These three cases are treated separately below.

CASE 1

$$IC2_1 \triangleq \mathrm{Re} \int_{C_2} I_1(t,v)\, dv = 0$$

CASE 2

$$IC2_1 = \mathrm{Re}\left[ i m_1 R^{-1} \zeta^3 \int_0^{\frac{1}{2}\pi} e^{i3\theta} d\theta \right]$$

$$= -\frac{1}{3} m_1 R^{-1} \zeta^3$$

CASE 3

$$IC2_2 = \mathrm{Re}\left[ i\eta\zeta \int_0^{\frac{1}{2}\pi} e^{i\theta} d\theta \right]$$

$$= -\eta\zeta$$

When $t < t_{nP}$ and $r < r_c$, the integral defining $x_{nP}$ is given by the expressions

$$x_{nP}(t,r,z) = -\frac{1}{\pi}\int_0^{\infty} I_n(t,v)\,dv = -\frac{1}{\pi}\lim_{\zeta\to\infty}\int_{C_1} I_n(t,v)\,dv$$

$$= -\frac{1}{\pi}\lim_{\zeta\to\infty} IC2_n \qquad \text{(D-13)}$$

From cases 1, 2, and 3 above, it is easy to see that $x_{1P}(t,r,z) = 0$ for a special solid-solid, but $x_{nP}(t,r,z)$ is otherwise unbounded and hence meaningless in the classical sense.

Equation (D-11) can be used to account for the results given by cases 1, 2, and 3. With $M = 0$, $x_{1P}(t,r,z) = 0$ for $t < t_{nP}$ which is consistent with case 1. As $M \to \infty$, $x_{nP}(t,r,z) \to \infty$ which is consistent with cases 2 and 3. More importantly, when equation (D-11) is differentiated twice with respect to t, an expression is obtained (eq. 12) which satisfies the displacement boundary conditions and yields numerical results which are consistent with plane wave theory.

# APPENDIX E

## EVALUATION OF THE WEIGHTS OF THE DOUBLET AND SINGLET TERMS OF THE BOUNDARY FUNCTIONS

As t decreases to the arrival time ($t \rightarrow t^{+}_{nP}$), two complex roots from both sheets of the Riemann surface for the function $Z_{nP} = (rv + i\tau_{nP})(rv - i\tau_{nP})$ merge on the real v-axis at $v_n$, forming a simple pole there. A similar situation occurs for the shear arrival time. Evaluation of the weights of the doublet and singlet terms of the boundary functions is predicated on determining the residue for this pole. This appendix pertains to the computation of residues of the poles for the compressional terms. Residues for the shear terms are obtained in the same manner.

An expression for the residue at $v_n$ may be obtained by expanding $rv - i\tau_{nP}$ in a Laurent series about its zero. The following notation will facilitate the expansion:

$$rv - i\tau_{nP} = Q_n(v) - t \qquad \text{(E-1)}$$

where

$$Q_n(v) = rv - i(a_1 h + |z| a_n)$$

The pole positions are given by the relations

$$v_1 = rS_1/R$$

$$v_2 = r_1S_1/R_1 = (r-r_1)S_2/R_2$$

The distances $r_1$, $R_1$, and $R_2$ are defined according to Figure 1. The distance R is given by

$$R = [r^2 + (h+z)^2]^{\frac{1}{2}}$$

In terms of $Q_n(v)$, the series expansion of equation (E-1) is given by the expression

$$rv - i\tau_{nP} = (v-v_n)Q_n'(v_n) + \frac{1}{2!}(v-v_n)^2Q_n''(v_n) + \frac{1}{3!}(v-v_n)^3Q_n'''(v_n) + \ldots \qquad \text{(E-2)}$$

The derivatives of $Q_n$ are given by the equations

$$Q_n'(v) = \frac{\partial Q_n}{\partial v} = r - iv(h/a_1 + |z|/a_n)$$

$$Q_n''(v) = \frac{\partial^2 Q_n}{\partial v^2} = -i(hS_1^2/a_1^3 + |z|S_n^2/a_n^3)$$

$$\begin{array}{ccc} \cdot & \cdot & \cdot \\ \cdot & \cdot & \cdot \\ \cdot & \cdot & \cdot \end{array}$$

It is easy to show that $Q_1'(v_1)$ vanishes:

$$Q_1'(v_1) = r - rS_1(h+z)/[S_1^2 - (rS_1/R)^2]^{\frac{1}{2}}$$

$$= r\,[1 - (h+z)/(R^2-r^2)^{\frac{1}{2}}]$$

$$= 0$$

It is considerably more difficult to show that $Q_2'(v_2)$ vanishes. Rather than do so, a technique due to Cagniard (1962, p. 89) is used to express the Laurent series (eq. E-2) in a form which contains only $Q_n''(v_n)$ and higher order terms. The development which follows will proceed with that objective.

A new function is introduced according to equations (E-1) and (E-2)

$$L_n(v) = \frac{Q_n(v) - t}{v_n - v}$$

$$= -Q_n'(v_n) - \frac{1}{2!}(v-v_n)Q_n''(v_n)$$

$$- \frac{1}{3!}(v-v_n)^2 Q_n'''(v_n) - \ldots \qquad \text{(E-3)}$$

By defining $a_n$ on the second sheet of the Riemann surface, the function $L_n(v)$ can be expanded about its zero $v = v_n^*$, where $v_n^*$ is the complex conjugate of $v_n$. This expansion gives

$$L_n(v) = (v-v_n^*)L_n'(v_n^*) + \frac{1}{2!}(v-v_n^*)^2 L_n''(v_n^*) + \ldots \qquad \text{(E-4)}$$

Successive differentiation of equation (E-3) gives the following expressions:

$$L_n'(v) = -\frac{1}{2}Q_n''(v_n) - \frac{1}{3}(v-v_n)Q_n'''(v_n) - \ldots$$

$$L_n''(v) = -\frac{1}{3}Q_n'''(v_n) - \frac{1}{8}Q_n^{iv}(v_n)(v-v_n) - \ldots$$

$$\vdots \qquad\qquad \vdots$$

Substituting the last expressions into equation (E-4) gives the following series for $L_n(v)$:

$$L_n(v) = (v-v_n^*)\left[-\frac{1}{2}Q_n''(v_n) - \frac{1}{3}(v_n^*-v_n)Q_n'''(v_n) - \ldots\right]$$
$$+ \frac{1}{2}(v-v_n^*)^2\left[-\frac{1}{3}Q_n'''(v_n) - \frac{1}{8}(v_n^*-v_n)Q_n^{iv}(v_n) - \ldots\right]$$
$$+ \ldots \qquad \text{(E-5)}$$

Substituting equation (E-5) into equation (E-3) gives the following series for equation (E-1):

$$Q_n(v) - t = (v-v_n^*)(v_n-v)\left[-\frac{1}{2}Q_n''(v_n) - \frac{1}{3}(v_n^*-v_n)Q_n'''(v_n) - \ldots\right]$$
$$+ (v-v_n^*)^2(v_n-v)\left[-\frac{1}{3}Q_n'''(v_n) - \frac{1}{8}(v_n^*-v_n)Q_n^{iv}(v_n) - \ldots\right]$$
$$+ \ldots \qquad \text{(E-6)}$$

Combining the higher-order terms of equation (E-6) into a single term gives

$$Q_n(v) - t = \frac{1}{2}(v-v_n)(v-v_n^*)[Q_n''(v_n) + \epsilon(v)]$$

where $\epsilon(v)$ is given by

$$\epsilon(v) = 2\sum_{m=3}^{\infty}(v-v_n^*)^{m-2}Q_n^{(m)}(v_n)/m$$

$$+ 2\sum_{j=3}^{\infty}(v_n^*-v_n)^{j-2}\sum_{m=j}^{\infty}\frac{m-1}{m!}(v-v_n)^{m-j}Q_n^{(m)}(v_n) \qquad \text{(E-7)}$$

As t decreases to the arrival time $t_{nP}$, the zeros of $Q_n(v)-t$ on the two sheets of the Riemann surface merge and the second term in equation (E-7) vanishes because $(v_n^*-v_n)\to 0$. In other words as $t \to t_{nP}^+$, $v_n^*$ tends to $v_n$ resulting in the limit

$$\lim_{v_n^*\to v_n}\epsilon(v) = 2\sum_{m=3}^{\infty}(v-v_n)^{m-2}Q_n^{(m)}(v_n)/m$$

$$= \hat{\epsilon}(v).$$

From the above result, equation (E-1) becomes

$$\lim_{t\to t_{nP}^+}[Q_n(v)-t] = \frac{1}{2}(v-v_n)^2[Q_n''(v_n) + \hat{\epsilon}(v)]$$

Since the derivatives of $Q_n$ are bounded, the error term $\hat{\epsilon}(v)$ in equation (E-8) vanishes as v tends to $v_n$ because it contains terms in $(v-v_n)$ of order two and greater. Consequently, in arbitrarily small neighborhoods of $v_n$, the following approximation is valid for $t = t_{nP}$

$$Z_{nP} \approx -(v-v_n)^2\left[\frac{1}{2}(rv+i\tau_{nP})|Q_n''(v_n)|\right] \qquad \text{(E-9)}$$

The following relationships facilitate the evaluation of equation (E-9)

$$a_1(v_1) = i(h+z)S_1/R$$

$$a_1(v_2) = ihS_1/R_1$$

$$a_2(v_1) = izS_2/R_2$$

$$rv + i\tau_{nP}\Big|_{v=v_n} = 2rv_n$$

$$Q_1''(v_1) = -R^3/[(h+z)^2 S_1]$$

$$Q_2''(v_2) = -R_1^3/[h^2 S_1 D]$$

$$D = [1 + (R_2/R_1)^3 (h/z)^2 (S_1/S_2)]^{\frac{1}{2}}$$

The residue for the $x_{1P}$ integrand is given by

$$(v-v_1)R_P(v)K_{1P}(t,r,z,v)\Big|_{v=v_1} = \frac{iR_P(v_1)v_1}{[rv_1\,|Q_1''(v_1)|]^{\frac{1}{2}}}$$

$$= i[(h+z)/R][S_1/R]R_P(v_1)$$

Residues for the other integrands are similarly obtained.

Inside the critical cone, the weights of the doublet are given by equation (13), namely $\pi i$ times the residue at $v_n$. For $r > 0$, the required weights of the doublet are found to be

$$y_{1P}(t_{1P}) = [(h+z)/R][S_1/R]$$

$$y_{2P}(r_{2P}) = (h/R_1)(S_1/R_1)(r_1/r)^{\frac{1}{2}}D^{-1}\mathrm{Re}[T_P(v_2)];\ z \neq 0$$

$$= (h/R)(S_1/R)\mathrm{Re}[T_P(v_2)];\ z = 0$$

$$y_{1P}(t_{1P}) = (r/R)(S_1/R)\mathrm{Re}[\overline{R}_P(v_1)]$$

$$\overline{y}_{2P}(t_{2P}) = (r_1/R_1)(S_1/R_1)(r_1/r)^{\frac{1}{2}}D^{-1}\mathrm{Re}[T_P(v_2)];\ z \neq 0$$

$$= (r/R)(S_1/R)\ \mathrm{Re}[T_P(v_2)];\ z = 0$$

The appropriate expressions for normal incidence ($r = 0$) may be obtained by replacing $(r_1/r)^{\frac{1}{2}}$ with the expression

$$(r_1/r) = [r_1/(r_1+r_2)]^{\frac{1}{2}} = [1+r_2/r_1]^{-\frac{1}{2}} \qquad \text{(E-10)}$$

where

$$r_2 = r - r_1$$

Using Snell's law, the ratio $r_2/r_1$ may be written as follows:

$$r_2/r_1 = \frac{S_1[r_2^2 + z^2]^{\frac{1}{2}}}{S_2[r_1^2 + h^2]^{\frac{1}{2}}} \qquad \text{(E-11)}$$

Substituting equation (E-11) into equation (E-10) gives

$$[r_1/r]^{\frac{1}{2}} = \left[1 + \frac{S_1[r_2^2 + z^2]^{\frac{1}{2}}}{S_2[r_1^2 + h^2]^{\frac{1}{2}}}\right]^{-\frac{1}{2}}$$

As r approaches zero, both $r_1$ and $r_2$ approach zero.

Consequently,

$$\lim_{r\to 0} [r_1/r]^{\frac{1}{2}} = [1 + S_1|z|/S_2 h]^{-\frac{1}{2}}$$

The following results are obtained for r = 0:

$$\bar{y}_{nP}(t_{nP}) = 0$$

$$y_{1P}(t_{1P}) = [S_1/(h+z)]\mathrm{Re}[R_P(0)]$$

$$y_{2P}(t_{2P}) = (S_1/h)[1 + S_1 z /S_2 h]^{-1}\mathrm{Re}[T_P(0)]$$

Weights of the Singlets

The weights of the singlet terms of the boundary functions are obtained by evaluating $y'_{nP}(t,r,z)$ and $\bar{y}'_{nP}(t,r,z)$ for $t = t_{nP}$. In integral form, the required derivatives for $t > t_{nP}$ are given by

$$y'_{1P}(t,r,z) = -\frac{1}{\pi}\,\mathrm{Re}\int_0^\infty R_P(v)\; K'_{1P}(t,r,z,v)\; dv$$
$$y'_{2P}(t,r,z) = -\frac{1}{\pi}\,\mathrm{Re}\int_0^\infty T_P(v)\; K'_{2P}(t,r,z,v)\; dv \qquad \text{(E-12)}$$

and similarly for the horizontal (overbar) components. When $t = t_{nP}$, equations (E-12) display a third order pole at $v_n$ on the path of integration (see equations B-8 and B-9, Appendix B). With a simple transformation, the integrals can be cast in a form involving only simple poles on the real v-axis. To do this, the t-variable differentiations of the kernels are interchanged with differentiations with respect to h or r (or z). Possible transformations are briefly discussed below.

In integral form, the t-variable derivatives of the kernels are given by

$$K'_{nP}(t,r,z,v) = iv \int_0^\infty \omega e^{-\omega \tau_{nP}} J_o(rv\omega)\, d\omega \qquad \text{(E-13)}$$

$$\bar{K}'_{nP}(t,r,z,v) = i(v^2/a_1) \int_0^\infty \omega e^{-\omega \tau_{nP}} J_1(rv\omega)\, d\omega. \qquad \text{(E-14)}$$

Recalling that $\tau_{nP} = [a_1 h + a_n z - it]$, it is easy to see that equation (E-13) is equivalent to

$$K'_{nP}(t,r,z,v) = -i \frac{\partial}{\partial h} \left[ (v/a_1) \int_0^\infty e^{-\omega \tau_{nP}} J_o(rv\omega)\, d\omega \right]$$

$$= -i \frac{\partial}{\partial h} \left[ a_1^{-1} K_{nP}(t,r,z,v) \right] . \qquad \text{(E-15)}$$

where the dependence on h, heretofore considered a parameter, is implied. Equation (E-15) can be generalized to higher order derivatives. By induction

$$K^{(m)}_{nP}(t,r,z,v) = (-i)^m \frac{\partial^m}{\partial h^m} \left[ a_1^{-m} K_{nP}(t,r,z,v) \right].$$

The Bessel function appearing in equation (E-14) may be replaced with the identity

$$J_1(rv\omega) = -\frac{1}{v\omega} \frac{d}{dr} \left[ J_o(rv\omega) \right]$$

Replacing $J_1(rv\omega)$ in equation (E-14) by the last expression gives

$$\bar{K}'_{nP}(t,r,z,v) = -i \frac{\partial}{\partial r} \left[ (v/a_1) \int_0^\infty e^{-\omega \tau_{nP}} J_o(rv\omega)\, d\omega \right]$$

$$= -i \frac{\partial}{\partial r} \left[ a_1^{-1} K_{nP}(t,r,z,v) \right] \qquad \text{(E-16)}$$

A general expression is similarly obtained by induction:

$$K_{nP}^{(m)}(t,r,z,h,v) = (-i)^m \frac{\partial^m}{\partial r \partial h^{m-1}} \left[ a_1^{-m} K_{nP}(t,r,z,h,v) \right]$$

Equations (E-15) and (E-16) transform equations (E-12) into integrals involving simple poles on the real path of integration. To see this, $K'_{nP}$ and $\bar{K}'_{nP}$ in equations (E-12) are defined according to equations (E-15) and (E-16), and the order of differentiation and integration is interchanged. The following equations result:

$$y'_{1P}(t,r,z) = \frac{1}{\pi} \mathrm{Re}\left[ i \frac{\partial}{\partial h} \int_0^\infty R_P(v) a_1^{-1} K_{1P}(t,r,z,v)\, dv \right] \quad \text{(E-17)}$$

$$y'_{2P}(t,r,z) = \frac{1}{\pi} \mathrm{Re}\left[ i \frac{\partial}{\partial h} \int_0^\infty T_P(v) a_1^{-1} K_{2P}(t,r,z,v)\, dv \right] \quad \text{(E-18)}$$

and similarly for the horizontal components. The integrands of equations (E-17) and (E-18) display simple poles for $t = t_{nP}$ and hence the residues may be evaluated.

It is interesting to note that in generalizing the argument to $y''_{nP}$, $\bar{y}''_{nP}$, and higher order derivatives, the $a_1^{-m}$ term contributes singularities of order greater than one, and hence non-integrable singularities. Fortunately, the weights of the doublets and singlets do not require these higher order derivatives.

Using equation (E-17) for $y'_{1P}(t,r,z)$, the residue at $v_1$ is given by

$$(v-v_1) R_P(v) K'_{1P}(t,r,z,v) \Big|_{v=v_1}$$

$$= i\, R_P(v_1)\, \frac{\partial}{\partial h}\left\{\left(\left[(v/a_1)\ \tfrac{1}{2}(rv+i\tau_{nP})\,|Q_1''(v_1)|\right]^{-\frac{1}{2}}\right)_{v=v_1}\right\}$$

$$= i\, R_P(v_1)\, \frac{\partial}{\partial h}\left(\frac{1}{R}\right)$$

$$= -i[(h+z)/R]R^{-2}R_P(v_1) \qquad \text{(E-19)}$$

Residues for the other corresponding integrands are similarly obtained. It is important to note that the residue for the $y'_{nP}$ integrand equals $(RS_1)^{-1}$ times the residue of the $y_{1P}$ integrand. Similarly, the residue for the $y'_{2P}$ integrand equals $(R_1S_1)^{-1}$ times the residue of the $y_{2P}$ integrand. The proof of the latter case is considerably more involved than the proof given above for the former case because of the required differentiation of terms containing the distances $r_1$, $R_1$, and $R_2$, which are implicit functions of r and h.

In summary, the weights of the singlet terms are given by the relations

$$y'_{1P}(t_{1P}) = (RS_1)^{-1}y_{1P}(t_{1P})$$

$$y'_{2P}(t_{2P}) = (R_1S_1)^{-1}y_{2P}(t_{2P})$$

$$\bar{y}'_{1P}(t_{1P}) = (RS_1)^{-1}\bar{y}_{1P}(t_{1P})$$

$$\bar{y}'_{2P}(t_{2P}) = (R_1S_1)^{-1}\bar{y}_{2P}(t_{2P})$$

The distances $r_1$, $R_1$, and $R_2$, which are required in order to compute the weights of the doublet and singlet

terms for medium 2, may be derived by solving a quartic equation in $r_1$, namely

$$r_1^4 + ar_1^3 + br_1^2 + cr_1 + d = 0 \qquad \text{(E-20)}$$

where

$$a = -2r$$

$$b = (S_1^2 z^2 - S_2^2 h^2)/\Delta + r^2$$

$$c = (2rS_2^2 h^2)/\Delta$$

$$d = -(S_2^2 h^2 r^2)/\Delta$$

$$\Delta = (S_1^2 - S_2^2)$$

The appropriate $r_1$ is chosen from the four roots of equation (E-20) on the basis of Snell's law:

$$S_1 r_1/R_1 = S_2(r-r_1)/R_2$$

wherein

$$R_1 = [h^2 + r_1^2]^{\frac{1}{2}}$$

$$R_2 = [z^2 + (r-r_1)^2]^{\frac{1}{2}}$$

# APPENDIX F

## CONTINUITY OF THE COMPONENTS OF DISPLACEMENT FOR z = 0

A mathematical demonstration that the displacement boundary conditions are fulfilled is given in this section (see Appendix A, cases 1: and 2:). The development is for the vertical component of displacement for a special solid-solid interface ($s_1 = s_2$, $\rho_1 = \rho_2$). A corresponding development for the horizontal component is essentially the same, thus obviating the need for its presentation. The development for the general solid-solid interface includes shear wave terms, but is otherwise the same as the development for the special solid.

The arrival times for the direct wave, the reflection, and the transmission are equivalent when the receiver is located at the interface. In other words, $t_o = R_o S_1 = t_{1P} = t_{2P}$ for $z = 0$, where $R_o = [r^2 + h^2]^{\frac{1}{2}}$. Therefore, the difference between the vertical components of displacement in the two media is given by

$$d_1(t,r,o) - d_2(t,r,o) = -P(t)*f(t)*[(h/R_o)g(t-t_o) + \Delta(t,r)] \quad (F-1)$$

where

$$g(t) = -(S_1/R_o)\delta'(t) - R_o^{-2}\delta(t)$$

$$\Delta(t,r) = x''_{1P}(t,r,o) + x''_{2P}(t,r,o)$$

The functions $x''_{nP}$ may be expressed in two forms. One form, which is obtained from equation (6), is given below.

$$x''_{1P}(t,r,o) = \frac{1}{2\pi i}\int_{Br}\int_{o}^{\infty} C_1 \lambda J_o(r\lambda) e^{-\alpha_1 h + pt} d\lambda dp$$

$$x''_{2P}(t,r,o) = \frac{1}{2\pi i}\int_{Br}\int_{o}^{\infty} C_2 \lambda J_o(r\lambda) e^{-\alpha_1 h + pt} d\lambda dp \quad (F-2)$$

Using the relationship $C_2 = 1 - C_1$, $\Delta(t,r)$ is expressible in the form

$$\Delta(t,r) = \frac{1}{2\pi i}\int_{Br}\int_{o}^{\infty} \lambda J_o(r\lambda) e^{-\alpha_1 h + pt} d\lambda dp$$

$$= -\frac{1}{2\pi i}\int_{Br} e^{pt} dp \frac{d}{dh}\int_{o}^{\infty} \frac{\lambda}{\alpha_1} J_o(r\lambda) e^{-\alpha_1 h} d\lambda \quad (F-3)$$

The inner integral in equation (F-3) will be recognized as the Sommerfeld integral whose value is given by

$$[R_o \exp(p\, R_o S_1)]^{-1}$$

Consequently, equation (F-3) is equivalent to

$$\Delta(t,r) = -\frac{1}{2\pi i}\int_{Br}\frac{d}{dh}\left[R_o^{-1}e^{-pR_oS_1}\right]e^{pt}dp$$

$$= -\frac{d}{dh}\left[\frac{1}{R_o}\,\delta(t-R_oS_1)\right]$$

$$= -\frac{h}{R_o}\frac{d}{dR_o}\left[\frac{1}{R_o}\,\delta(t-R_oS_1)\right]$$

$$= -(h/R_o)g(t-t_o) \qquad \text{(F-4)}$$

Substituting equation (F-4) into equation (F-1) causes the bracketed term to vanish. Consequently,

$$d_1(t,r,o) - d_2(t,r,o) = 0$$

which verifies that the first of equations (6) satisfies the displacement boundary conditions for a special solid-solid interface.

Using the relationships

$$J_1(r\lambda) = -\frac{d}{dr}\left[\frac{1}{\lambda}\,J_o(r\lambda)\right]$$

$$\bar{C}_2 = 1 + \bar{C}_1,$$

it is easy to show that the third of equations (6) also satisfies the displacement boundary conditions. The development for the general solid is the same as that given above, only more terms are involved.

The second form for the functions $x''_{nP}$ involves the doublet and singlet terms (eq. 12). Actually, it is better to use the form given by equation (12) because it is from expressions such as these that the numerical computations are performed. Moreover, fulfillment of the displacement boundary conditions serves as a partial check that the mathematical development leading from equations (6) to equations (12) is correct.

The following equation for $\Delta(t,r)$ can be derived from equation (12) by setting $z = 0$:

$$\Delta(t,r) = \delta'(t-t_o)[y_{1P}(t_{1P}) + y_{2P}(t_{2P})]_{z=0} + \delta(t-t_o)[y'_{1P}(t_{1P}) + y'_{2P}(t_{2P})]_{z=0} + \delta^{-1}(t-t_o)[y''_{1P}(t,r,o) + y''_{2P}(t,r,o)] \qquad \text{(F-5)}$$

The required weights are given below for $z = 0$.

$$y_{1P}(t_{1P}) = (h/R_o)(S_1/R_o)\mathrm{Re}[R_P(v_1)]$$

$$y_{2P}(t_{2P}) = (h/R_o)(S_1/R_o)\mathrm{Re}[T_P(v_1)]$$

$$y'_{1P}(t_{1P}) = (h/R_o)R_o^{-2}\mathrm{Re}[R_P(v_1)]$$

$$y'_{2P}(t_{2P}) = (h/R_o)R_o^{-2}\mathrm{Re}[T_P(v_1)] \qquad \text{(F-6)}$$

The following relationships are used to reduce the bracketed terms shown in equation (F-5) and its horizontal component analogs:

$$T_p(v) = 1 - R_p(v)$$

$$\bar{T}_p(v) = 1 + \bar{R}_p(v)$$

$$K_{1p}(t,r,o,v) = K_{2p}(t,r,o,v)$$

$$\bar{K}_{1p}(t,r,o,v) = \bar{K}_{2p}(t,r,o,v) \qquad \text{(F-7)}$$

Using equation (F-6), together with the appropriate relationships from equation (F-7), it is easy to show that equation (F-5) reduces to the following form:

$$\Delta(t,r) = -(h/R_o)g(t-t_o) - \delta^{-1}(t-t_o)\,I(t,r) \qquad \text{(F-8)}$$

where

$$I(t,r) = \frac{1}{\pi}\,\mathrm{Re}\int_o^\infty K''_{1p}(t,r,o,v)\;dv$$

Substituting equation (F-8) into equation (F-1) gives

$$d_1(t,r,o) - d_2(t,r,o) = P(t) * f(t) * \delta^{-1}(t-t_o)\,I(t,r) \qquad \text{(F-9)}$$

The integral definition of the kernel (eq. 8) is used to evaluate I(t,r). This gives

$$I(t,r) = -\frac{1}{\pi}\,\mathrm{Re}\int_o^\infty dv\; v\int_o^\infty \omega^2\,\exp[-\omega(a_1 h - it)]J_o(rv\omega)\;d\omega$$

$$= \frac{1}{\pi}\,\mathrm{Re}\int_o^\infty \omega e^{i\omega t}d\omega\;\frac{d}{dh}\int_o^\infty \frac{v}{a_1}\,e^{-\omega a_1 h}J_o(rv\omega)\;dv \qquad \text{(F-10)}$$

The inner integral in equation (F-10) is a form of the Sommerfeld integral. Its value is given by

$$[\omega R_o \exp(-i\omega R_o S_1)]^{-1}$$

Consequently, $I(t,r)$ may be expressed as an inverse Fourier transform:

$$I(t,r) = \frac{1}{\pi} \mathrm{Re} \int_o^\infty \frac{d}{dh} [R_o^{-1} \exp(-i\omega R_o S_1)] e^{i\omega t} d\omega \qquad \text{(F-11)}$$

Inverting equation (F-11) gives the following result:

$$I(t,r) = \frac{d}{dh} [R_o^{-1} \delta(t-R_o S_1)]$$

$$= (h/R_o)[-(S_1/R_o)\delta'(t-R_o S_1) - R_o^{-2}\delta(t-R_o S_1)]$$

$$= (h/R_o) g(t-t_o) \qquad \text{(F-12)}$$

Equation (F-9) now becomes

$$d_1(t,r,o) - d_2(t,r,o) = (h/R_o) P(t) * f(t) * [\delta^{-1}(t-t_o) g(t-t_o)] \qquad \text{(F-13)}$$

The bracketed term in equation (F-13) represents the product of generalized functions. Unfortunately, it is not possible to define such an operation in general. There does not seem to be any natural way to define the product of two arbitrary generalized functions because the product does not always exist. It is natural, however, to define one of the generalized functions as the limit of a sequence $\gamma_k(t)$ of ordinary differentiable functions. Then, since it is possible

to define the product of any generalized function and an infinitely differentiable function, the limit of this product, if it exists, yields the required result.

A convenient description of a family of functions with derivatives of arbitrarily high order is given by

$$\gamma_k(t) = (k/\pi)^{\frac{1}{2}} \int_{-\infty}^{t} e^{-kx^2} dx \qquad \text{(F-14)}$$

From the properties of the Gaussian error function it can be shown that

$$(k/\pi)^{\frac{1}{2}} \int_{-\infty}^{\infty} e^{-kx^2} dx = 1$$

for all k. Since the integrand is positive, it follows that

$$0 < \gamma_k(t) < 1$$

for all t. If k is large $\gamma_k(t)$ is practically zero for $t < 0$ and practically unity for $t > 0$, except in a small neighborhood of $t = 0$ (Figure F-1a). By shifting the function an amount $\epsilon$ to the right, $\gamma_k(t-\epsilon)$ can be made arbitrarily small for $t < 0$ (Figure F-1b). Thus, the larger k and the smaller $\epsilon$, the more closely $\gamma_k(t-\epsilon)$ approximates the unit step $\delta^{-1}(t)$. In fact,

$$\lim_{\substack{k\to\infty \\ \epsilon\to 0}} \gamma_k(t-\epsilon) = \delta^{-1}(t) = \begin{cases} 1 \text{ for } t > 0 \\ 0 \text{ for } t \leqslant 0 \end{cases}$$

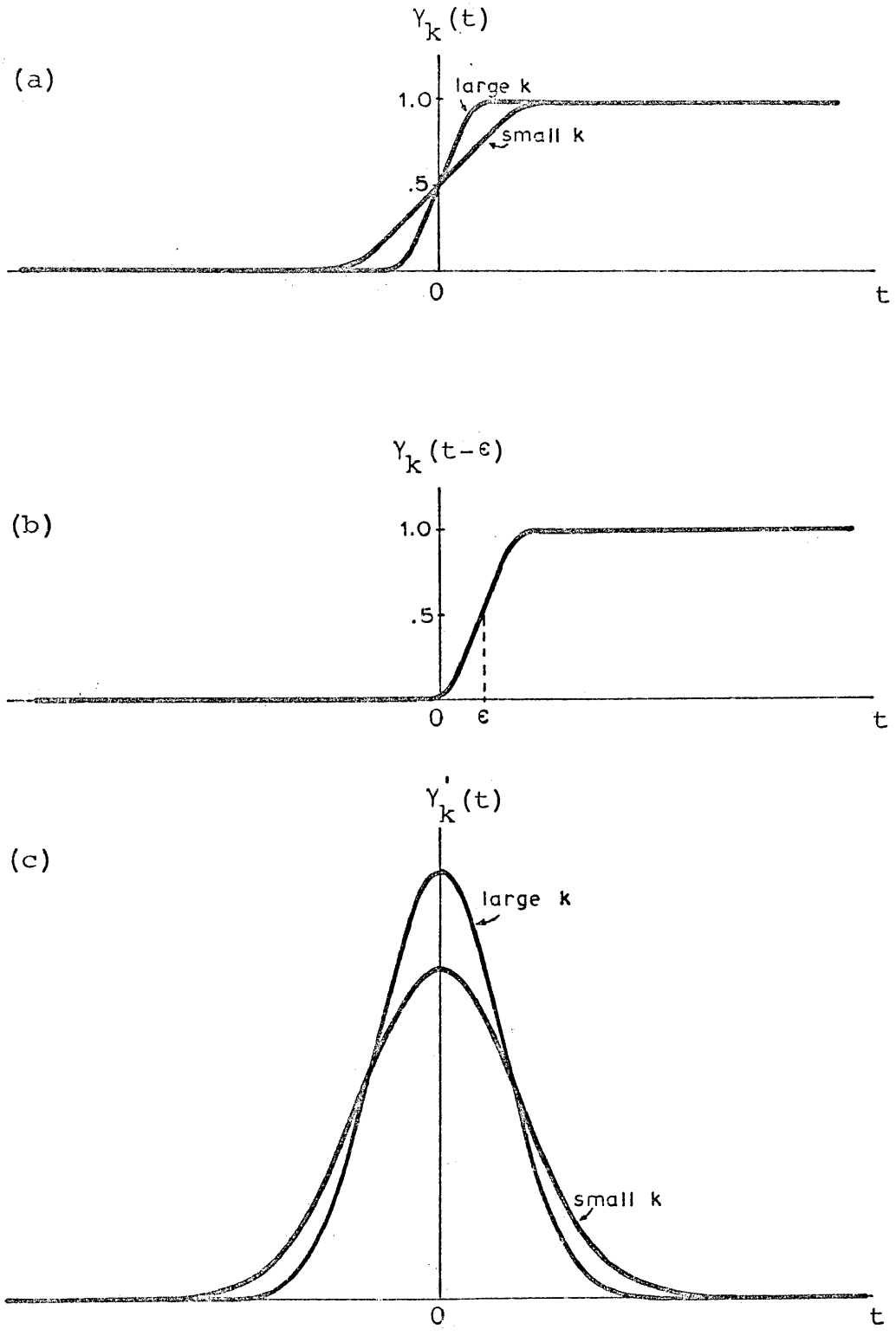


FIGURE F-1. Examples of the sequences $\gamma_k(t)$, $\gamma_k(t-\varepsilon)$, $\gamma_k'(t)$. $\gamma_k'(t)$ is shown on an expanded scale in t.

where the order of the limit is from top to bottom; that is, (1) $k \to \infty$ and then (2) $\epsilon \to 0$.

With the step function defined as a generalized limit of a sequence $\gamma_k(t-\epsilon)$ of ordinary functions, the following meaning is given to the bracketed term in equation (F-13):

$$[\delta^{-1}(t-t_o)g(t-t_o)] = c_1 \lim_{\substack{k\to\infty \\ \epsilon\to 0}} [\gamma_k(t-t_o-\epsilon)\delta'(t-t_o)] + c_2 \lim_{\substack{k\to\infty \\ \epsilon\to 0}} [\gamma_k(t-t_o-\epsilon)\delta(t-t_o)] \qquad \text{(F-16)}$$

Here, $c_1$ and $c_2$ are the constants $-S_1R_o^{-1}$ and $R_o^{-2}$, respectively. The properties of generalized functions yield the following expressions for the bracketed terms in equation (F-16) (Papoulis, 1962, p. 274):

$$[\gamma_k(t-t_o-\epsilon)\delta'(t-t_o)] = \gamma_k(-\epsilon)\delta'(t-t_o) - \gamma_k'(-\epsilon)\delta(t-t_o)$$

$$[\gamma_k(t-t_o-\epsilon)\delta(t-t_o)] = \gamma_k(-\epsilon)\delta(t-t_o)$$

Equation (F-16) therefore becomes

$$[\delta^{-1}(t-t_o)g(t-t_o)] = [c_1\delta'(t-t_o) + c_2\delta(t-t_o)] \lim_{\substack{k\to\infty \\ \epsilon\to 0}} \gamma_k(-\epsilon) - [c_1\delta(t-t_o)] \lim_{\substack{k\to\infty \\ \epsilon\to 0}} \gamma_k'(-\epsilon) \qquad \text{(F-17)}$$

From equation (F-15) it follows that the first term of equation (F-17) vanishes. The derivative of $\gamma_k(t)$, namely

$$\gamma_k'(t) = (k/\pi)^{\frac{1}{2}} e^{-kt^2}$$

looks like Figure (F-1c). The larger k is, that is, the more closely $\gamma_k(t)$ approximates a step, the narrower the curve representing $\gamma_k'(t)$ becomes and the higher the peak is at $t = 0$. In the limit as $k \to \infty$, $\gamma_k'(t) \to \delta(t)$, which is entirely consistent with the properties of generalized functions. Consequently,

$$\lim_{\substack{k\to\infty \\ \epsilon\to 0}} \gamma_k'(-\epsilon) = \lim_{\epsilon\to 0} \left[ \lim_{k\to\infty} \gamma_k'(-\epsilon) \right]$$

$$= \lim_{\epsilon\to 0} [0] = 0$$

With the result $[\delta^{-1}(t-t_o)g(t-t_o)] = 0$, it follows immediately that

$$d_1(t,r,o) - d_2(t,r,o) = 0$$

when the second form of $x''_{nP}$ is used in the analysis.

It is instructive to note that two other forms of $\delta^{-1}(t)$ may be obtained from the sequence $\gamma_k(t)$. These are given by the limits:

$$\lim_{k\to\infty} \gamma_k(t) = \begin{cases} 1 \text{ for } t > 0 \\ \frac{1}{2} \text{ for } t = 0 \\ 0 \text{ for } t < 0 \end{cases} \qquad \text{(F-18)}$$

and

$$\lim_{\substack{k\to\infty \\ \epsilon\to 0}} \gamma_k(t+\epsilon) = \begin{cases} 1 \text{ for } t \geq 0 \\ 0 \text{ for } t < 0 \end{cases} \qquad \text{(F-19)}$$

Equations (F-15) and (F-19) are equivalent to equation (F-18) when the order of the limits is interchanged; that is, when (1) $\epsilon\to 0$ and then (2) $k\to\infty$.

An interpretation of $\delta^{-1}(t)$ based on either equation (F-18) or equation (F-19) gives

$$[\delta^{-1}(t-t_o)g(t-t_o)] = [c_1\delta'(t-t_o) + c_2\delta(t-t_o)]w - [c_1\delta(t-t_o)]\delta(o) \qquad \text{(F-20)}$$

where w is either $\frac{1}{2}$ or 1, depending on whether equation (F-18) or equation (F-19) is used. No meaning can be attached to the second term in equation (F-20) because it makes no sense to talk about the value of $\delta(t)$ for a fixed t. Furthermore, equation (F-20) does not cause equation (F-13) to vanish, meaning that the first and second forms of $x''_{nP}$ (eqs. 6 and eqs. 12) are not equivalent when $\delta^{-1}$ is interpreted according to either equation (F-18) or equation (F-19).

Equation (F-15) is certainly not an unreasonable interpretation of the step function when used in the context of equation (12). The integral $x''_{nP}(t,r,z)$ strictly does not

exist at the arrival time $t_{nP}$, and $\delta^{-1}(t-t_{nP})y''_{nP}(t,r,z)$ gives meaning to such a function for all t.

Fulfillment of the displacement boundary conditions for several values of r and h has been demonstrated numerically for both vertical and horizontal components. A special solid-solid interface was used. The second form of $x''_{nP}$ and $\bar{x}''_{nP}$, interpreted according to equation (F-15), was used for all computations.

# APPENDIX G

## BIBLIOGRAPHY

### Spherical Wave Propagation in Bounded Media

Abramovici, F., and Alterman, Z., 1965, Computations pertaining to the problem of propagation of a seismic pulse in a layered solid: in Methods in Computational Physics, v. 4, p. 349-379.

Ben-Menahem, A., and Cisternas, A., 1963, The dynamic response of an elastic half-space to an explosion in a spherical cavity: Jour. Mathematics and Physics, v. 42, p. 112-125.

Bortfeld, R., 1962a, Exact solution of the reflection and refraction of arbitrary spherical compressional waves at liquid-liquid interfaces and at solid-solid interfaces with equal shear velocities and equal densities: Geophys. Prosp., v. 10, no. 1, p. 35-67.

_____1962b, Reflection and refraction of spherical compressional waves at arbitrary plane interfaces: Geophys. Prosp., v. 10, no. 4, p. 515-538.

_____1967, Elastic waves in layered media: Geophys. Prosp., v. 15, no. 4.

Brekhovskikh, L.M., 1948, The reflection of spherical waves at a plane interface: Jour. Tech. Physics (U.S.S.R.), v. 18, p. 455.

_____1960, Waves in layered media: (Transl. by D. Lieberman Ed. by R.T. Beyer), Academic Press, New York.

Cagniard, L., 1939, Reflection et refraction des ondes progressives seismiques: Gauthier-Villars, Paris (Transl. by E.A. Flinn and C.H. Dix, New York, McGraw-Hill Cook Co., Inc., 1962).

Dix, C.H., 1954, The method of Cagniard in seismic pulse problems: Geophysics, v. 19, no. 4, p. 722-738.

_____1961, The seismic head pulse, reflection, and pseudo-reflection pulses: Jour. Geophys. Research, v. 66, p. 2495-2951.

Doak, P.E., 1952, The reflection of a spherical acoustic pulse by an absorbent infinite plane and related problems: Royal Soc. London Proc., Ser. A, v. 215, p. 233-254.

Ewing, M.W., and Jardetzky, W.S., and Press, F., 1957, Elastic waves in layered media: New York, McGraw-Hill Book Co., Inc.

Flinn, E.A., 1961, Exact transient solution of some elementary problems of elastic wave propagation: Jour. Acoustical Soc. America, v. 33, p. 623-627.

Gerjuoy, E., 1948, Refraction of waves from a point source into a medium of higher velocity: Phys. Rev., v. 73, p. 1442-1449.

_____1953, Total reflection of waves from a point source: Commun. Pure Appl. Mathematics, v. 6, p. 73.

Gilbert, F., and Laster, S.J., 1962, Excitation and propagation of pulses on an interface: Seismol. Soc. America Bull., v. 52, p. 299-319.

Go, J.C., 1964, Surface elastic waves of a surface layer overlying a half-space due to an internal point source: Seattle, Wash., Report D2-22965, The Boeing Co.

_____1965, Dynamic ground responses due to an impulsive moving pressure: Seattle, Wash., Report D2-23440, The Boeing Co.

Grant, F.S., and West, G.F., 1965, Interpretation theory in applied geophysics: New York, McGraw-Hill Book Co., Inc.

Harkrider, D.G., 1964, Surface waves in multilayered elastic media. I. Rayleigh and Love waves from buried sources in a multilayered elastic half-space: Seismol. Soc. America Bull., v. 54, no. 2, p. 627-680.

Ingard, V., 1951, On the reflection of a spherical sound wave from an infinite plane: Jour. Acoustical Soc. America, v. 23, p. 329-355.

Knopoff, L., Gilbert, F., and Pilant, W.L., 1960, Wave propagation in a medium with a single layer: Jour. Geophys. Research, v. 65, p. 265-278.

Kogan, S.Y., 1963, The seismic energy generated by a surface source: (Izvestiya) Acad. Sci., U.S.S.R., Geophysics Ser.

Koo, B., and Loux, P., 1967, Ray theory seismic pulse (rats pulse): Math. Report, Environmental Research Corp., Alexandria, Virginia. Prepared under contract AT(29-2)-1163 for the Nevada Operations Office, U.S. Atomic Energy Comm.

Lamb, H., 1904, On the propagation of tremors over the surface of an elastic solid: Royal Soc. Phil. Trans., A203-1.

Ott, H., 1942, Reflection and refraction of spherical waves - effects of the second order: Annalen Der Physik, v. 41, p. 443-446.

Pekeris, C.L., 1940, A pathological case in the numerical solution of integral equations: U.S. Natl. Acad. Sci. Proc., v. 26, p. 433-437.

_____1941, The propagation of an SH pulse in a layered medium: Am. Geophys. Union Trans., v. 22, p. 392.

_____1948, Theory of propagation of explosive sound in shallow water: Geol. Soc. America Mem. 27.

_____1955a, The seismic surface pulse: U.S. Natl. Acad. Sci. Proc., v. 41, p. 469-480.

_____1955b, The seismic buried pulse: U.S. Natl. Acad. Sci. Proc., v. 41, p. 629-639.

_____1960, Propagation of seismic pulses in layered liquids and solids: in Internatl. Symp. on stress wave propagation in materials, Interscience, New York.

Pekeris, C.L., Alterman, Z., Abramovici, F., and Jarosch, H., 1965, Propagation of a compressional pulse in a layered solid: Reviews of Geophysics, v. 3, no. 1, p. 25-47.

Pekeris, C.L., and Lifson, H., 1957, Motion of the surface of a uniform elastic half-space produced by a buried pulse: Jour. Acoustical Soc. America, v. 29, p. 1233-1238.

Pekeris, C.L., and Longman, I.M., 1958a, The motion of the surface of a uniform elastic half-space produced by a buried torque-pulse: Geophys. Jour., v. 1, p. 146-153.

_____1958b, Ray-theory solution of the problem of propagation of explosive sound in a layered liquid: Jour. Acoustical Soc. America, v. 30, p. 323-328.

Pekeris, C.L., Longman, I.M., and Lifson, H., 1959, Application of ray-theory to the problem of long-range propagation of explosive sound in a layered liquid: Seismol. Soc. America Bull., v. 49, p. 247-250.

Petrashen, G.I., 1965, The work of the Leningrad school on seismic wave propagation: Review of Geophysics, v. 1, no. 3, p. 199-209.

Phinney, R., 1965, Theoretical calculation of the spectrum of first arrivals in layered elastic mediums: Jour. Geophy. Research, v. 70, no. 20.

Pinney, E., 1954, Surface motion due to a point source in a semi-infinite elastic medium: Seismol. Soc. America Bull., v. 44, p. 571-596.

Pod"yapol'skii, G.S., 1966, A ray-series expansion for reflected and transmitted waves: (Izvestiya) Acad. Sci., U.S.S.R., Physics of the Solid Earth Ser.

Roever, W.L., Vining, T.F., and Strict, E., 1959, Propagation of elastic wave motion from an impulsive source along a fluid-solid interface -- I. Experimental pressure response, II. Theoretical pressure response, III. The pseudo-Rayleigh wave: Royal Soc. London Philos. Trans., Ser. A, v. 251, p. 455-523.

Roy, A., 1965, On the general solution of elastic wave equations in a homogeneous medium with applications to the study of earthquake source mechanisms: Seismol. Soc. America Bull., v. 55, no. 2, p. 283-301.

Savage, J.C., 1958, Reflection from a fluid of higher sound velocity: Jour. Acoustical Soc. America, v. 30, p. 974-978.

Sherwood, J.W.C., 1960, Transient sound propagation in a layered liquid medium: Jour. Acoustical Soc. America, v. 32, p. 1673-1684.

Smirnov, V., and Sobolev, S., 1932, On a new method in the problem of elastic vibrations: Trudy Inst. Seism. Akad. Nauk U.S.S.R., no. 20.

_____1932a, Sur le problem plan des vibrations elastiques: Acad. sci Paris Comptes rendus, v. 194, p. 1437-1439.

_____1932b, Sur quelques problems des vibrations elastiques: Acad. sci Paris Comptes rendus, v. 194, p. 1797-1799.

_____1933, On the application of a new method of investigation of the elastic vibrations in space with axial symmetry: Trudy Inst. Seism. Akad. Nauk U.S.S.R., no. 29.

Sobolev, S., 1932, Application de la theorie des ondes planes a la solution du probleme de H. Lamb: Trudy Inst. Seism. Akad. Nauk U.S.S.R., no. 18.

_____1933, Sur les vibrations d'un demiplan et d'une couce a conditions initiales arbitraires: Sbornik Mat. (Moscow), v. 40.

_____1937, Some aspects of the theory of propagation and vibrations: in P. Frank and R. Von Mises, Differential and integral equations of mathematical physics, pt. 2, (only in the Russian edition).

Spencer, T.W., 1960, The method of generalized reflection and transmission coefficients: Geophysics, v. 25, no. 3, p. 625-641.

_____1965a, Long-time response predicted by exact elastic ray theory: Geophysics, v. 30, no. 3, p. 363-368.

_____1965b, Refraction along a layer: Geophysics, v. 30, no. 3, p. 369-388.

Whitley, V.W., 1967, Ray theory seismic pulse (rats pulse): Program Report, Environmental Research Corp., Alexandria, Virginia. Prepared under contract AT(29-2)-1163 for the Nevada Operations Office, U.S. Atomic Energy Comm.

Weyl, H., 1919, Ausbreitung elektromagnetischer wellen uber einem ebenen leiter: Annalen Physik, v. 60, p. 481-500.

Zvolinskii, N.V., 1957-58, Reflected waves and head waves arising at a plane boundary between two elastic media, I, II, III: (Izvestiya) Acad. Sci., U.S.S.R., Geophysics Ser.

Spherical Wave Propagation in Unbounded Media

Barnes, C., and Anderson, D.V., 1952, The sound field from a pulsating sphere and the development of a tail in pulse propagation: Jour. Acoustical Soc. America, v. 24, p. 229.

Blake, F.G., Jr., 1952, Spherical wave propagation in solid media: Jour. Acoustical Soc. America, v. 24, p. 211-215.

Case, K.M., and Colwell, J.F., 1967, Elastic waves radiated by a small source: Geophysics, v. 32, p. 52-59.

Duvall, W.I., and Atchison,T.C., 1950, Vibrations associated with a spherical cavity in an elastic medium: Bur. of Mines Rept. of Inv. 4692, 9p.

Eason, G., 1963, Propagation of waves from a spherical and cylindrical source of finite length: ZAMP, v. 14, p. 12-23.

Eringen, A.C., 1957, Elasto-dynamic problem concerning the spherical cavity: Quart. Jour. Mech. and Appl. Math., v. 10, pt. 3.

Gurvich, I.I., 1965, The theory of spherical radiators of seismic waves: (Izvestiya) Acad. Sci., U.S.S.R., Physics of the Solid Earth Ser.

_____1966a, The excitation function of a spherical detonation emitter: (Izvestiya) Acad. Sci., U.S.S.R., Physics of the Solid Earth Ser.

_____1966b, Spectra of waves from a spherical emitter in a homogeneous absorbing medium: (Izvestiya) Acad. Sci., U.S.S.R., Physics of the Solid Earth Ser.

_____1967, The dependence of seismic wave spectra in an absorbing medium on weight of a charge: (Izvestiya) Acad. Sci., U.S.S.R., Physics of the Solid Earth Ser.

Hirasawa, T., and Sato, R., 1963, Propagation of elastic waves from a spherical origin-Part 1, Part 2: Zisin 2, v. 16, p. 52-64, 65-77 (in Japanese).

Honda, H., 1959, The elastic waves generated from a spherical source: Sci. Reports Tohoku Univ., Ser. 5, Geophysics, v. 11, p. 178-183.

Sabodash, P.F., 1966, Propagation of spherical waves in an elastic-plastic medium: (Izvestiya) Acad. Sci., U.S.S.R., Physics of the Solid Earth Ser.

Selberg, H.L., 1952, Transient compression waves from spherical and cylindrical cavities: Arkiv, Fysik., v. 5, p. 97-108.

Sezawa, K., and Kanai, K., 1941, Transmission of arbitrary elastic waves from a spherical source, solved with operational calculus: Tokyo Univ. Earthquake Research Inst. Bull., v. 19, p. 151-161.

Sharpe, J.A., 1962, The propagation of elastic waves by explosive pressures: Geophysics, v. 7, p. 144-154, 311-321.

Vodicka, V., 1963, Radial vibrations of an infinite medium with a spherical cavity: ZAMP, Brief Reports, v. 14, p. 745-748.

White, J.E., 1965, Seismic waves-radiation, transmission, and attenuation: New York, McGraw-Hill Book Co., Inc.

Mathematical Techniques Employed For Certain Spherical Wave Propagation Problems

Hoop, A.T., de, 1961, A modification of Cagniard's method for solving seismic problems: Appl. Sci. Res., sec. B, v. 8, p. 349-356.

Longman, I.M., 1961, Solution of an integral equation occurring in the study of certain wave-propagation problems in layered media: Jour. Acoustical Soc. America, v. 33, p. 954-958.

_____1965, Comments on a paper by Papadopoulos on the use of singular integrals in wave propagation problems: Seismol. Soc. America Bull., v. 55, no. 2, p. 303-318.

Love, A.E.H., 1944, The mathematical theory of elasticity, 4th ed.: New York, Dover Pub. Inc.

Papoulis, A., 1962, The Fourier integral and its applications: New York, McGraw-Hill Book Co., Inc.

Pekeris, C.L., 1956, Solution of an integral equation occurring in impulsive wave propagation problems: U.S. Natl. Acad. Sci. Proc., v. 42, p. 439-443.

Pinney, E., 1951, A theorem of use in wave theory: Jour. Mathematics and Physics, v. 30, p. 1-10.

Rabinowitz, P., 1966, Automatic integration of a function with a parameter: Comm. Assoc. Computing Machinery, v. 9, p. 804-806.

Sokolnikoff, I.S., 1956, Mathematical theory of elasticity: New York, McGraw-Hill Book Co., Inc.

Watson, G.N., 1944, A treatise on the theory of Bessel functions: 2nd ed. Cambridge.

Parameters of Explosive Sources of Spherical Waves

Berg, J.W., Jr., and Papageorge, G., 1964, Elastic displacement from explosive sources: Seismol. Soc. America Bull., v. 54, no. 3, p. 947-959.

Kisslinger, C., 1963, The generation of the primary seismic signal by a contained explosion: Vesiac State of the Art Report, Inst. of Sci. and Tech., Univ. of Michigan, p. 1-85.

Latter, A.L., Martinelli, E.A., and Teller, E., 1959, Seismic scaling laws for underground explosions: Phys. of Fluids, v. 2, p. 280-282.

Molotova, L.V., 1964a, The relationship between the frequency spectra of seismic vibrations and explosion conditions I. Results of experimental investigations: (Izvestiya) Acad. Sci., U.S.S.R., Geophys. Ser.

_____1964b, The relationship of the frequency spectra of seismic vibrations and explosion conditions II. Comparison of the experimental results with the theory: (Izvestiya) Acad. Sci., U.S.S.R., Geophys. Ser.

O'Brien, P.N.S., 1960, Seismic energy from explosions: Geophys. Jour., v. 3, no. 1, p. 29-44.

Peet, W.E., 1960, A shock wave theory for the generation of the seismic signal around a spherical shot hole: Geophys. Prosp., v. 8, no. 4, p. 509-533.

Toksöz, M.N., Ben-Menahem, A., and Harkrider, D.G., 1964, Determination of source parameters of explosions and earthquakes by amplitude equalization of seismic surface waves. 1. underground nuclear explosions: Jour. Geophys. Research, v. 69, no. 20, p. 4355-4365.